

**FRAGILITY CURVES FOR RESIDENTIAL BUILDINGS IN DEVELOPING
COUNTRIES**

**FRAGILITY CURVES FOR RESIDENTIAL BUILDINGS IN DEVELOPING
COUNTRIES: A CASE STUDY ON NON-ENGINEERED
UNREINFORCED MASONRY HOMES IN BANTUL, INDONESIA**

By

Miqdad Khalfan, B. Eng

A Thesis Submitted to the School of Graduate Studies in Partial Fulfillment
of the Requirements for the Degree of Master of Applied Science

McMaster University
Hamilton, Ontario, Canada
January 2013

© Copyright by Miqdad Khalfan, January 2013

Master of Applied Science (2013)
(Civil Engineering)

McMaster University
Hamilton, Ontario

TITLE: FRAGILITY CURVES FOR RESIDENTIAL
BUILDINGS IN DEVELOPING COUNTRIES: A CASE
STUDY ON NON-ENGINEERED URM HOMES IN
BANTUL, INDONESIA

AUTHOR: Miqdad Khalfan

SUPERVISORS: Dr. Wael El-Dakhakhni, Dr. Michael J. Tait

PAGES: xv, 137

Abstract

Developing countries typically suffer far greater than developed countries as a result of earthquakes. Poor socioeconomic conditions often lead to poorly constructed homes that are vulnerable to damage during earthquakes. Literature review in this study highlights the lack of existing fragility curves for buildings in developing countries. Furthermore, fragility curves derived using empirical data are almost nonexistent due to the scarcity of post-earthquake damage data and insufficient ground motion recordings in developing countries. Therefore, this research proposes a methodology for developing empirical fragility curves using ground motion data in the form of USGS ShakeMaps.

The methodology has been applied to a case study consisting of damage data collected in Bantul Regency, Indonesia in the aftermath of the May 2006 Yogyakarta earthquake in Indonesia. Fragility curves for non-engineered single-storey unreinforced masonry (URM) homes have been derived using the damage dataset for three ground motion parameters; peak ground acceleration (PGA), peak ground velocity (PGV), and pseudo-spectral acceleration (PSA). The fragility curves indicate the high seismic vulnerability of non-engineered URM homes in developing countries. There is a probability of 80% that a seismic event with a PGA of only 0.1g will induce significant cracking of the walls and reduction in the load carrying capacity of a URM home, resulting in moderate damage or collapse. Fragility curves as a function of PGA and PSA were found to reasonably represent the damage data; however, fits for several PGV fragility curves could not be obtained. The case study illustrated the extension of ShakeMaps to fragility curves, and the derived fragility curves supplement to the limited collection of empirical fragility curves for

developing countries. Finally, a comparison with an existing fragility study highlights the significant influence of the derivation method used on the fragility curves. The diversity in construction techniques and material quality in developing countries, particularly for non-engineered cannot be sufficiently represented through simplified or idealized analytical models. Therefore, the empirical method is considered to be the most suitable method for deriving fragility curves for structures in developing countries.

Acknowledgements

In the name of God, to Him all praise and gratitude belongs. I thank Him for the blessings and opportunities that He has bestowed upon me.

This thesis would not have been possible without the support and guidance of my supervisors, Dr. Wael El-Dakhakhni and Dr. Michael Tait. Their unwavering faith in me provided comfort during the challenging times, and their patience with me during the last three years is sincerely appreciated. They have guided and mentored me while giving me the freedom to research and investigate subjects of my interest. I would like to thank them for their invaluable advice and ideas on the research, and their extensive feedback on the thesis.

I would like to thank Dr. Norman Kerle from the University of Twente, Netherlands, and Dr. Junun Sartohadi from the University of Gadjah Mada for making accessible the data used in the case study. I would also like to thank Kishor Jaiswal from US Geological Survey for the providing the updated ShakeMaps used in this research.

I would like to acknowledge my friends and colleagues for providing excellent company during the long days at school. Special thanks to Sean Cianflone for the valuable lessons on Matlab that have been very beneficial.

Finally, this step in my career would not have been possible without my family. I would like to recognize my grandparents who instilled in me the value of education and specifically, my late grandmother who constantly encouraged me to pursue further education despite having no formal education herself. I am grateful to God for granting me a family who have been nothing but supportive of my ambitions and dreams. A special note of thanks to my sister, Fatema, for her invaluable comments on the earlier versions of this thesis. Behind every successful man is a woman; Raihanna, my wife is my rock who has believed in me and has supported me in every way possible, and without her, any achievement would be meaningless.

Table of Contents

Abstract	iii
Acknowledgements	v
Table of Contents	vi
List of Figures	ix
List of Tables.....	xiii
List of Acronyms and Abbreviations	xiv
1 Introduction.....	1
1.1 Problem Overview	1
1.2 Socioeconomic Characteristics of Developing Countries	2
1.3 International Disaster Reduction Agreements	5
1.4 Structural Typologies of Homes in Developing Countries	7
1.5 Seismic Risk Assessment	11
1.6 Fragility and Vulnerability Assessment.....	13
1.7 Organization of thesis.....	15
2 Fragility Curves.....	16
2.1 Fragility Curves in Seismic Risk and Loss Assessment Tools	16
2.2 Methods of Deriving Fragility Curves.....	20
2.2.1 Empirical Fragility Curves	20
2.2.2 Analytical Fragility Curves.....	26
2.2.3 Expert-Opinion Fragility Curves	32

2.2.4	Hybrid Fragility Curves.....	34
2.3	Existing Fragility Curves for Homes in Developing Countries	36
3	Derivation of Empirical Fragility Curves	42
3.1	General.....	42
3.2	Post-earthquake Data Collection.....	42
3.3	Damage Classification.....	44
3.4	Ground Motion Parameters and USGS ShakeMaps	48
3.5	Data Processing using GIS	54
3.6	Damage Probability Matrices (DPMs) and Fragility Curves	56
3.7	Conclusion.....	63
4	Fragility of Single-storey URM Houses: Case Study on the 2006 Yogyakarta Earthquake	64
4.1	General.....	64
4.2	Indonesia	64
4.2.1	Socio-economic Profile	64
4.2.2	Seismic History and Tectonic Setting	65
4.3	Yogyakarta Earthquake, May 2006	67
4.4	Available Dataset.....	68
4.5	Damage Classification.....	74
4.6	Ground Motion – USGS ShakeMaps.....	75
4.7	Damage Probability Matrices.....	77
4.8	Derivation of Fragility Curves	90

4.9 Discussion on the Derived Fragility Curves.....	98
4.9.1 Data Points and Fragility Curves	98
4.9.2 Curve Fitting Statistics	101
4.9.3 Comparable Fragile Structures.....	105
4.10 Comparison with existing fragility curves.....	106
4.11 Conclusion.....	112
5 Conclusions and Recommendations.....	114
5.1 Summary	114
5.2 Conclusions.....	115
5.3 Recommendations.....	118
Bibliography.....	120
Appendix A Fragility Curves (PSA and PGA).....	132

List of Figures

Figure 1.1 Risk Management (Stanganelli 2008)	12
Figure 1.2 Vulnerability curve (left) and fragility curve (right)	14
Figure 2.1 Example Capacity Curve and Spectral Demand (FEMA 2012a)	17
Figure 2.2 Fragility curves of RC buildings as a function of S_d -elastic (above) and S_d -inelastic (below) (Rossetto & Elnashai (2003) found in: Crowley et al. (2011b))	22
Figure 2.3 Fragility curves for URM building with tie rods and tie beams (above) and without tie rods and tie beams (below) (Rota et al. (2008a) found in: Crowley et al. (2011a)).....	24
Figure 2.4 Fragility curves for masonry buildings (Colombi et al. (2008) found in: Crowley et al. (2011a)).....	25
Figure 2.5 Fragility curves for low rise infilled RC frames (Rossetto and Elnashai (2005) found in: Crowley et al. (2011b))	28
Figure 2.6 Illustration of fragility surfaces (above) and projected fragility curve (below) (Seyedi et al. 2010)	30
Figure 2.7 Fragility curve for 3-storey masonry building (Rota et al. (2010) found in: Crowley et al. (2011a)).....	31
Figure 2.8 Fragility curves for typical URM structures in Trinidad & Tobago (Clarke 2010)	38

Figure 3.1 Example USGS ShakeMap uncertainty grading (USGS 2010a)	53
Figure 3.2 Fragility curve derivation flow chart for PGA range 0.3-0.34g	57
Figure 4.1 Pacific Ring of Fire, Indonesia located along the Sunda trench (http://commons.wikimedia.org/wiki/File%3APacific_Ring_of_Fire.svg)	67
Figure 4.2 Damage data distribution based on building typologies	70
Figure 4.3 Building occupancy distribution	70
Figure 4.4 Data distribution of storeys	71
Figure 4.5 One (or One and half) brick thick masonry buildings (Boen 2006)	72
Figure 4.6 Half brick thick masonry building without reinforcements (Boen 2006)	72
Figure 4.7 Damage distribution of brick masonry buildings	73
Figure 4.8 Damage distribution of RC buildings	73
Figure 4.9 Illustration of USGS Shakemap and damage data overlay in ArcGIS (black markers are individual buildings)	76
Figure 4.10 Damage Distribution as a function of PGA	78
Figure 4.11 Damage distribution as a function of PGV	78
Figure 4.12 Damage distribution as a function of PSA-03	79
Figure 4.13 Distribution of collapsed (above) and lightly damaged (below) buildings as a function of PGA	80

Figure 4.14 Distribution of collapsed (above) and lightly damaged (below) buildings as a function of PGV.....	81
Figure 4.15 Damage Probability Matrices in PGA	84
Figure 4.16 Damage Probability Matrices in PGV	85
Figure 4.17 Damage Probability Matrices in PSA.....	86
Figure 4.18 Cumulated DPMs for PGA intervals	87
Figure 4.19 Cumulated DPMs for PGV intervals	88
Figure 4.20 Cumulated DPMs for PSA (0.3s Period, 5% damping) intervals	89
Figure 4.21 Cumulative lognormal distribution fragility curves in PGA.....	91
Figure 4.22 Cumulative beta distribution fragility curves in PGA.....	91
Figure 4.23 Exponential fragility curves in PGA	92
Figure 4.24 Comparison of fitted functions in PGA.....	92
Figure 4.25 Comparison of fitted functions in PGV.....	93
Figure 4.26 Cumulative lognormal distribution fragility curves in PSA (0.3s period, 5% damping).....	94
Figure 4.27 Cumulative beta distribution fragility curves in PSA (0.3s period, 5% damping).....	95
Figure 4.28 Exponential fragility curves in PSA (0.3s period, 5% damping)	95

Figure 4.29 Comparison of fitted functions in PSA.....	96
Figure 4.30 Fragility curves fitted with and without the last data point (cumulative lognormal fragility curve in terms of PGA).....	99
Figure 4.31 Fragility curves for building typology IMA2 (Rota et al. (2008b) found in: Crowley et al. (2011a)).....	101
Figure 4.32 In-plane failure fragility curves (Tarque et al. 2010)	106
Figure 4.33 Comparison with Turkish fragility curves (moderate damage state).....	108
Figure 4.34 Comparison with Turkish fragility curves (collapse damage state).....	109
Figure A.1 Cumulative lognormal fragility curve in terms of PGA.....	132
Figure A.2 Cumulative beta fragility curve in terms of PGA.....	133
Figure A.3 Exponential fragility curve in terms of PGA.....	134
Figure A.4 Cumulative lognormal fragility curve in terms of PSA	135
Figure A.5 Cumulative Beta fragility curve in terms of PSA.....	136
Figure A.6 Exponential fragility curve in terms of PSA	137

List of Tables

Table 3.1 EMS-98 Damage descriptions for masonry buildings (Grünthal 1998).....	47
Table 4.1 Damage states and definitions (Boen 2010).....	75
Table 4.2 Fragility curve results.....	97
Table 4.3 Descriptions of Turkish building sub-classes (Erberik 2008) ..	108

List of Acronyms and Abbreviations

ARMA	Autoregressive Moving Average
ASTM	American Society for Testing and Materials
ATC	Applied Technology Council
CAV	Cumulative Absolute Velocity
CM	Confined Masonry
CSA	Canadian Standards Association
DBELA	Displacement-Based Earthquake Loss Assessment
DI _{HRC}	Damage Index (Homogenized Reinforced Concrete)
DPM	Damage Probability Matrix
EERI	Earthquake Engineering Research Institute
EIS	Earthquake Impact Scale
EMS	European Macroseismic Scale
FEMA	Federal Emergency Management Agency
GDP	Gross Domestic Product
GEM	Global Earthquake Model
GIS	Geographic Information System
GMPE	Ground Motion Prediction Equation
GNI	Gross National Income
GPS	Global Positioning System
HAZUS-MH	Hazard US-Multi Hazard
HDI	Human Development Index
HRC	Homogenized Reinforced Concrete
IAEE	International Association for Earthquake Engineering
ICG	International Centre of Geohazards
IDA	Incremental Dynamic Analysis
IHDI	Inequality adjusted Human Development
IMF	International Monetary Fund
IPE	Intensity Prediction Equations

ISD	Inter-Storey Drift
ISDR	Inter-Storey Drift Ratio
LAR	Least Absolute Residuals
LMA	Levenberg-Marquardt Algorithm
MDG	Millennium Development Goal
MMI	Modified-Mercalli Index
MSK	Medvedev-Sponheuer-Karnik
NGO	Non-Governmental Organizations
NIBS	National Institute of Building Sciences
PAGER	Prompt Assessment of Global Earthquakes for Response
PGA	Peak Ground Acceleration
PGV	Peak Ground Velocity
PPP	Purchasing Power Parity
PSA	Pseudo-Spectral Acceleration
RC	Reinforced Concrete
RMSE	Root Mean Square Errors
SDOF	Single-Degree of Freedom
SELENA	SEismic Loss Estimation using a logic tree Approach
SSE	Sum of Squared Errors
SSR	Sum of Square of Regression
SST	Sum of Squares Total
TR	Trust Region
UN	United Nations
UNDP	United Nations Development Programme
URM	Unreinforced Masonry
USGS	United States Geological Survey
WB	World Bank
WCNDR	World Conference on Natural Disaster Reduction
WHE	World Housing Encyclopedia

1 Introduction

1.1 Problem Overview

The Annual Disaster Statistical Review (Guha-Sapir et al. 2011) reported that 1,888 people were killed due to 22 earthquakes in 2009 while affecting an additional 3.2 million people and causing damages amounting to 6.2 billion US dollars. This review also points out that in 2010, 25 seismic events caused 46.2 billion US dollars worth of damage while claiming 226,735 lives and affecting 7.2 million people. Although there has been no significant increase in the number of earthquakes over the last 20 years, the statistics of property damage and human loss is rising, and most of the human loss is found to occur in developing countries (Kenny 2009). The effects of seismic disasters on developing countries are long lasting and often crippling their already struggling economy (Meli and Alcocer 2004) thus rendering such countries more vulnerable and highly dependent on post-disaster relief aid.

The seismic vulnerability of buildings in developing countries can be observed from the recent earthquake in Haiti on January 12th, 2010 where the 7.0 magnitude earthquake caused severe damage or destruction to almost 300,000 homes and over 300,000 lives were lost (DesRoches et al. 2011). The well-known saying that *earthquakes don't kill people, buildings do*, holds particularly true for developing countries where lives lost are generally a result of poorly constructed structures. The social, economical, and political makeup of these countries make them more susceptible to loss of human lives and property damage.

International disaster risk reduction agreements such as the Yokohama Strategy (IDNDR 1994) and Hyogo Framework (ISDR 2005) have

advocated a paradigm shift from post-disaster relief efforts towards pre-disaster planning. These international disaster risk reduction principles also recognize the need to focus risk reduction strategies towards developing nations and this has led to significant efforts in the last decade towards developing seismic risk assessment and management programs with a more global focus. Given the uncertain nature of seismic events, damage risk assessment in a pre-disaster framework is established by examining the vulnerability or fragility of structures through vulnerability and fragility curves (Porter 2003). This thesis aims to provide a methodology for deriving fragility curves for single-storey unreinforced masonry (URM) homes in the context of developing countries that can be used in assessing their seismic risks and consequently in developing risk reduction strategies.

1.2 Socioeconomic Characteristics of Developing Countries

The terms ‘developed’ and ‘developing’ are commonly used to suggest the status of a country’s development level. However, no universally accepted classification system exists and several multinational organizations have adopted different designations for their own mandates. As of 2004, the International Monetary Fund (IMF) has categorized countries as either advanced economies or emerging and developing economies (IMF 2011). The method used for classification is not explicit and is based on the economic and financial data provided by the member countries (Nielsen 2011). Some key indicators used in the classification by IMF are the countries’ gross domestic product (GDP) measured by their purchasing-power parity (PPP), total exports of goods and services, and populations (IMF 2011).

The World Bank (WB) in their yearly development report presents socioeconomic data for 130 countries, which is in addition to its database of 237 economies and regions on the Open Data website. The WB classification of countries as low-, middle- or high-income is based on their gross national income (GNI) per capita ranges of US\$995 or less, US\$996 to US\$12,195, and US\$12,196 or more, respectively (WB 2011). All WB member countries and countries with a population of more than 30,000 are included in this classification (WB 2011).

In contrast to the IMF and WB, the United Nations Development Programme (UNDP) has used socioeconomic indicators to classify countries using the Human Development Index (HDI). Health, education, and income are three socioeconomic dimensions that are combined to form the HDI and are measured using indicators such as life expectancy at birth, mean years and expected years of schooling, and GNI per capita. In 2010, the UNDP introduced the Inequality-adjusted HDI (IHDI), which accounts for the variance in human development across the population where the HDI only reflects the averages. The countries are classified into four categories; low, medium, high, and very high human development, where for convenience, the countries in the very high HDI category are known as developed and the rest being developing (UNDP 2010). Natural disasters affect human development progress and therefore this work defines developing countries according to UNDP's classification system.

Diversity in politics, culture, history, geography, and size make it a complex task to characterize developing countries, but it is possible to identify common trends using UNDP's HDI. These common characteristics are considered for the purpose of understanding the effects of socioeconomic dynamics of developing countries on general risk assessment and management methodologies. Lower income levels, low

levels of human capital, high levels of poverty, higher population growth rates, larger rural population, and higher rate of rural-to-urban migration rates are some common indicators of developing countries (Todaro and Smith 2009) that exacerbate the impacts of seismic disasters on such countries.

The GNI per capita in terms of purchasing power parity (PPP) for medium and low HDI groupings were \$5,276 and \$1,585, respectively, while that for the very high HDI grouping was \$33,352 (UNDP 2011). Countries with lower income levels are more susceptible to human losses from natural disasters than those with higher income levels given the same number of disasters (Kahn 2005). The lower levels of income force the prioritization of needs for well-being, and most often health and education are deprioritized and, as a result, the nations' productivity levels decline thus leading to an income level stagnate or perpetual poverty (Todaro and Smith 2009).

Increasing population levels in developing countries and the migration trends from rural to urban areas contribute to socioeconomic vulnerability. The population growth projected in 2010 for the next five years in the low and medium HDI groupings are 2.2% and 1%, respectively, while the very high HDI category expects a growth of 0.5% (UNDP 2011). The migration of people from rural to urban areas seeking a better quality of life leads to development of overpopulated cities and urban slums that are highly vulnerable to seismic disasters. Demographic trends given by UNDP show that urban population of low and medium human development countries from 1990 to 2010 have increased by 38% and 40% (UNDP 2010), respectively, and this growth is partly contributed by rural-to-urban migration.

Socioeconomic standing of developing countries largely decide the consequences of seismic events and as seen in the case of Haiti can be devastating. The direct losses as a result of structural destruction and loss of human lives are detrimental to the already vulnerable socioeconomic structure of developing countries. Developing countries also suffer larger indirect losses from the loss of economic activities and social infrastructure in contrast to developed countries (Noy 2009). These characteristics indicate the existing seismic risks and highlight the importance of seismic risk assessment and management programs for developing countries.

1.3 International Disaster Reduction Agreements

In 1994, the participants of the World Conference on Natural Disaster Reduction (WCNDR) adopted the *Yokohama Strategy and its Plan of Action* (IDNDR 1994). The Yokohama Strategy recognized the vulnerability of developing countries to natural disasters, and placed strong emphasis on disaster prevention, mitigation, and preparedness rather than disaster response alone. The Yokohama Strategy also called for improved risk assessments as part of a broader management strategy.

A review of the Yokohama Strategy requested by the General Assembly of the United Nations (UN) in 2004 noted that amongst the remaining challenges, “*greater awareness of the social and economic dimensions of vulnerability*” was needed in the context of risk identification. The review presented several areas of progress; however, it also outlined several gaps and challenges that needed to be addressed to adequately respond to disaster risks.

The WCNDR was held again in Hyogo, Japan in 2005 to address the inadequacies outlined in the review of the Yokohama Strategy. The outcome of the 2005 WCNDR meeting was the proposal and adoption of

the Hyogo Framework for Action 2005-2015 titled *Building the Resilience of Nations and Communities to Disasters* (ISDR 2005). The Hyogo Framework acknowledges that for an effective disaster risk management initiative, its efforts must be incorporated into broader socioeconomic goals that promote sustainable development and poverty reduction. Similar to the preceding UN resolution that formed the Yokohama Strategy, the Hyogo Framework recognizes that disaster risks were higher for developing countries as a result of vulnerabilities that were characteristic of such countries.

The WCNDR outlined a number of priorities in the Hyogo Framework among which was the need to focus on developing countries because of their vulnerability to disaster and their inability to adequately respond and recover. The WCNDR recognized that disaster risk reduction was intertwined with the broader issue of sustainable development and to address this, the Hyogo Framework's action plan addresses key social and economic components of development. The Hyogo Framework is therefore considered to be an essential component towards the realizations of the Millennium Declaration¹.

The Yokohama Strategy and Hyogo Framework have established the need for focusing disaster risk prevention and mitigation in the context of developing countries. The socioeconomic vulnerabilities compounded by structural vulnerabilities pose a great challenge for developing countries

¹ The Millennium Declaration is a resolution adopted by the United Nation's general assembly whose outcome resulted in the establishment of the Millennium Development Goals (MDGs). The MDGs are targeted at addressing the challenges faced by developing countries and they include: eradicating extreme poverty; achieving universal primary education for all; promoting gender equality and empowering women; reducing child mortality; improving maternal health; combating HIV/AIDS, malaria and other diseases; ensuring environmental sustainability; and developing a global partnership for development.

that are prone to seismic events. Many recent seismic risk reduction strategies have incorporated the assessment of socioeconomic vulnerabilities. However, it is necessary to examine the complexities that characterize developing countries in context of their socioeconomic status and the vulnerability of their infrastructure.

1.4 Structural Typologies of Homes in Developing Countries

The consequences of housing damage or collapse are devastating not only from the loss of lives but also loss of security, and socioeconomic stability. This is particularly true for populations in developing countries whose homes are an essential fabric of their socioeconomic security. Furthermore, the loss of shelter usually results in their entrapment in a perpetual cycle of poverty. The results of housing losses in addition to civilian infrastructure damage escalate the effects of existing low productivity levels and impede the progress of developing economies making it a key component in any vulnerability or risk study.

There is a rich diversity of housing structures in the developing world resulting from its geography, colonial history, and level of economic growth. This diversity is also exhibited within each country where rural dwellings can be significantly different from urban homes as a result of disproportionate economic and social progress. Earthquake Engineering Research Institute (EERI) and the International Association for Earthquake Engineering (IAEE) in a recent project has attempted to collect different house construction types found globally through expert opinion and classified them into structural categories in an online repository (<http://www.world-housing.net/>) called the World Housing Encyclopedia (WHE). Non-engineered houses that are constructed without the technical

expertise of engineers or architects are most vulnerable. Using the WHE structural categories, some of the common vulnerable construction types are described in this section to assess the diversity that is generally encountered in establishing seismic risk assessment programs for developing countries.

Adobe mud block construction is very popular in rural and urban parts of South America, Asia, and Africa, which often experience earthquakes (Blondet et al. 2011). Adobe structures are considered to be non-engineered structures which are generally constructed by the owner or local builders (Blondet and Villa-Garcia 2004). The seismic forces are resisted by the adobe block walls which vary in thickness from 250mm to 850mm (Blondet et al. 2011) without any specific out-of-plane force resisting systems. The roof construction varies depending on the region and the availability of materials and this is noted in southern and western Iran where wood and mud are used to construct flat roof structures whereas in the hot and dry areas of central and eastern parts of the country many adobe homes can be found to have dome-shaped roofs (Bakhshi et al. 2005; Maheri et al. 2005). In many parts of South America, adobe construction features pitched roofs that are constructed using wooden beams and trusses with clay tiles or corrugated steel sheets (French 2007a,b,c; Lang et al. 2007; Lopez et al. 2012). The roof structures are supported by the adobe block walls and in most cases lack wall-to-roof connections (Blondet et al. 2011).

Adobe mud blocks are heavy and brittle offering inadequate seismic resistance, which is also attributed to the inferior material properties exacerbated by contact with water (Meli et al. 1980). Seismic damage patterns of adobe structures include vertical and diagonal cracking, out-of-plane failure of the walls, and wall detachments at corners leading to

collapse of the roof structure (Blondet et al. 2011; Meli et al. 1980). In the 1976 Guatemala earthquake, failure of 250,000 adobe homes led to the death of 25,000 people (Meli et al. 1980). Earthquakes in El Salvador (2001), Peru (2001), Iran (2003), Peru (2007), and even more recently in China (2008) and Chile (2010) have led to many deaths due to the failure of adobe homes, however, adobe homes will continue to persist due to their low cost and availability of materials.

Unreinforced masonry (URM) construction using stone, rubble, brick or concrete blocks with mud or mortar joints is a popular choice in developing countries due to its simple construction process and low material costs (Mayorca and Meguro 2004). URM can be found in both urban and rural areas and construction is most often carried out without technical input from engineers (Abrams 2000). The choice of poor quality materials and lack of seismic resistant design make this type of construction extremely vulnerable.

URM walls are designed to carry the gravity loads and they vary in thickness depending on the materials being used and their manufacturing process. Stone masonry homes extend across many parts of the developing world including North Africa, the Middle East, and South Asia. They are constructed by arranging stone boulders from a variety of sources and are bonded using weak mud and lime mortars or sometimes stronger cement mortar (Bothara and Brzev 2011). Fired clay brick masonry walls vary in thickness from 125mm to 250mm depending on the owner's financial status (Ali 2006; Ansary 2003). Concrete block units in developing countries are a relatively new development in contrast to other URM types. They are manufactured by mixing cement and aggregates with very low cement ratios resulting in low compressive strengths (Marshall et al. 2011). The blocks come in a variety of sizes and can be

solid, cellular, or hollow. Roof structures for this type of construction incorporate an array of roof configurations such as flat roofs with wood framing or pitched wood trusses with clay tiles or corrugated iron sheets, concrete slabs, cold-form steel purlins with corrugated iron sheets, and straw covered with mud supported on wooden framing (Ahari and Azarbakht 2005; Ali 2006; Ali and Muhammad 2007; Ansary 2003; Clarke and Ramnath 2009). URM homes similar to adobe structures, lack adequate lateral load resisting systems and have poor or no connection details. Collapse of URM structures are governed by out-of-plane failures, in-plane shear failures, wall detachments at intersections, and roof collapse, all of which can be attributed to lack of adequate connections that tie the structure together (Bothara and Brzev 2011). Major earthquakes in Kashmir (Pakistan in 2005) and Bhuj (India in 2001) have exhibited the vulnerability of URM structures that have resulted in considerable damage (Bothara and Brzev 2011).

Confined masonry (CM) system is another construction type that is used in several earthquake-prone developing countries in South America, Iran, Indonesia, and China (Brzev 2007). The system is very similar in appearance to the reinforced concrete RC moment frame construction; however, the construction sequence is reversed and the unreinforced masonry walls using hollow or solid blocks are constructed prior to the beams and columns. A variation in the construction of CM structures is also encountered where hollow masonry blocks are used to construct the columns, which are then reinforced with steel bars and grout (Rodriguez 2007). CM structures resist lateral loads using both, the frame and the masonry walls. Housing structures using CM construction have generally performed well when built to design codes as demonstrated in the February, 2010 earthquake in Chile (Astroza et al. 2012).

RC construction is quite extensive in many parts of Latin America, North Africa, and the Middle East. RC is commonly used in multi-storey homes and its seismic load resisting systems are moment frames or shear walls. Moment frame structures support the gravity loads and usually employ masonry infill walls as non-structural elements between the columns. This type of construction contains many essential engineered details; however, in most parts of the developing world they are built without the involvement of engineers or design codes.

In addition to the deficiencies of adopted structural systems, the quality of construction and materials in developing countries are below par, which attributes to their vulnerability. Many developing countries have limited or no building codes and where building codes are present, the governments fail to enforce or revise building codes to address the construction practices. The socioeconomic conditions together with the structural variety and vulnerability of the building stock require a systematic but focused seismic risk assessment and management effort in developing countries.

1.5 Seismic Risk Assessment

The move towards prevention, preparedness, and mitigation of disasters as recommended by the Hyogo Framework underlines seismic risk management as an essential component of a seismic risk reduction program. Risk in the context of natural disasters can be defined as the expectation of losses or damage both direct and indirect, as a result of natural hazards (ISDR 2009). Seismic risk management is the development of policies, procedures, and strategies to limit the extent of disaster caused by earthquakes. Seismic risk assessment is an integral component of seismic risk management and it involves the evaluation of

the risk of a disaster due to potential hazards given the vulnerability of the region or area.

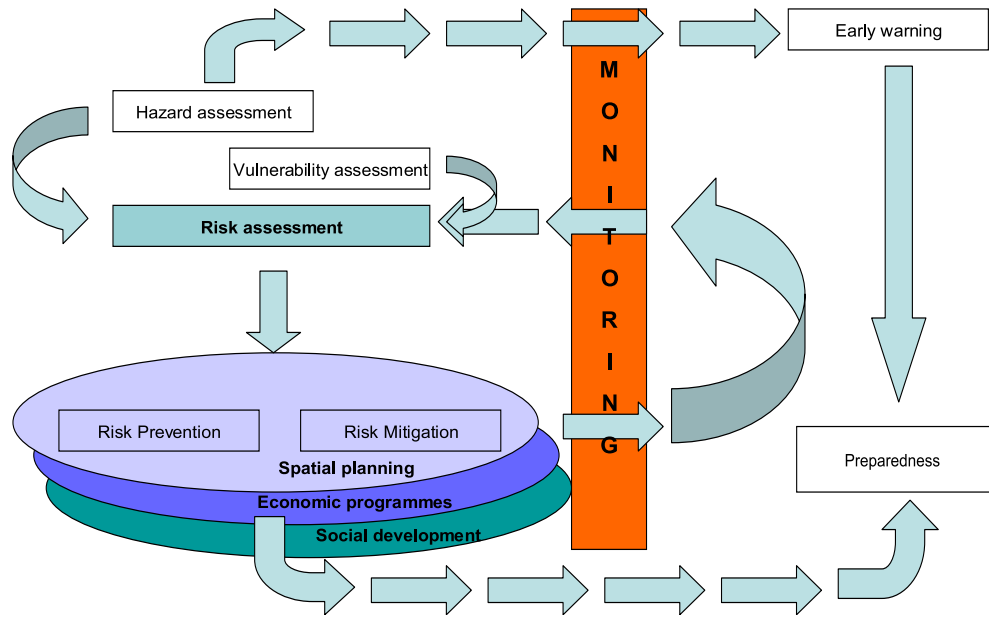


Figure 1.1 Risk Management (Stanganelli 2008)

Seismic vulnerability assessments of the built environment evaluate the extent of potential damage that could be experienced as a consequence of a seismic event. The uncertain nature of seismic events and the variability in the construction of structures require the use of a probabilistic approach in the form of fragility and vulnerability curves (or functions) to assess the seismic vulnerability. Seismic events include hazards other than ground shaking such as liquefaction, tsunamis, landslides, and surface fault ruptures. However, these impacts are localized and therefore, ground shaking is the only significant impact in any loss modeling involving larger parts of the affected regions (Bird and Bommer 2004) and seismic vulnerability assessments are generally carried out with this understanding.

1.6 Fragility and Vulnerability Assessment

Fragility and vulnerability curves that take on the form of analytical functions are commonly used in seismic risk assessment and loss estimation applications (Khater et al. 2003). As illustrated in Figure 1.2, fragility and vulnerability curves look similar and the terms are often used interchangeably and while both are used to assess risk, they are distinct in their description of information (Crowley, Colombi, et al. 2010; Porter 2003). Use of either largely depends on its particular application in the assessment study and they can be derived using empirical, analytical, judgment-based, and hybrid methods depending on their source of data (Rossetto and Elnashai 2003).

Fragility of a structure can be defined as its damageability while the structure's vulnerability is a consequence of this damageability. Fragility curves describe the probability of reaching or exceeding specific damage levels as a function of seismic intensity measure, whereas vulnerability functions relate the probability of losses to the seismic intensity measures (Porter 2003). Vulnerability functions relate the probability of losses as a result of damage to a ground motion measure. Some types of losses that can be used in developing seismic vulnerability functions for structures include repair cost, repair time, casualties, environmental impacts (ATC 2011), or a damage factor given as a ratio of loss cost suffered to replacement cost (ATC 1985). The data used in the derivation of vulnerability functions are region specific and can be collected using an inventory method (ATC 1985). However, the use of this method can lead to issues with data unavailability and inconsistency. Obtaining data estimates from experts or using relative losses expressed as a ratio of reported losses from the seismic event to the GDP, which is more readily

available, can simplify the process (Yong et al. 2001). Vulnerability functions can be directly derived using the data discussed above or through the use of fragility and consequence functions (Crowley et al. 2011a).

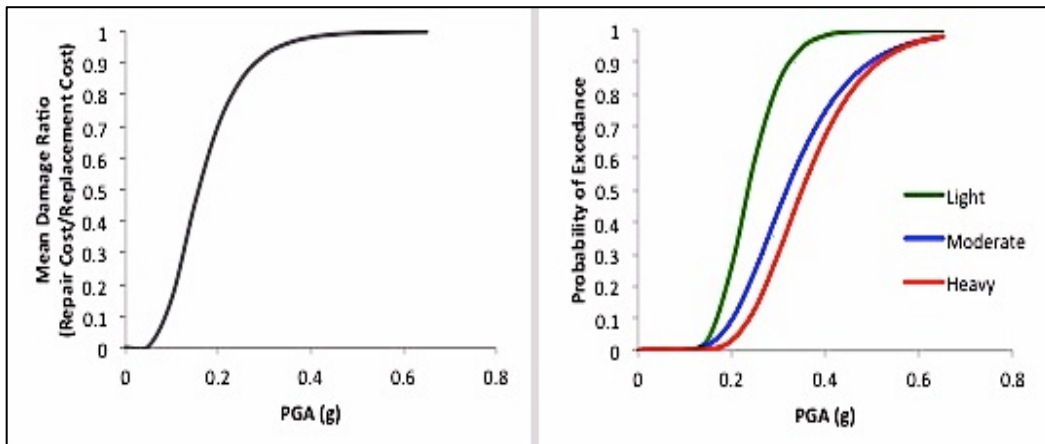


Figure 1.2 Vulnerability curve (left) and fragility curve (right)

Although fragility curves are specific to structural typologies, they are versatile in their use for seismic risk assessment purposes as they can be adapted to any region for similar building typologies and ground conditions, and they can also be used to derive vulnerability functions using consequence functions. In addition to their use in seismic risk assessments, fragility functions are also used to understand structural response to seismic forces particularly given the current shift in seismic design philosophy towards a performance-based earthquake engineering methodology (Porter et al. 2007). The use of fragility curves within performance-based design is done through evaluation of the fragility of building components, structural and non-structural, while fragility curves for seismic risk assessments evaluate overall structural performance. This research focuses on the development of overall structural fragility functions for the purpose of seismic risk assessments.

1.7 Organization of thesis

The thesis has been divided into five chapters. Chapter 1 introduces the problem, provides an overview of socioeconomic characteristics, and existing structural typologies that exist in developing countries. It also introduces the concepts of fragility and vulnerability curves, and discusses the differences between the two. Chapter 2 discusses fragility curves in the context of seismic risk and loss assessment tools. A thorough literature review of existing fragility curves derived using the empirical, analytical, expert-opinion, and hybrid methods are presented in this chapter. The chapter concludes with a discussion on existing fragility curves for homes in developing countries. Chapter 3 outlines a methodology for deriving fragility curves using post-earthquake damage data. The methodology includes the use of USGS ShakeMaps as a valuable tool to address the lack of ground motion data, particularly in developing countries. A curve fitting procedure is discussed and descriptions of analytical and distribution functions that are used to fit curves to the empirical data are also provided in this chapter. A case study implementing the methodology discussed in Chapter 3 is presented in Chapter 4. The case study involves damage data collected after the Yogyakarta earthquake in May, 2006, in Indonesia. Fragility curves are developed for single-storey URM homes using cumulative lognormal, cumulative beta, and exponential functions for the case study data. The fragility curves are developed in terms of PGA, PGV, and PSA. A comparison between the curves derived in this study and other existing curves is presented. The study concludes with Chapter 5 providing a brief summary of the conducted research and recommendations that need to be considered for future work.

2 Fragility Curves

2.1 Fragility Curves in Seismic Risk and Loss Assessment Tools

Risk is defined differently among different professions. However, in the context of natural disasters, risk can be defined as the potential of negative consequences as a result of a natural disaster given the vulnerability and exposure of people, buildings, and infrastructure to such disasters. Loss estimation is a key component to seismic risk assessment as it gives decision-makers critical information in developing and planning pre- and post-disaster policies. There are several loss estimation tools and methodologies available; however, only those utilizing fragility curves are discussed here.

HAZUS (Hazard US) is a popular loss estimation methodology that is implemented through a GIS-based software application, HAZUS MH (FEMA 2012b). The HAZUS methodology was developed as a national methodology for seismic loss estimation by the Federal Emergency Management Agency (FEMA) in cooperation with the National Institute of Building Sciences (NIBS) (Kircher et al. 2006). Earthquake demand is represented in terms of spectral response for a probabilistic study or it can be used for scenario earthquakes. The software is designed to allow the use of user-supplied GIS-based ground shaking maps and building stock inventory. The methodology defines five damage states: none, slight, moderate, extensive, and complete, using physical (qualitative) descriptions of damage to building elements. Fragility curves are derived using the capacity spectrum method where the intersection of the response spectrum with the capacity curve in an S_a - S_d space, known as the *performance points* shown in Figure 2.1, are used as inputs to the

fragility functions. Loss estimates are developed using the probability of damage in the fragility curves as inputs to building loss functions. Loss estimates in HAZUS are based on the capacity and fragility curves of the US building stock, therefore, its application at a global scale requires additional capacity and fragility computations. The HAZUS methodology has been applied to several seismic risk assessment studies by adapting the capacity and fragility curves for buildings in specific regions (Gulati 2006; Levi et al. 2010; Yeh et al. 2000; 2006).

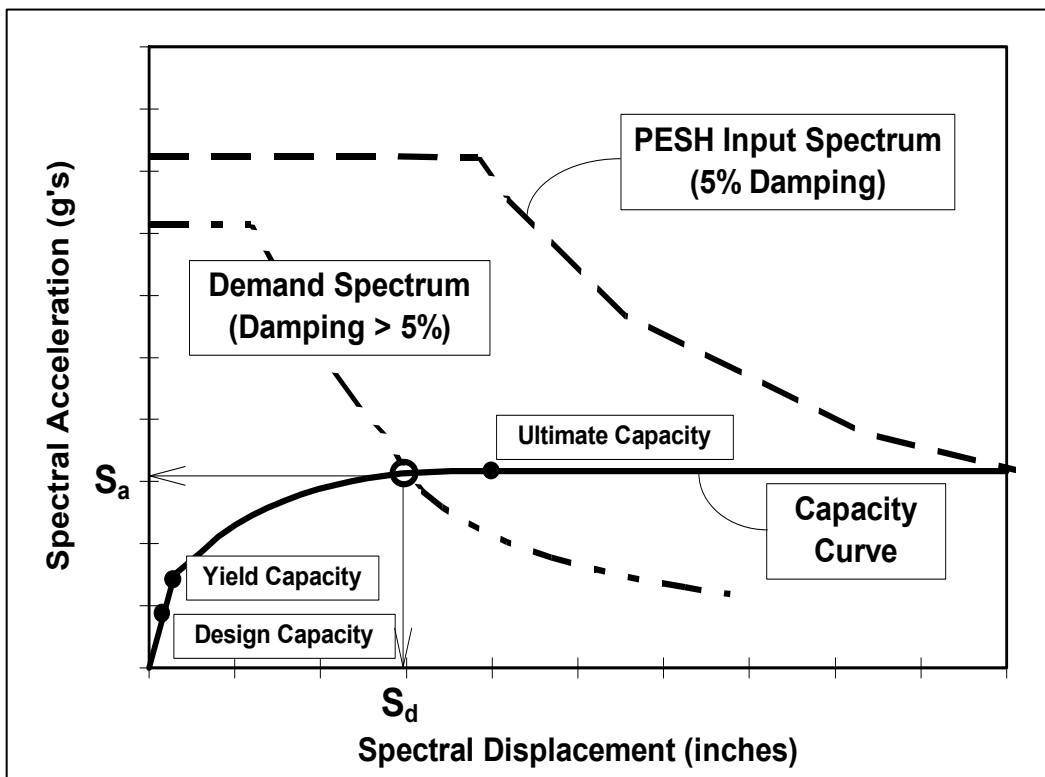


Figure 2.1 Example Capacity Curve and Spectral Demand (FEMA 2012a)

The European seismic risk assessment project, RISK-UE utilized fragility and vulnerability functions to assess direct and indirect losses from an earthquake scenario to seven European cities that include: Barcelona, Bitola, Bucharest, Catania, Nice, Sofia, and Thessaloniki (Mouroux and Brun 2006; Mouroux et al. 2004). The fragility and vulnerability

assessments were carried out for regular buildings as well as historical monuments using analytical and empirical methods depending on the nature of data available. The analytical method used the capacity spectrum method similar to that employed by HAZUS (Kappos et al. 2006; Lagomarsino and Giovinazzi 2006).

Empirical collapse fragility curves for global building types developed from the WHE-PAGER survey (to be discussed in Section 2.2.3) are intended to be incorporated into the Prompt Assessment of Global Earthquakes for Response (PAGER) model developed by U.S. Geological Survey (USGS) (Jaiswal et al. 2011). PAGER (Wald et al. 2010) provides seismic impact assessments through an automated system that includes estimates of possible fatalities and economic losses. Additional information in PAGER notifications includes types of vulnerable buildings in the region, exposure and fatalities from previous nearby earthquakes, and information concerning the potential for secondary hazards. An earthquake impact scale (EIS) based on estimated cost of damage and estimated range of fatalities is used to provide the level of impact expected as a result of seismic event.

The International Centre of Geohazards (ICG) based in Norway, through the contributions of NORSAR (Norway) and the University of Alicante (Spain) developed the seismic risk assessment MATLAB-based software SELENA (SEismic Loss Estimation using a logic tree Approach) (Molina et al. 2010b). Fragility curves derived using the capacity spectrum method are used to provide estimates on building damage distributions and subsequently economic losses and human casualties. While SELENA is based on the HAZUS methodology, it differs from HAZUS from an operational perspective. SELENA allows the flexibility of using any GIS

software unlike HAZUS, which is linked to ArcGIS. Also, unlike other seismic loss estimation tools, SELENA is structured using a logic tree approach applying weighted parameters at each level to account for uncertainties (Molina et al. 2010a).

The Global Earthquake Model (GEM) has been established by the Global Science Forum to provide risk assessment at a global level (GEM Foundation 2010). GEM's risk engine referred to as *OpenQuake* was developed to provide a comprehensive global earthquake risk model (Crowley et al. 2011). *OpenQuake* software consists of two main components: seismic hazard and seismic risk. Probabilistic and deterministic seismic hazard analyses are carried out using a logic-tree process found in SELENA and Monte Carlo sampling. Seismic risk is estimated through exposure and physical vulnerability models. Physical vulnerability is determined using vulnerability and fragility functions. However, only discrete vulnerability functions are available in the current version, and continuous fragility functions are planned to be implemented in future versions of the software.

The discussed loss estimation and risk assessment tools indicate the extensive work carried out in this area. Most tools are developed for specific regions, and while these tools are flexible to assess seismic risks globally, a comprehensive seismic risk assessment tool to incorporate the multiple dimensions of vulnerability in a developing country is yet to be developed. The GEM project is promising in this regard, as it is comprehensive in its seismic hazard and risk analysis, and is utilizing a wealth of expertise from around the world that are participating and developing GEM's global hazard, exposure, and vulnerability (of which, fragility curves are essential) components.

2.2 Methods of Deriving Fragility Curves

As mentioned earlier, the method of deriving fragility curves is dependent on the type of damage distribution data source used and the four main types of data sources are post-earthquake surveys, analytical models and simulations, expert-opinions, and a combination of these. Presented below are some noteworthy works that highlight the diversity of approaches available in the development of fragility curves within the four methods and the limitations of these methods are also discussed herein.

2.2.1 Empirical Fragility Curves

Post-earthquake data surveys are used to collect vital information on the impacts of the seismic event on people and infrastructure. This data presents itself as results of a real-life experiment that includes building inventory information and inherent seismic characteristics such as soil-structure interaction, site profile, regional topography, path, and source (Rossetto and Elnashai 2003). Data collection methods vary depending on the experience of the surveyors and the purpose of the surveys, which is usually to assess occupancy safety and estimate losses.

Sabetta et al. (1998) derived empirical fragility curves for three structural classes using six damage levels according to the Medvedev-Sponheuer-Karnik (MSK) macroseismic scale. The data collected through damage survey after the 1980, Irpinia and 1984, Abruzzo earthquakes in Italy were utilized in the methodology. A mean damage index was used to describe the damage and was calculated as a weighted average of the frequencies of each damage level. Fragility curves for each structural type were fitted using a binomial distribution as a function of seismic demand in terms of PGA, Arias Intensity, and effective peak acceleration.

Empirical fragility curves for the Japanese building stock developed by Yamaguchi and Yamazaki (2000) and Murao and Yamazaki (2000) used multiple datasets collected after the 1995 Kobe earthquake. The studies involved the estimation of ground motion measures in terms of PGV using building damage surveys for tax reduction purposes from the Hanshin area and Kobe city. The PGV estimates and building damage data collected from Nishinomiya City (Yamaguchi and Yamazaki 2000) and Nada Ward (Murao and Yamazaki 2000) were used to construct the fragility curves represented by a cumulative lognormal distribution function.

Fragility curves for RC buildings were developed by Rossetto and Elnashai (2003) using a data bank comprising of 340,000 structures from 29 post-earthquake surveys over 19 earthquakes. The data pertains primarily to European seismic events. However, damage statistics from non-European data have been included to extend the range of ground motions. A new damage scale called the homogenised reinforced concrete (HRC) damage scale using a HRC-damage index (DI_{HRC}) is defined to address the variety of structural composition in the data using seven damage limit states. Seismic DI_{HRC} is related to the inter-storey drift ratio ($ISD_{max\%}$) and calibrated using experimental results from dynamic tests on RC bare and infilled frames, and shear wall structural specimens. Ground motion measures of PGA, spectral acceleration and displacement, and inelastic spectral displacement derived from ground motion records or attenuation relationships were used in the study. The empirical fragility curves were fitted with the functional form in Eq. (2.1) that was seen to give the best fit to the observational data (see Figure 2.2).

$$P(d \geq DI_{HRC} | GM) = 1 - \exp(-\alpha \cdot GM^\beta) \quad (2.1)$$

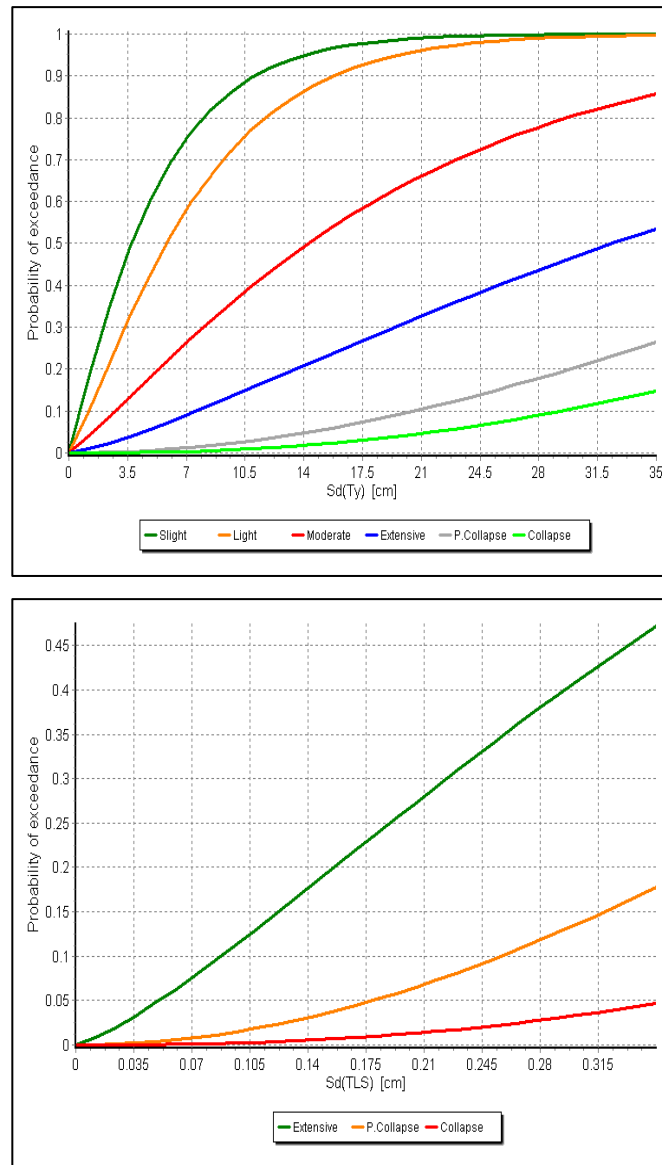


Figure 2.2 Fragility curves of RC buildings as a function of S_d -elastic (above) and S_d -inelastic (below) (Rossetto & Elnashai (2003) found in: Crowley et al. (2011b))

King et al. (2004) and Sarabandi et al. (2004) produced empirical fragility curves for steel moment frame, RC frame, RC shear wall, wood frame, and rehabilitated URM buildings by extending the methodology proposed by Singhal and Kiremidjian (1996b). Fragility curves were derived using empirical data from the 1994 Northridge, California and the 1999 Chi-Chi, Taiwan earthquakes. Data for buildings near the free-field strong motion

recording stations and on similar site conditions were extracted using spatial mapping in a Geographic Information System (GIS). The purpose of only selecting buildings near stations was to reduce the uncertainties from the use of ground motion attenuation relationships. Seismic performance of the each building was defined according to the damage states and performance classification schemes from ATC-13, HAZUS99, FEMA 273/356, and Vision2000. Correlation of building performance to 22 ground motion intensity and building demand measures were explored and fragility curves described using cumulative lognormal distribution functions were developed for ground motion measures that indicated a higher correlation.

Rota et al. (2008a) derived fragility curves for several building typologies characterizing the Italian building stock using a dataset of about 150,000 buildings from post-earthquake surveys. Seismic severity was represented as PGA for each municipality evaluated from attenuation relationships. Structural damage identifying five performance levels were adopted from the European Macroseismic Scale (EMS). Since the dataset was compiled from several different events referring to different damage scales, the authors converted the different scales to a unique one. The buildings in the dataset are classified using RISK-UE building typologies and include several RC and masonry construction types. The fragility curves were represented by a cumulative lognormal distribution that was fitted to the data and some of them are presented in Figure 2.3 as an illustration.

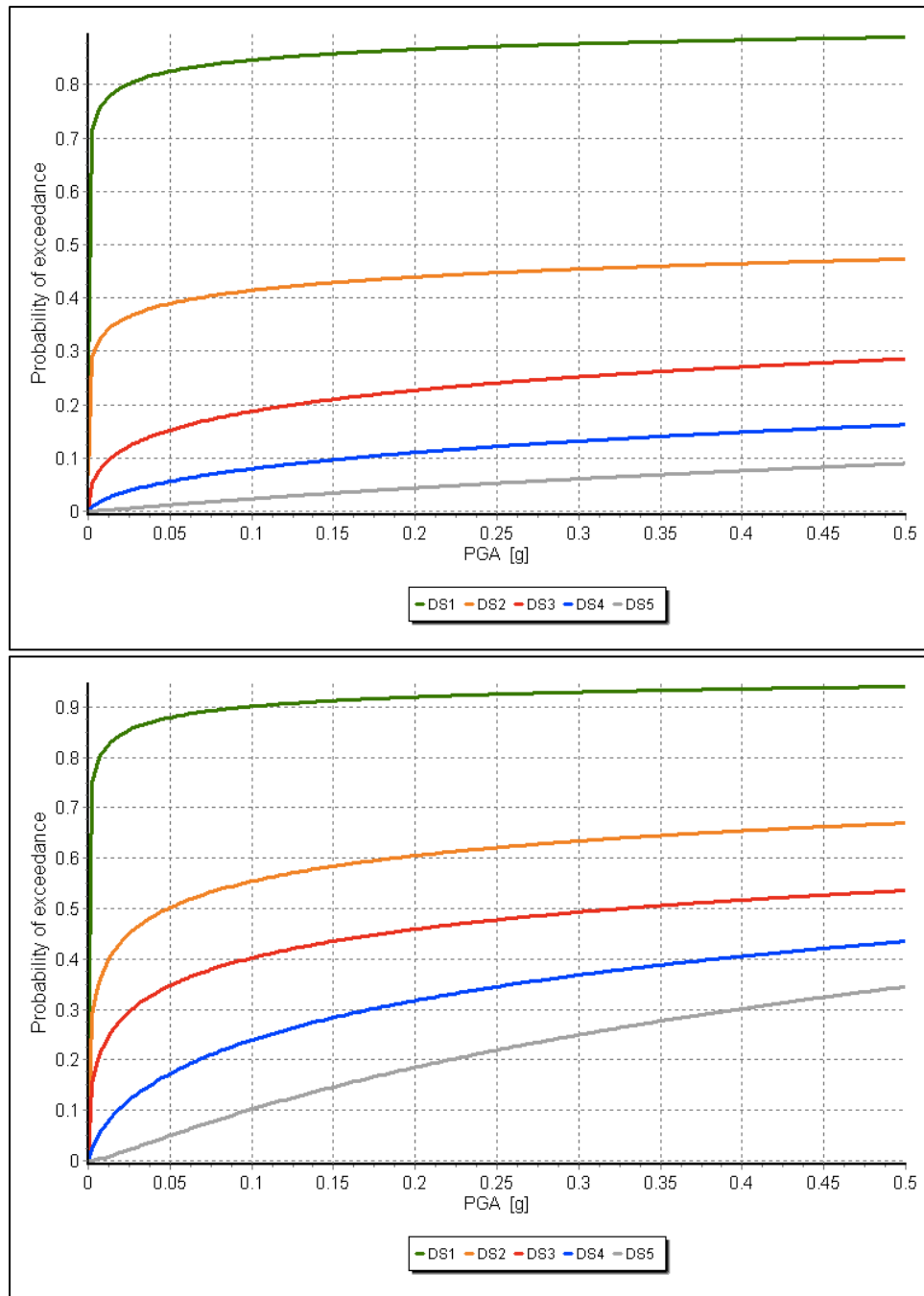


Figure 2.3 Fragility curves for URM building with tie rods and tie beams (above) and without tie rods and tie beams (below) (Rota et al. (2008a) found in: Crowley et al. (2011a))

Colombi et al. (2008) obtained fragility curves for RC, masonry (see Figure 2.4), and hybrid (RC and masonry) buildings, using Italian earthquake

damage data with the purpose of comparing them to curves derived using mechanics. Therefore, a spectral displacement is used to represent seismic demand. Spectral displacement is calculated from attenuation equations using estimated mean period of vibration, which is estimated through an equivalent linearization approach considering a mean limit state ductility for each building type. The damage levels of none, slight, significant, and collapse were used in this work.

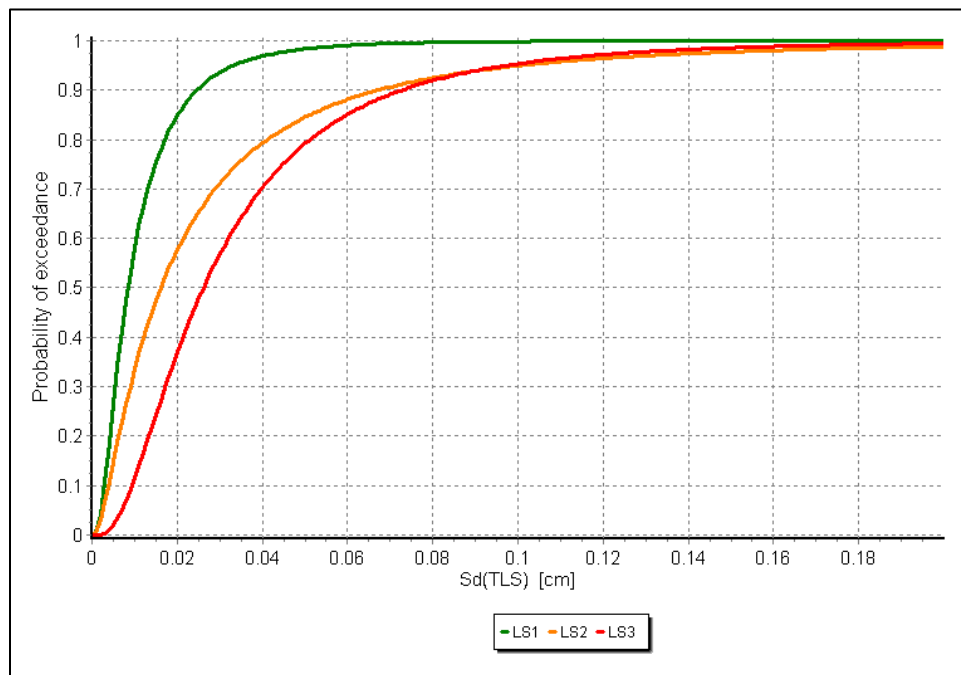


Figure 2.4 Fragility curves for masonry buildings (Colombi et al. (2008) found in: Crowley et al. (2011a))

Empirical fragility curves are limited by the data available. In order to alleviate this limitation, multiple data sets from variety of earthquakes with similar ground conditions are used (Calvi et al. 2006). However, large uncertainties are introduced when data sets from different regions are used since construction practices for similar structural typologies vary greatly. Lack of standardized post-earthquake surveys, and the variety of available and the introduction of new damage scales require extensive

data processing that is usually simplified with several assumptions. Empirical data often include building damage as a result of aftershocks from a single event or earthquake phenomena besides ground shaking (Rossetto and Elnashai 2003). Issues resulting from data collection and use of multiple data sets require reliability and uncertainty analysis to be integrated in empirical fragility analyses.

2.2.2 Analytical Fragility Curves

Data for analytical fragility curves is compiled through seismic simulation of structural analysis models using idealized and simplified structural representations. The analytical method is favourable in cases where there is a lack of data on specific structural typologies or where particular structural response is of interest. The analytical procedures used in assessing structural response to seismic demands vary in complexity from linear static to non-linear dynamic analysis (Rossetto and Elnashai 2003) and some of the major studies are presented below.

Fragility curves for low-, mid-, and high-rise RC frames were developed by Singhal (1996a) based on non-linear dynamic analysis of structures. Ground motion represented by spectral acceleration was generated using an autoregressive moving average (ARMA) model and five damage levels characterized using Park-Ang's global index. Input variables for non-linear dynamic analysis were obtained through Monte Carlo simulation and sampled using Latin hypercube sampling method. Fragility curves were fitted to the damage distributions from the analyses using lognormal distribution functions.

An analytical procedure to derive displacement-based fragility curves for RC structures was applied by Rossetto and Elnashai (2005). Combined use of adaptive pushover analysis and capacity spectrum method avoids

repetition of analyses for increasing ground motions and reduces computational effort. The HRC damage scale index (DI_{HRC}) developed by Rossetto and Elnashai (2003) is used to define the damage levels used in the fragility curves. The procedure consists of four steps: system definition, ground motion definition, model evaluation, and statistical processing of analysis results. A structural archetype is selected to represent the material, configuration, and seismic resistance characteristics of the building class being examined. Seismic records are selected for the analyses that are consistent with the damage states defined. The structural model is evaluated using adaptive pushover analysis that updates the applied load distribution at each load increment. A modified Capacity Spectrum Method is adopted to assess the seismic performance where inelastic seismic demand and building capacity curves are plotted in S_a - S_d coordinates. Performance points at the intersection of the demand and capacity curves are used to determine the damage state of the building. The results of the model evaluation are used to construct response surfaces from which statistical analysis are carried out to determine the proportion of buildings exceeding the HRC damage states and are plotted against the spectral displacements. The fragility curves are then developed using the points and are characterized using parameters of a lognormal cumulative probability function. The methodology was applied to a three-storey infilled RC frame (see Figure 2.5) and was shown to compare reasonably well with observational data and empirical curves.

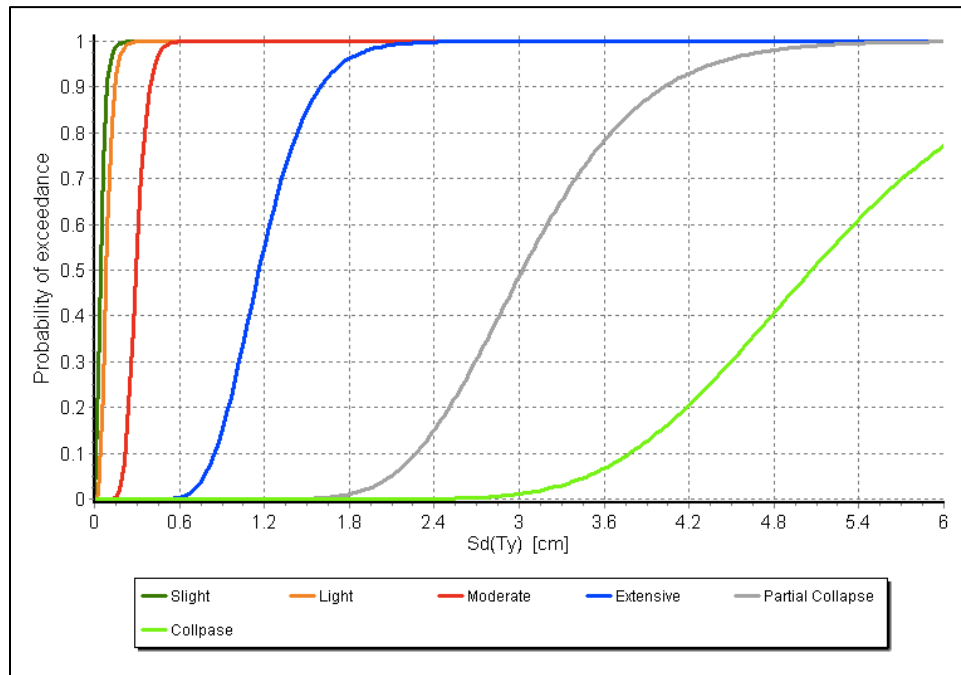


Figure 2.5 Fragility curves for low rise infilled RC frames (Rossetto and Elnashai (2005) found in: Crowley et al. (2011b))

Erberik (2008) developed fragility curves to assess the in-plane failure modes for 120 classes of masonry buildings representing the Turkish masonry building stock. The buildings were classified using structural parameters that influence seismic performance such as the number of stories, load bearing wall material, regularity in plan, and the arrangement of walls. Two limit states considered correspond to the damage states, which are the base shear capacity at the threshold of linear elastic behavior and the ultimate base shear capacity of the specific masonry structure. Capacity and demand curves from pushover and time-history analyses, respectively, were used to derive fragility curves for the masonry buildings. The fragility curves indicated that the number of stories and wall material strength significantly influenced the damage state probabilities.

Fragility curves relate a single ground motion parameter to structural damage; however, this relationship can be extended to two parameters in

a fragility surface. Omine et al. (2008) used PGA and PGV to develop fragility surfaces and found that PGV is better for expressing fragility for severe damage while both PGA and PGV are useful at lower damage levels. Seyedi et al. (2010) proposed a methodology for developing fragility surfaces utilizing the spectral displacement at the first and second natural periods of an eight-storey regular RC frame structure as the ground motion parameters. The ground motion parameters were selected based on the strength of their correlation to the inter-storey drift ratio (ISDR), which is used to assess structural damage. In addition, the DI_{HRC} correlation to ISDR proposed by Rossetto and Elnashai (2003) was selected to define the damage levels. The fragility surfaces were described by parameters of an adapted lognormal cumulative distribution and the surfaces can be converted to fragility curves for comparison purposes by projecting the surface onto either ground motion parameter's plane (spectral displacement at the first or second natural period) (see Figure 2.6). The advantage of fragility surfaces over fragility curves is the incorporation of the variability as a result of other ground motion characteristics and this can be beneficial when assessing the risks from different types of seismic events.

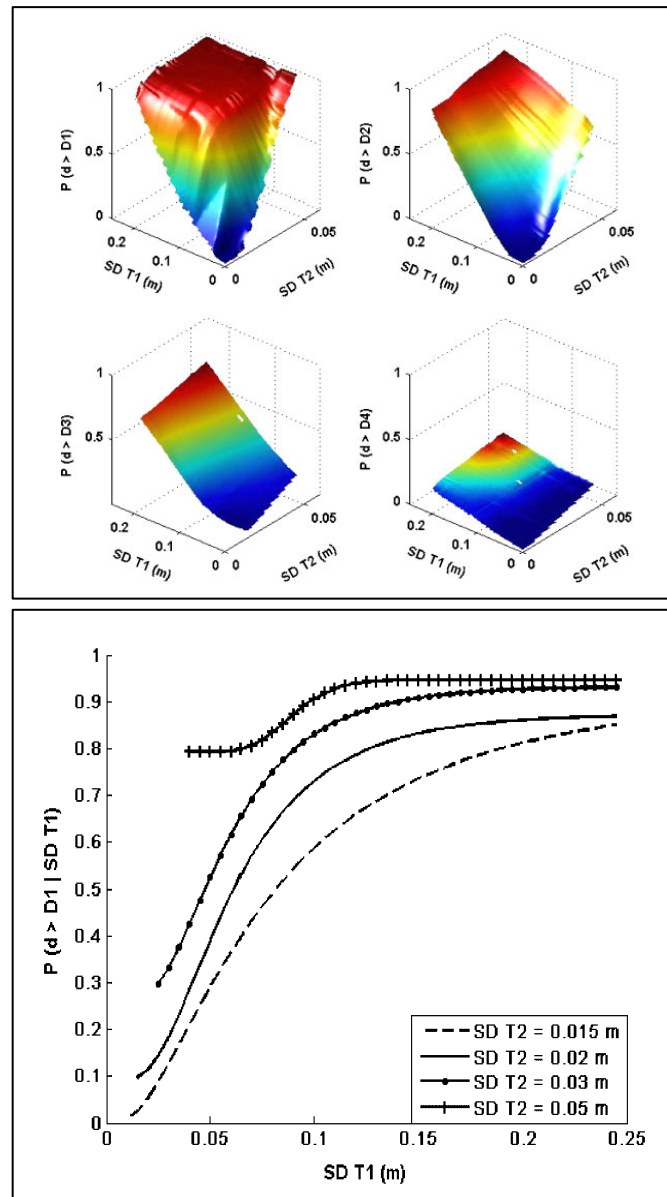


Figure 2.6 Illustration of fragility surfaces (above) and projected fragility curve (below) (Seyedi et al. 2010)

Rota et al. (2010) developed an analytical approach to derive fragility curves for masonry structures. The methodology allows a prototype to represent the class of building with similar structural characteristics whose mechanical properties can be obtained through Monte Carlo simulations using realistic ranges of variation that were determined from experimental

tests. Probability density functions of each damage state were obtained from nonlinear static pushover analyses. Time history analyses were carried out to determine the probability density function of the displacement demands on the structure from seismic forces. The cumulative distribution function of the displacement demands was determined and convolved with the probability density functions of the damage states (i.e. structural capacity) to derive the fragility points which were fitted with lognormal distributions to obtain the analytical fragility curves (see Figure 2.7).

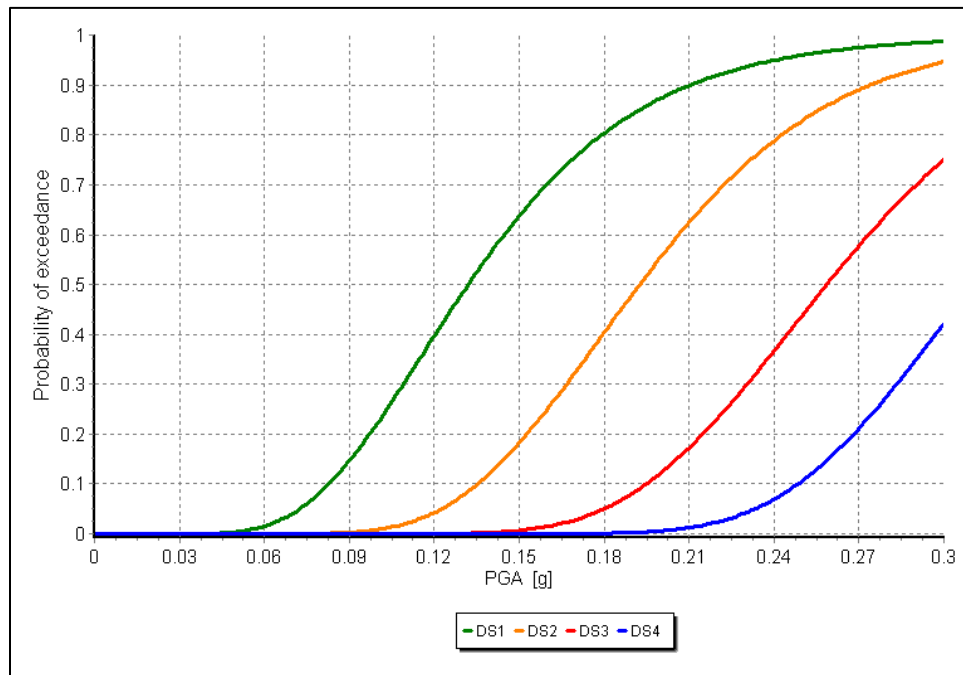


Figure 2.7 Fragility curve for 3-storey masonry building (Rota et al. (2010) found in: Crowley et al. (2011a))

Displacement-based fragility functions of URM buildings made of solid brick derived using a nonlinear static procedure was presented in Ahmad et al. (2010a). Buildings were idealized as a single degree-of-freedom (SDOF) representing their mechanical properties such as the secant vibration period, displacement energy, displacement capacity, and energy

dissipation capability. Monte Carlo simulations were carried out to account for the geometrical and material properties in the building stock and the uncertainties introduced by actual seismic loading. Building capacity was determined using a probabilistic displacement-based earthquake loss assessment approach developed for RC buildings by Crowley et al. (2004) and extended to masonry structures by Ahmad et al. (2010b). Seismic demand was obtained by randomly generating a 5% damped linear displacement response spectra. Probability of exceedance for a damage state was estimated by the proportion of buildings whose capacities were less than the demand over the total population of the building type. The probability of exceedance is plotted against the median displacement demand and the points were fitted using lognormal distribution functions.

Model idealization, choice of analytical method, and seismic hazard and damage models add bias in the fragility assessment. Soil-structure interaction, non-structural elements and small structural details are often also not included in the models. The use of non-linear dynamic structural analysis can also lead to numerical rather than structural failure of the model when subject to large seismic demands (Rossetto and Elnashai 2003). These modeling complications have been addressed with the development of complex analysis software such as *OpenSees* that allow more detailed analysis of the structures. However, the computational effort required in this method is still significant for seismic risk assessments involving many structural typologies.

2.2.3 Expert-Opinion Fragility Curves

Expert-opinion or judgment-based methods rely on estimates provided by earthquake engineering experts on potential building damage distributions when subjected to seismic events of different intensities. Estimates are

collected through the use of questionnaire surveys or Delphi methods (ATC 1985; Jaiswal and Wald 2009) that also inquire into the structural characteristics influencing the vulnerability (Vamvatsikos et al. 2010). Fragility curves are obtained by fitting probability distribution functions to the expert's estimates to relate the extent of damage to ground motion parameters.

A joint study on the fragility of buildings was carried out by National Center for Earthquake Engineering Research (NCEER) and the Applied Technology Council (ATC) (Anagnos et al. 1995) where improvements and modifications to the ATC-13 (1985) were identified and developed. The study developed fragility curves for 40 building classes by fitting lognormal functions to expert opinions provided in the ATC-13 (1985). The experts provided the probability of achieving the none, slight, light, moderate, heavy, major, and destroyed damage states, given the seismic intensity in terms of modified Mercalli intensity (MMI). The damage states were expressed as damage factors relating repair costs to structural damage, which is inconsistent with the definition of fragility functions. Standard damage state definitions for all building types in terms of repair costs is problematic since repair costs for the same damage state might be different for the building classes (Anagnos et al. 1995). Nevertheless, the study highlights the use of expert opinions in developing fragility curves.

The WHE-PAGER project is a joint undertaking by WHE of EERI and the PAGER project by USGS (D'Ayala et al. 2010). Under the WHE-PAGER project, estimates of building inventory of residential types and probability of collapse for given seismic intensities in terms of MMI and PGA were collected from experts from over 30 countries (Jaiswal et al. 2011). Jaiswal

et al. (2011) derived fragility functions by fitting the expert estimates provided for the WHE-PAGER project using a three parameter power function. A beta distribution was used to model the uncertainty in the collapse probabilities provided by the experts and the resulting beta curve estimates collapse fragility at intermediate intensities and extend the fragility curves beyond the shaking intensity range. The study also provides a hybrid extension to the method using a procedure to update the curves using Bayesian principles as new field data becomes available.

The fragility curve derivations using expert estimates are subjective to the experience of the experts involved, and the level of conservatism present in their judgment cannot be evaluated. Regional structural types and construction practices are intrinsic to the experts' opinions, therefore, vulnerability assessments using such data could only be applied to similar structures (Jaiswal et al. 2011; Rossetto and Elnashai 2003). Expert opinions are reasonable as first estimates. However, they require reliability analysis to assess and quantify the uncertainty for seismic risk assessment purposes.

2.2.4 Hybrid Fragility Curves

Results from analytical models can supplement insufficient empirical data in a hybrid approach to develop fragility curves encompassing all seismic intensities. The hybrid approach attempts to reduce the computational effort of analytical modeling and compensates for the subjective bias of expert judgment method (Kappos et al. 2006). Hybrid methods also incorporate results from large-scale experimental tests that can reasonably mimic real structural response. However, more often they are used for verification only, as such tests are costly and time consuming (Rossetto and Elnashai 2003).

Further to their earlier work on developing analytical fragility curves (Singhal and Kiremidjian 1996a), Singhal & Kiremidjian (1998) presented a method to update fragility curves using damage data from earthquakes through a Bayesian statistical analysis method. The Park and Ang damage index at specified ground motion intervals followed a lognormal probability distribution shown in Singhal and Kiremidjian (1996a) whose parameters were treated as prior estimates in the Bayesian analysis for each ground motion level. Uncertainty arising from the use of finite data set was addressed through confidence bounds around the median fragility curves. This methodology was applied using data from the January 17, 1994, Northridge earthquake in California. Updated fragility curves were found to have little difference to the earlier work and this was attributed to the small sample size.

Kappos et al. (2006; 2010) developed a hybrid method to derive fragility curves by combining statistical data and analytical procedures whose data are unavailable. The curves were derived for RC and URM building types in terms of PGA and S_d . Several configurations of RC building types that were representative of buildings in Greece and southern European countries in terms of their structural system, height, and seismic design code level were analyzed as 2D structures using incremental dynamic analysis (IDA). Loss values in data from the 1978 Thessaloniki earthquake in Greece were correlated to structural damage indices and fragility curves for five damage states were established assuming a lognormal distribution. Inelastic static method using the capacity spectrum approach and data from the 1978 Thessaloniki as well as from the 1995 Aegion events in Greece were utilized to develop fragility curves. Different analytical approaches were required as inelastic time-history analysis for URM buildings was found not to be as straightforward in comparison to RC

buildings. Kappos et al. (2006) illustrates the use of empirical data in calibrating as well as extending analytically derived fragility curves.

The hybrid method addresses the limitations of the empirical and analytical methods, however this method also has some drawbacks. Aleatory uncertainty arising from the natural variability of earthquakes is present in the ground motion data in addition to the epistemic uncertainty related to the lack of knowledge or information, which is present in the empirical damage data. Both these categories of uncertainties add to the uncertainty involved in analytical models resulting in significant dispersion in the risk assessment models whereby requiring reliability and sensitivity analysis. Furthermore, the idealization of building models within the analytical method ignores the variation in construction techniques and materials that are inherently considered in the empirical data. Therefore the hybrid method incorporating damage datasets collected in areas of significant structural diversity should be used with caution.

2.3 Existing Fragility Curves for Homes in Developing Countries

Vulnerable homes are ubiquitous around the developing world and many of the earthquake-prone countries fall within this category. Earthquakes in Iran, Pakistan, Indonesia, and most recently in Haiti caused widespread devastation in terms of lives lost and structural damage as a result of poorly built houses. The fragilities of diverse construction types within developing countries need to be examined in order to assess seismic risks and develop disaster mitigation and prevention programs. As a consequence of recent catastrophes, there has been an attempt to understand the fragility of buildings in developing countries, some of which are presented here.

Clarke (2010) carried out fragility analysis of single story URM homes, which make up two-thirds of Trinidad and Tobago's building stock. Analytical fragility curves were derived using the incremental dynamic analysis method (IDA) on 3-dimensional models of a typical URM residential structure whose lateral loads are resisted by shear walls. Four damage states of slight, moderate, extensive, and complete as defined by HAZUS-MH MR4 (FEMA 2003) using story drift ratio were employed to assess in-plane response of the walls. The out-of-plane dynamic instability was observed by comparing the calculated displacement to the displacement capacity using an energy approach. The ground motion parameter selected for the analysis was S_a , and the fragility function was expressed by the cumulative lognormal distribution function. The derived fragility curves revealed a higher probability of exceedance for the dynamic instability limit state and this was explained by the slenderness and high flexibility of the walls, and the lack of cross-walls also contributed to this failure mechanism.

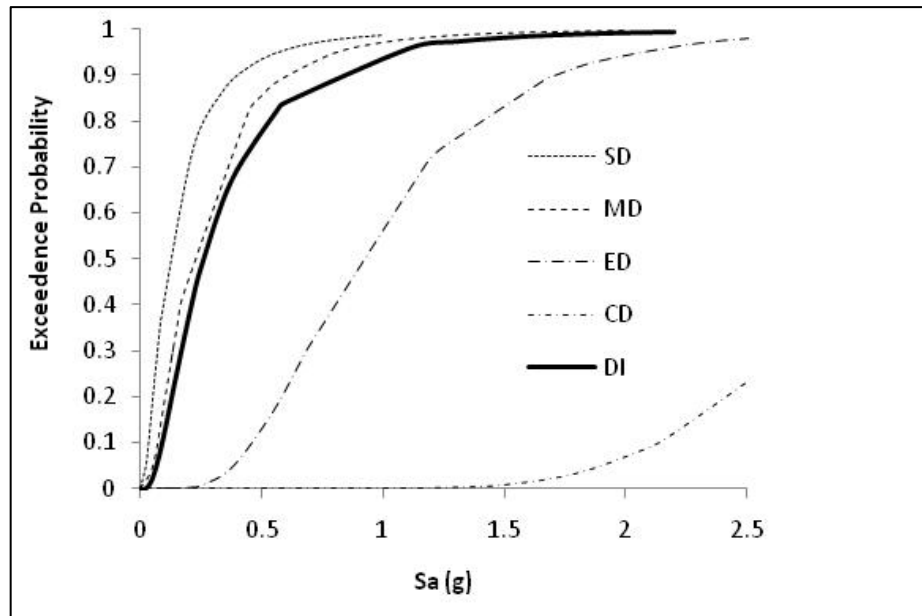


Figure 2.8 Fragility curves for typical URM structures in Trinidad & Tobago (Clarke 2010)

As in other developing countries, URM homes are also commonly found in Iran and their vulnerability has been exposed during past earthquakes. Bakhshi and Karimi (2006) have derived fragility curves to assess seismic performance of masonry structures with and without seismic provisions. The ground motion parameter selected for the procedure was the Cumulative Absolute Velocity (CAV) and a total of twelve earthquake records were used for ground motion input to account for different site conditions. Material uncertainty was accounted for by adopting probabilistic distributions for the parameters and generating samples through the Monte Carlo Simulation. Nonlinear dynamic analyses were carried out in IDARC 2D v4.0 program where the masonry walls were modeled as shear walls with masonry material properties. Fragility curves were derived for five damage states defined using the Park and Ang damage index through 450 nonlinear analyses for one- and three-story URM buildings with and without ties, and one-story reinforced masonry buildings. The fragility curves exposed the benefits of seismic provisions

as the probability of severe damage and collapse for buildings with ties and the probability of all damage states for the reinforced single story building were insignificant.

As part of a loss assessment methodology, Moharram et al. (2008b) derived fragility curves for non-ductile RC and URM buildings that are commonly found in the Greater Cairo area in Egypt. The typical RC building that was analyzed using the capacity spectrum method consisted of non-ductile, masonry in-filled RC frames that were not designed for seismic forces. Results from earlier work by Moharram et al. (2008a) where representative low-, medium-, and high-rise buildings were designed and analyzed were used in this methodology. The main material parameters were treated as random variables using probability density functions to address the uncertainty in material properties and samples were generated using Latin Hypercube procedure. Displacement-Based Earthquake Loss Assessment (DBELA) approach by Bommer and Crowley (2006) was used to treat the ground motion variability to derive fragility curves for four limit states defined in terms of inter-story drift ratios. Fragility curves for URM structures were derived using capacity and demand curves for the 'URM bearing wall model' as set out in the HAZUS 1999 methodology.

Earthquakes have caused widespread devastation in Latin and South American developing countries as a result of vulnerable residential dwellings. Much work has been done to develop retrofitting techniques and reinforcing existing vulnerable homes to reduce and prevent seismic damage in South American countries (Blondet et al. 2011; Mayorca and Meguro 2004). Ruiz-Garcia and Negrete (2009) produced fragility curves for CM walls that are used to resist lateral loads in home construction that

is popular in Latin-America. The data used in this study was obtained from experimental results of 118 full-scale or nearly full-scale CM wall specimens tested under cyclic loading in Mexico, Chile, Peru, Venezuela, and Colombia. Drift-based fragility curves for two damage states were derived; Damage State 1 would suffice minor repairs to close cracks closer than 0.1mm and Damage State 2 was described by X-shaped cracking of about 5mm, concrete crushing at the base of tie-columns and hairline cracking along the height of the columns. The empirical data was fit using the cumulative lognormal distribution and the study accounted for uncertainty due to specimen-to-specimen variability, limited experimental data, mechanical properties of masonry, and geometric configuration of the wall specimens. Influences from type of masonry-brick used, horizontal steel reinforcement, and vertical compressive stress were also investigated. The fragility curves were also used to define and calibrate drift-limits in relation to damage-based limit states for CM structures for design codes.

Fragility curves for single-storey adobe homes located in Cusco, Peru were developed by Tarque et al. (2010) by comparing the displacement capacity of the buildings to the seismic demand as outlined in the DBELA methodology (Crowley et al. 2004). An artificial sample of 1,000 buildings was generated using Monte Carlo simulation by using statistics and probability density functions of geometrical properties from an earlier building survey carried out in Cusco. Building capacities were assessed in terms of their in-plane and out-of-plane wall displacement capacity, and seismic demand was represented by the displacement response spectra. The probability of exceedance was calculated by comparing the capacity with the demand, and the resulting fragility curves indicated the

vulnerability of adobe homes where complete overturning of walls from out-of-plane failure for seismic PGA higher than 0.25g was highly probable.

There are far less works available on fragility curves for buildings in developing countries, and even less on single-storey homes, which are the building blocks of socioeconomic stability. Many of the fragility models for dwellings in developing countries have applied the analytical method, as empirical data is scarce due to the lack of local resources to establish data collection procedures after seismic events.

3 Derivation of Empirical Fragility Curves

3.1 General

Fragility curves describe the probability of reaching or exceeding different damage states at given ground motion intensities. Empirical fragility curves make use of damage distribution data collected through post-earthquake damage surveys. The damage is categorized through broad terms such as “light”, “moderate”, “collapse” and other similar labels. Depending on the damage scale used during the surveys, these terms are defined using physical damage descriptions. Ground motion parameters are selected and applied to fragility studies using attenuation relationships. The damage distribution data is processed to develop damage probability matrices (DPMs) that are statistically analyzed to create fragility curves and are described using analytical functions. The advancement and application of GPS technology in post-earthquake surveying allows the recording of damage data geospatially in a GIS format that has been utilized together with USGS ShakeMaps (in GIS format) in this study to derive damage probability matrices and empirical fragility curves.

3.2 Post-earthquake Data Collection

Data collected from earthquakes that have caused significant damage provide researchers with the opportunity to understand the performance of different types of structures. Rehabilitated and seismic resistant structures are *tested* during seismic events and their performances can be investigated with the aim of providing improvements or developing design codes. Private NGOs and government authorities collect post-earthquake damage data for several different purposes, and the extent of data collected varies accordingly. Post-earthquake reconnaissance or field

surveys collect data to assess the performance of infrastructure, evaluate societal impacts, and study the effects of other secondary phenomena such as liquefaction, landslides and tsunamis (EERI 1996; Rossetto and Elnashai 2003). Seismic damage data is also collected to evaluate the need for relief efforts, loss estimation, earthquake insurance and government statistics purposes. Timelines within which data is collected also vary depending on the purpose. However, for infrastructure performance and relief needs assessment, damage investigations and assessments often take place within days to several weeks of an earthquake to secure perishable data and ensure timely humanitarian response. Damage data is the first component in the derivation of a fragility curve that essentially determines the method to be used for deriving fragility curves. Therefore, empirical method is utilized in the case of damage data collected through post-earthquake surveys.

Damage data collected after earthquakes is often limited and assumptions have to be made for the data to be utilized in the derivation of empirical fragility curves. Statistical treatment of the data requires a sufficiently large sample size to make meaningful inferences about the building population. The damage surveys are often inconsistent in their reporting of damage and require judgment that is subjective to the format of the survey and the experience of the surveyor. Damage data is also generally collected in the most affected areas; hence it does not cover a large range of ground motions.

Combining data from several earthquakes improves the statistical sample and ground motion coverage, however it increases the inconsistencies related to the survey format and subjectivity of the surveyor. The details collected in post-earthquake field surveys are different as they are conducted by different agencies for their specific purposes. Furthermore,

fragility curves developed using data from several post-earthquake surveys in different regions implicitly include the uncertainty from the differences in construction practice and detailing (Goretti and Di Pasquale 2002; Rossetto and Elnashai 2003). The ideal data set would be one that is collected by experienced engineers immediately after the earthquake using a standardized reporting format with clear damage level descriptions. The data should be collected over a large area with similar soil conditions in order to cover a sufficient range of ground motion intensities from a single earthquake (Rossetto and Elnashai 2003; Rota et al. 2008b). However, these criteria are quite unrealistic in general and particularly in the case of developing countries with limited resources. Therefore, any reasonable damage data available should be utilized with sound assumptions, and appropriate statistical methods applied to account for the uncertainty and reliability of the empirical fragility curves.

3.3 Damage Classification

The second component in the derivation of empirical fragility curves involves the classification and description of structure's damage levels indicated in the empirical data. Several classifications of building damage have been developed and they vary in extent and detail depending on: the aim of damage collection; the discipline of the personnel conducting the collection; and the time of collection either as pre-event or post-event (Goretti and Di Pasquale 2002; Rota et al. 2008b). Damage classifications of structural typologies are applied in vulnerability and fragility assessments and they are categorized generally as economic damage, apparent or physical damage, and mechanical damage (FEMA 2012b; Rota et al. 2008b). Apparent or physical damage descriptions are most commonly used in post-earthquake surveys as they are visual and they can be recorded. The structural, and in some cases non-structural

damage classifications adopted in the surveys are generally applied in the derivation of fragility curves, however, the damage classification is often modified to suit the derivation of empirical fragility curves.

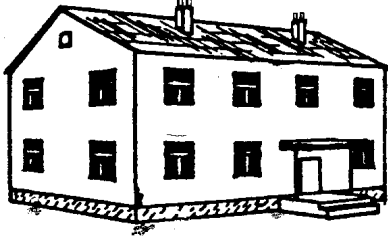
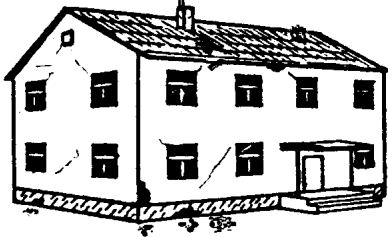


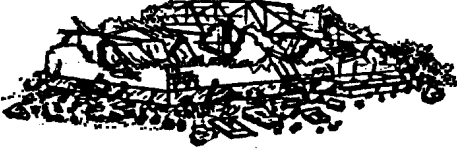
Apparent or physical damage classifications that are used in damage surveys or fragility curves include clear descriptions of the damage sustained within each category. The damage descriptions include extent of cracking, material deterioration, local and global displacements, and deformation of structural members (Grünthal 1998; Rota et al. 2008b). These damage descriptions also vary according to the construction material. Some of the main damage classifications that have been used in damage assessments and subsequently in fragility and vulnerability assessments include: HAZUS, EMS-98, and MSK-64. The US-based hazard assessment framework and software, HAZUS, provides damage descriptions for 16 building types using four general damage states: Slight, Moderate, Extensive, and Collapse (FEMA 2012b). The damage states are also used within the framework to develop fragility curves. European Macroseismic Scale (Grünthal 1998) provides a damage scale that uses five damage states to generally describe damage of masonry (see Table 3.1) and reinforced concrete structures. Damage classification provided in the MSK-64 Seismic Intensity Scale provides descriptions for five levels of damage: slight, moderate, heavy, destruction, and total damage. These classifications provide broad descriptions of damage and do not address regional variations in construction details and therefore it is necessary to adapt them in order to adequately describe the damage.

Empirical fragility curve derivations rely on post-earthquake surveys that are carried out in different locations and times, and the survey methods and forms vary accordingly, therefore, when data from different earthquakes are combined, they need to be converted or calibrated to a

single damage scale. Colombi et al. (2008) used slight damage, significant damage, and collapse as damage states that are defined in Italian seismic design and assessment regulations to develop fragility curves. Various assumptions were then made to relate the damage reported in the post-earthquake surveys to these damage states. Similarly, Rota et al. (2008a) developed fragility curves by converting the damage levels used in four different surveys to a single damage scale based on EMS-98, described above.

Building damage classifications generally exist for engineered and well-defined structure types. However, most vulnerable structures in developing countries are non-engineered and incorporate locally specific construction techniques and materials. This reality, in addition to the variety of non-engineered constructions, makes it extremely difficult to adopt standard definitions of damage states for structures in developing countries. The idea of a homogenized damage scale for a composition of structure types as one developed by Rossetto and Elnashai (2003) is appealing, however, such a task either requires a large data set (which is not always available) or a good understanding of the various non-engineered structures present in the regions of interest. Hill and Rossetto (2008) critically evaluated several damage scales with the intent of its application in earthquake loss modeling in Europe. All damage scales considered were based on well defined structural types found in developed countries and the applicability of even the most comprehensive damage scale in another developed country was found to be limited. Therefore, damage classification using damage scales calibrated for developed countries should be used with caution in seismic fragility assessment for their developing counterparts.

Table 3.1 EMS-98 Damage descriptions for masonry buildings (Grünthal 1998)

Classification of damage to masonry buildings	
	<p>Grade 1: Negligible to slight damage (no structural damage, slight non-structural damage)</p> <p>Hair-line cracks in very few walls. Fall of small pieces of plaster only. Fall of loose stones from upper parts of buildings in very few cases.</p>
	<p>Grade 2: Moderate damage (slight structural damage, moderate non-structural damage)</p> <p>Cracks in many walls. Fall of fairly large pieces of plaster. Partial collapse of chimneys.</p>
	<p>Grade 3: Substantial to heavy damage (moderate structural damage, heavy non-structural damage)</p> <p>Large and extensive cracks in most walls. Roof tiles detach. Chimneys fracture at the roof line; failure of individual non-structural elements (partitions, gable walls).</p>
	<p>Grade 4: Very heavy damage (heavy structural damage, very heavy non-structural damage)</p> <p>Serious failure of walls; partial structural failure of roofs and floors.</p>
	<p>Grade 5: Destruction (very heavy structural damage)</p> <p>Total or near total collapse.</p>

The large variety of non-engineered structural types also makes it extremely difficult to develop a standard damage classification that will address the entire building stock of developing countries. Damage characteristics and mechanisms vary according to the construction materials and structural details, therefore, descriptions for the damage states may not be valid for all building types (Rota et al. 2008b). Hence, it is important for seismic-prone developing countries to examine its building stocks individually and develop unique descriptive damage classification schemes or modify existing schemes to ensure applicability in developing countries. The damage scale developed or adopted should provide adequate descriptions of damage and failure mechanisms for each damage level enabling a straightforward identification during post-earthquake surveys (Hill and Rossetto 2008).

3.4 Ground Motion Parameters and USGS ShakeMaps

The final component required in the derivation of fragility curves is the selection of ground motion parameters that indicate the severity of ground shaking during an earthquake. The severity of ground shaking related to an earthquake is expressed using macroseismic intensity scales or ground motion parameters. Macroseismic intensity scales measure the severity of ground shaking based on observed or felt effects of the earthquake on the earth's surface, humans, and structures. Intensity scales such as Modified Mercalli Intensity (MMI), Medvedev-Sponheuer-Karnik (MSK81) and European Macroseismic Scale (EMS-98) include twelve levels where each level is identified based on detailed observations of human and animal reactions, and physical damages.

Ground motion parameters on the other hand express the severity of ground shaking measured using instrumental recordings or through analyses of recorded accelerograms. Structural response and damage is caused directly by ground shaking during earthquakes as well as other phenomena such as landslides and liquefaction that occur as result of ground shaking. Therefore, ground motion parameters are a better choice for developing damage-ground motion relationships. Macroseismic intensity scales have been used in risk assessments; however, their use in fragility curves is limited for several reasons. Intensity scales are not continuous and fragility curves require the use of continuous variables that can be obtained through attenuation equations (Rota et al. 2008a) also known as ground motion prediction equations (GMPE) that relate the ground shaking parameter to the magnitude, distance, and site of the earthquake. In addition, empirical fragility curves relate levels of damage to ground shaking using post-earthquake damage surveys and intensity scales are also based on damage observations after the earthquakes, hence, developing probabilistic relationships between the two is redundant. Furthermore, macroseismic intensity scales are subjective as human and structural responses can vary based on sensitivity and predisposed vulnerability, and the responses could be very different at similar levels of ground shaking. However, the intent is not to completely disregard the usefulness of macroseismic intensity scales, but rather to acknowledge the drawbacks when utilizing such scales for fragility curves. Several relationships between MMI and ground motion parameters have been developed for different regions (Linkimer 2008; Tselentis and Danciu 2008; Wald et al. 1999) to accommodate for regions that lack sufficient seismic recording instruments.

A variety of ground motion parameters have been adopted in the derivation of fragility curves, however, the most commonly applied are the peak ground motion values and spectral ordinates. Typically, ground motion parameters are evaluated using ground motion records where available, otherwise appropriate attenuation relationships are selected depending on the site location and seismic fault mechanism. Colombi et al. (2008) and Rota et al. (2008a) have used PGA that was derived based on an attenuation relationship developed by Sabetta and Pugliese (1987) assuming rock site conditions and using the event magnitude and distance to site as inputs. Rota et al. (2008a) also assessed the influence of the evaluated PGA using the attenuation relationship on the lognormal fragility curves and the results indicated that effect on the fragility curves was limited despite significant scatter in PGA. Fragility curves derived by Rossetto and Elnashai (2003) utilized a large dataset from several seismic events that required the use of several region-specific attenuation relationships to evaluate PGA and spectral acceleration values. These works highlight the need for careful selection of attenuation relationships to represent the regional site specifications and seismic fault characteristics.

Evaluation of appropriate attenuation relationships to estimate the severity of ground motion experienced by an entire city or municipality is tedious and the fact that a municipality depending on its size, could have experienced several levels of ground shaking is understandably ignored. However, with the advancement in technology, damage surveys can be carried out using Global Positioning System (GPS) devices to record the spatial location of buildings during post-earthquake surveys and enables the data to be presented in Geographic Information System (GIS) format. Therefore, data in this format can be used to estimate the exact level of

ground shaking experience by a building depending on its distance from the epicenter, and the rock and soil conditions at the site; however, this approach is also quite cumbersome for the purpose of deriving fragility curves.

USGS provides a feasible option through its catalogue of ground shaking maps referred to as *ShakeMaps* (Wald et al. 1999; 2006) that are available on the USGS website (<http://earthquake.usgs.gov/earthquakes/shakemap>) and have been used in this study. A ShakeMap is a near real-time map of ground motion and shaking intensity produced by an earthquake. ShakeMaps were originally developed for southern California, U.S., however, the program was extended in 2004 to produce *Global ShakeMaps* (Allen et al. 2008; Worden et al. 2010) for earthquakes occurring anywhere in the world. The program also provided a set of ShakeMaps for historical earthquakes since 1973 where significant human populations were exposed.

The ShakeMaps are produced in terms of: PGA; PGV; 5% critically damped pseudo-spectral acceleration (PSA) at periods of 0.3s, 1s, and 3s (PSA); and macroseismic intensity. The methodology used to produce the maps involves a systematic process to combine data acquired from seismic recording stations, where available with site geology and ground motion attenuation for the distance to the epicenter of causative fault. A uniformly spaced grid of “phantom” stations are created and peak ground motions are calculated for each station using Ground Motion Prediction Equations (GMPE) based on the magnitude and distance from the epicenter of causative fault. Three tectonic regimes are considered when selecting the GMPEs including shallow active tectonic crust, subduction zone (intraplate and intraslab), and stable continent. Site corrections and amplification factors are then applied to the stations based on geological

or topographic maps and contouring is carried out using the grid stations. The ShakeMaps are eventually refined to reflect the available data on the geometry and dimensions of the fault. ShakeMaps that are produced in near real time apply an automatic earthquake discrimination scheme leading to an appropriate selection of the GMPEs while manual revisions are applied to the maps in the case of complex earthquake scenarios or as more accurate and recent site information becomes available.

Many parts of the world lack sufficient seismic recording stations, therefore, observed or felt macroseismic intensities such as MMI are used to measure the severity of ground shaking. Similarly, the ShakeMap methodology has adopted the use of MMI in two ways. Firstly, where there are adequate seismic recording stations, the peak ground motion values are converted to MMI and then contoured. Secondly, in areas that lack ground motion recordings, macroseismic observations are obtained through various sources including USGS's *Did you Feel It?* (DYFI?) program; the observations are added to the ShakeMap intensity map. In addition, the intensity values are converted to peak ground motions using the inverted equations of Wald et al. (1999) and are used in the peak ground motion maps. A subsequent revision to this ground-motion and intensity interpolation scheme allows the combined use (through a weighted approach) of: direct observations of measured ground motions or reported intensities; converted observations (intensity to ground motion or vice versa); and estimated ground motions and intensities from GMPEs or intensity prediction equations (IPE) (Worden et al. 2010).

The ShakeMap program has developed algorithms to assess the uncertainty associated with the spatial variability of peak ground motions near recording stations, and the uncertainty associated with GMPEs used for interpolation, quantitatively and qualitatively. The algorithm produces a

quantitative variance associated with each point of calculated peak ground motion value and a qualitative letter grading is applied to describe the uncertainty of the entire ShakeMap (see Figure 3.1). Uncertainty assessments of ShakeMaps ascertain a level of confidence with the use of a ShakeMap and allow the uncertainties to be accounted for in risk assessments and loss estimation studies.

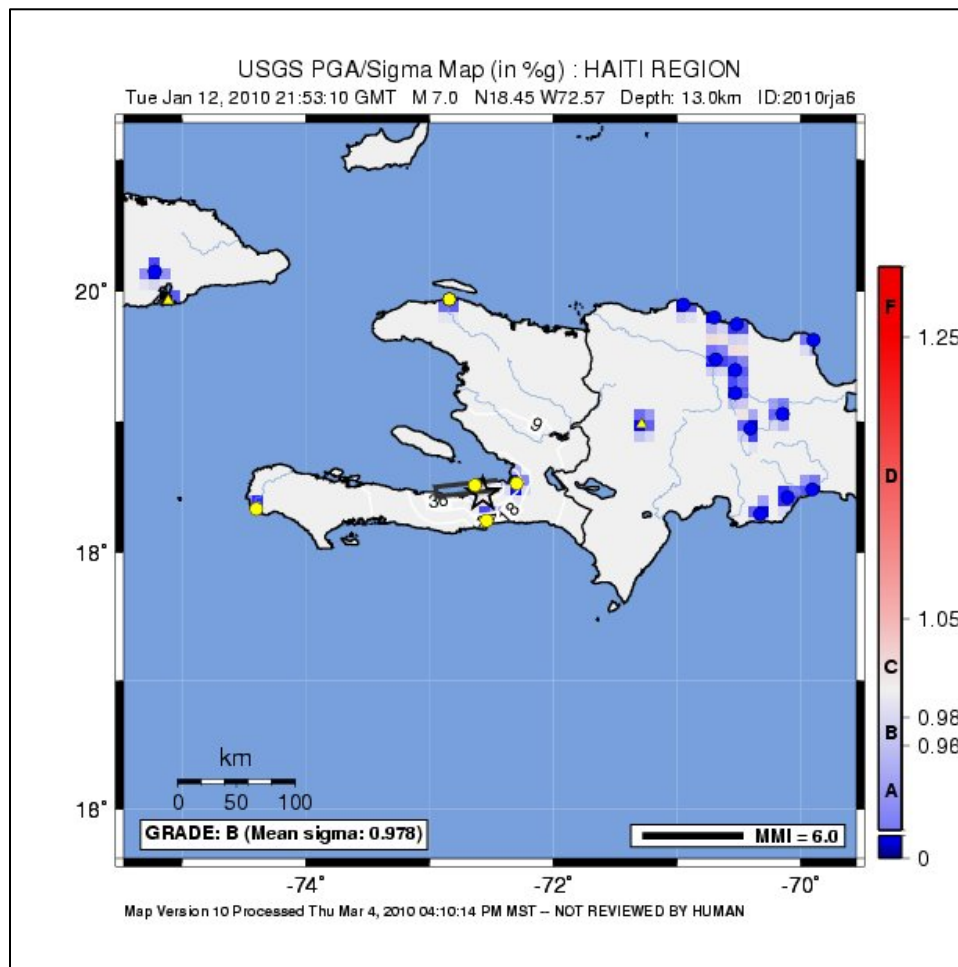


Figure 3.1 Example USGS ShakeMap uncertainty grading (USGS 2010a)

In addition to being an integral part of the USGS PAGER loss estimation methodology, ShakeMap applications can be extended to disaster response planning, and research and education. HAZUS, a GIS-based

loss estimation software allows ShakeMaps to be directly imported into its framework and be used for loss and damage estimation. Luco et al. (2007) developed maps for seismic risk to structures in the U.S. by combining USGS National Seismic Hazard Maps and ShakeMaps with fragility curves partly derived from FEMA's HAZUS-MH earthquake model. Currently, the Global Earthquake Model (GEM) is also using ShakeMaps to perform event-based loss assessments (Crowley, Cerisara, et al. 2010) and future applications of ShakeMaps are also expected in the GEM framework (So and Pomonis 2011).

The availability of global ShakeMaps provides an opportunity to utilize them in the derivation of fragility curves. The most common method of evaluating ground motion values for fragility curves is done through GMPEs and applied at the municipal or regional level. The use of ShakeMaps allows the application of spatial ground motion values to each building providing a more detailed assessment of ground shaking experienced by the building. Uncertainties involved in the ShakeMap methodology are detailed in the Uncertainty Maps and they provide an input in uncertainty evaluations of seismic risk assessments and loss estimation procedures. Derivation of fragility curves using empirical data can be time-consuming and cumbersome, as large amounts of damage data have to be processed, and ground motion values have to be computed, therefore, the use of ShakeMaps provides a more efficient and consistent way to obtain ground motion values.

3.5 Data Processing using GIS

The use of empirical data requires diligent processing techniques to ensure efficient use of the data to generate reliable fragility curves. The inconsistencies in damage data recording and collection discussed earlier

have to be addressed. The damage classifications have to be unified for data that is combined from several earthquakes. Structural typologies have to be organized and grouped for the derivation of typological fragility curves. Error inputs in survey collection as a result of surveyor inexperience need to be removed prior to statistical analysis. Data processing includes removing data points with missing entries or errors and organizing the data, and the extent of data processing required usually depends on the quality of data obtained. The process can be conducted visually by examining each data entry, and can be organized and grouped accordingly. This is possible for small data sets; however, it is not feasible for larger data sets containing thousands of data points. The alternative is to use database software or computer algorithms that systematically sift through and process the raw data.

The use of GPS during post-earthquake surveys allows the data to be spatially represented in a GIS framework. Commercial or open-source GIS software can be used to access and process the data. ArcGIS 10 software (ESRI 2011) was selected for the purpose of this study as it provided the functionality required to process the data. The ArcMap component within the ArcGIS framework is used to view, analyze, and process the data. ShakeMaps that are available in GIS *shapefile* format are *overlaid* on and *merged* with, the damage data layers, to obtain the levels of ground motion experienced by each building. Given the geospatial nature of GIS, it is important that the geographic coordinate systems and 2D map projections are defined and aligned prior to merging. This merged dataset that includes building damage data and ground motion measures are used in subsequent analysis.

Sub-datasets for the structures of interest are generated through database **query** and **select by attributes** commands. The data can be viewed as a

map or database table that can be exported and saved as comma separated value (.csv) or other formats. The .csv files are imported into statistical software that is used to further analyze the data, and develop damage probability matrices and fragility curves.

3.6 Damage Probability Matrices (DPMs) and Fragility Curves

Amongst the earliest derivations of damage probability matrices (DPMs) using empirical damage data were those by Whitman et al. (1973) whereby a damage probability matrix was defined as a set of probability mass functions for damage for a given seismic intensity. More generally, DPMs express the conditional probability of occurrence of a damage level j , given a ground motion intensity i , $P[D = j|i]$. The merged database described in the previous section is used to derive the damage probability matrices. The procedure used to derive the fragility curves in this report has been adapted from the methodologies outlined in Rota et al. (2008a) and Singhal and Kiremidjian (1996b).

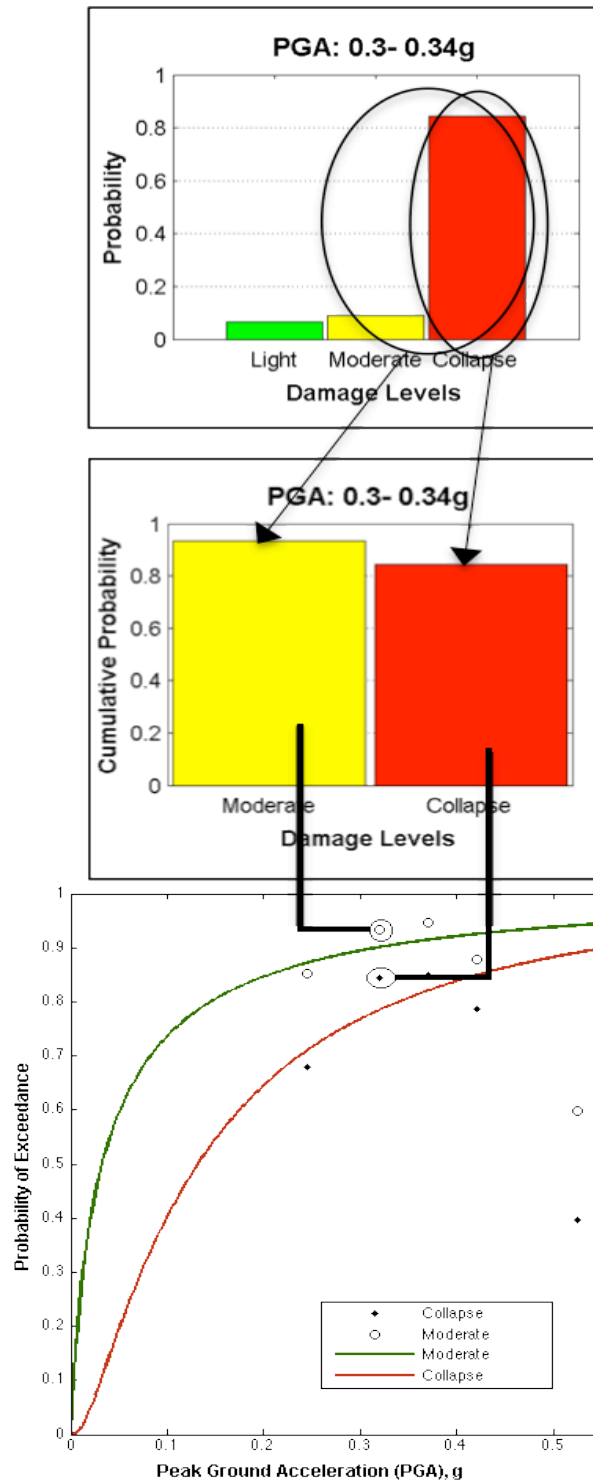


Figure 3.2 Fragility curve derivation flow chart for PGA range 0.3-0.34g

The first step in deriving the fragility curves after processing the raw data is to specify the bin size or allocate the ground motion ranges where each bin or range should have sufficient data to carry out statistical analysis. The probability of occurrence of each damage state is subsequently calculated by dividing the number of buildings having experienced the damage state by the total number of buildings, within each ground motion range. Cumulative probabilities expressing the probability of reaching or exceeding a damage level at a given ground motion value are calculated by adding the probabilities of occurrence from the highest damage levels to the damage levels of interest. The cumulative probability points are then fitted with a curve (fragility curve) that is expressed using an analytical function (i.e. fragility function). The lowest damage level is not included in the cumulative exercise as it results in the accumulation of all probabilities of occurrences, which is always 1, as illustrated in the flow chart in Figure 3.2.

The curve fitting exercise is carried out using the Curve Fitting toolbox in MATLAB (Mathworks 2012). Curve fitting in MATLAB utilizes the method of least squares to fit data which is based on minimizing the summed square of residuals. Residuals are defined as the difference between the observed values y_i and fitted values \bar{y}_i for each data point. The summed square S of residuals r_i for n data points is therefore expressed as:

$$S = \sum_{i=1}^n r_i^2 = \sum_{i=1}^n (y_i - \bar{y}_i)^2 \quad (3.1)$$

Nonlinear least squares fitting is used to estimate the parameters of the nonlinear analytical function describing the fitted curve (i.e. fragility curve). The formulation used to obtain a nonlinear least squares fit involves an

iterative approach using either the Levenberg-Marquardt algorithm (LMA) or the Trust Region (TR) method.

The LMA minimizes the sum of squared residuals or errors using the gradient descent method, and the Gauss-Newton method. The gradient descent method evaluates the optimal parameter by iteratively searching for a local minimum in the direction of the negative gradient of the least squares objective function while the Gauss-Newton method minimizes the sum of the squared errors by calculating the minimum of the least squares function, which is approximated as a local quadratic. The LMA uses the gradient descent method in its early iterations and the Gauss-Newton method when approaching the minimum or optimal solution. A vector \mathbf{p} constituting of n -parameters of a nonlinear function is evaluated iteratively with the sequence terminating as error function \mathbf{d} nears a minimum. In the LMA framework, this problem becomes:

$$[\mathbf{J}^T \cdot \mathbf{J} + \lambda \cdot \text{diag}(\mathbf{J}^T \cdot \mathbf{J})] \mathbf{p} = \mathbf{J}^T \cdot \mathbf{d} \quad (3.2)$$

In Eq. (3.2), \mathbf{J} represents the $m \times n$ Jacobian matrix containing the partial derivatives of the error function with respect to the parameters in \mathbf{p} , and, in the case of fragility curves, m is the number of selected ground motion classes and n is number of parameters. The non-zero scalar λ , also known as the damping factor, is used to control the direction and step size of each iteration.

The TR method presents an improvement over the LMA as it introduces a trust region approach where the direction and magnitude of subsequent iterations is bound in a finite radius around the current approximation. The step size s is approximated using a localized quadratic model in Eq. (3.3)

also known as the trust region sub problem, where \mathbf{g} is the gradient of the objective function f at the current point x , \mathbf{H} is the symmetric matrix of second derivatives also known as the Hessian matrix, \mathbf{D} is a diagonal scaling matrix, Δ is a positive scalar trust region radius, and $\|\cdot\|$ is the 2-dimensional norm. The solution to the TR sub problem is approximated in a restricted two-dimensional subspace based on the works of Branch et al. (Branch et al. 1999) and Byrd et al. (Byrd et al. 1988).

$$\psi(\mathbf{s}) = \mathbf{g}^T \mathbf{s} + \frac{1}{2} \mathbf{s}^T \mathbf{H} \mathbf{s} : \|\mathbf{D}\mathbf{s}\| \leq \Delta \quad (3.3)$$

In addition to the algorithm options, the Curve Fitting toolbox in Matlab also provides an option to use robust least squares fitting methods dealing with the effects of outliers in the data. The robust methods available include the bisquare weights method and the least absolute residuals (LAR) method. The bisquare weights method achieves the fit by minimizing a weighted sum of squares where data points closer to the fitted line get higher weights while those further from the line get reduced weights. The LAR method estimates a curve that minimizes the absolute difference of the residuals instead of the squared difference, hence, allowing extreme values a lesser influence on the fitted curve. While both methods are efficient in dealing with outliers, the bisquare method is usually preferred over the LAR method as it minimizes the outliers while also trying to find the curve that fits most of the data using the least squares method (Mathworks 2012).

Fragility curves are fitted to the cumulative probabilities using functional forms or known distributions. The lognormal cumulative distribution function has been the most popular choice in the derivation of fragility

curves (King et al. 2004; Rota et al. 2008a; Sarabandi et al. 2004; Singhal and Kiremidjian 1996b). The lognormal cumulative distribution function in Eq. (3.4), expressed using two parameters μ and σ , gives the probability of a certain damage level being exceeded given a ground motion value. Lognormal distribution function has been a reasonable model for fragility curves; however, other distributions and functions have also been used.

$$F(x|\mu, \sigma) = \frac{1}{t\sigma\sqrt{2\pi}} \int_0^x e^{-\frac{(\ln(t)-\mu)^2}{2\sigma^2}} dt \quad (3.4)$$

Several studies have used the functional form of the cumulative beta distribution to describe fragility curves. ATC-13 (1985) fit a generalized cumulative beta distribution in Eq. (3.5) to expert opinions on damage of a variety of building types. Similarly, Penelis et al. (2002) used the beta distribution to derive fragility curves for Greek URM single and two-storey buildings using observed damage data collected after several Greek earthquakes. The beta distribution is useful for cases with extreme levels of ground motion because of its shape parameters, v and ω , which allow the distribution to skew to the left or right (ATC 1985).

$$F(x|v, \omega) = \int_0^x \frac{(t-a)^{v-1}(b-t)^{\omega-1}}{B(v, \omega)(b-a)^{v+\omega-1}} dt \quad (3.5)$$

where: $B(v, \omega) = \int_0^1 u^{v-1}(1-u)^{\omega-1} du$; and

$$a \leq x \leq b$$

There are several distributions other than those discussed above that have been used in past derivations of fragility curves and have been

discussed in detail in Rota et al. (2008b); however, the lognormal distribution is the most popular.

Functional forms besides commonly known statistical distribution functions have been used to represent the cumulative probability distribution (i.e. fragility curve) and have shown to adequately represent building damage-ground motion relationships. Penelis et al. (2002) used an exponential function in Eq. (3.6) to fit observational data from a Greek earthquake, and the same functional form was used by Kappos et al. (2006) to develop fragility curves for unreinforced masonry buildings using a hybrid methodology. After a trial of various functional forms, an exponential expression (Eq. (3.7)) was selected by Rossetto and Elnashai (2003) to represent fragility curves for European-type reinforced concrete structures where damage levels were assessed using the homogenized reinforced concrete damage index, DI_{HRC} .

$$P(D > DS|I) = e^{a+b(pga)} \quad (3.6)$$

$$P(d \geq DI_{HRC}|GM) = 1 - e^{(-\alpha.GM^\beta)} \quad (3.7)$$

A variety of functional forms and distributions are available in the literature and are applicable in this work. However, the three that are considered in the subsequent chapters are the cumulative lognormal distribution, cumulative beta distribution, and the functional form used by Rossetto and Elnashai (2003) herein known as the exponential function.

3.7 Conclusion

A thorough methodology for deriving fragility curves using empirical data has been presented in this chapter. The methodology utilizes ShakeMaps that reduces the computational effort required to derive fragility curves and it provides ground motion data in GIS format that can be incorporated into other tools. However, most importantly it also provides the ground motion data, which is quite often not readily available in developing countries. The chapter also highlights the variety of distribution and analytical functions available that can be used to represent the fragility curves. The subsequent chapters illustrate the application of the methodology in a case study comprising of damage data collected after the May 2006, Yogyakarta earthquake in Indonesia.

4 Fragility of Single-storey URM Houses: Case Study on the 2006 Yogyakarta Earthquake

4.1 General

Indonesia is an archipelago consisting of about 17,500 islands located between the Indian and Pacific Oceans. The estimated population of Indonesia is approximately 237 million people making it the fourth largest population in the world after China, India, and United States. Indonesia has experienced several devastating natural disasters including several earthquakes and tsunamis. A high population density, developing socioeconomic status, and presence of non-engineered buildings makes Indonesia extremely vulnerable to earthquakes. The Yogyakarta earthquake of May 2006 resulted in widespread devastation in the Central Java region of Indonesia where 5,700 lives were lost with an estimated 154,000 homes completely destroyed and 260,000 homes suffering some form of damage (BAPPENAS et al. 2006). Data collected in the aftermath of the earthquake are used to derive fragility curves herein for unreinforced masonry homes.

4.2 Indonesia

4.2.1 Socio-economic Profile

Indonesia is a developing country that ranks 124th out 187 countries in terms of the HDI reported by the UNDP (2011). Some common socioeconomic characteristics of developing countries that Indonesia exhibits include lower income levels, low levels of human capital, high

levels of poverty, higher population growth rates, larger rural population, and higher rural-to-urban migration rates.

Indonesia has experienced significant economic growth in the last decade and it has also achieved a number of critical MDGs or is on-target to achieve them by 2015. The percentage of its population living in extreme poverty, or under US\$1 a day, has dropped significantly from 20.6% in 1990 to about 6% in 2008 (BAPPENAS 2010). Furthermore, over 13% of its population still live under the national income poverty line of US\$1.5 (PPP) per capita per day (BAPPENAS 2010) and 20% of the population or over 48 million people are still suffering from *multidimensional poverty*¹ (UNDP 2011). Indonesia is experiencing an urban population growth of 3.1% a year while the rural population is steadily declining at a rate of 1.4% (WB 2012a,b) and this urbanization results from rural-to-urban migration as well as urban sprawl into surrounding rural areas. The rapid increase in urban population induces strain on the health, housing, education, and infrastructure sectors as a result, over 12% of the urban population resort to living in slums (BAPPENAS 2010). While Indonesia's economic progress is a testament to the country's fiscal policies, this is yet to translate into natural disaster preparedness and resilience consequently making it imperative to consider the socioeconomic complexity within a disaster risk assessment strategy.

4.2.2 Seismic History and Tectonic Setting

Indonesia lies along the Pacific *Ring of Fire*, which is a region that experiences frequent earthquakes and volcanoes. The overall tectonic setting in the Indonesian region involves the subduction of the Indo-

¹ Multidimensional poverty (MP) is measured using several indicators such as poor health, lack of education, and poor living standards in contrast to poverty, which is measured solely on the level of income.

Australian plate under the Eurasian plate at an average rate of 5cm/year with the slip rates in some sections of the mechanism reaching about 7cm/year (Elnashai et al. 2007). Yogyakarta has experienced several recorded earthquakes since the early 19th century, however, of significance are the events of June 10, 1867, and July 23, 1943. Records from the 1867 seismic event indicate the City of Yogyakarta felt intensities of VIII – IX on the MMI scale. The 1943 event had an intensity of MMI VII-VIII and as a result about 213 people were killed and 3,900 people injured in addition to the collapse and damage of several thousand homes (Husein et al. 2007). In addition to its seismic history, the Central Java and Yogyakarta area is also home to Mt. Merapi volcano, one of the world's most active volcanoes. The devastating effects of its violent eruptions include the destruction of villages and thousands of acres of farmland and forests resulting in over 130,000 casualties (Voight et al. 2000).

The geological setting of the region is as complex as its tectonic and volcanic history. Yogyakarta is located in a depression zone between two faults: the Progo River fault which is bordered by the West Progo Mountains, and the Opak River fault to the east. Young volcanic deposits from Mt. Merapi consisting of volcanic tuff and ash, breccia, agglomerates, and lava cover the Yogyakarta depression (Pramumijoyo and Sudarno 2007). Setijadji et al. (2007) suggest that destructed areas were concentrated within the low-land areas, and the dominant geological factors contributing to the extensive damage consisted of unconsolidated Quaternary volcanic deposits from the Mt. Merapi Volcano in addition to other secondary geological conditions. As a result of the geological conditions, directivity and soil amplification significantly contributed to the damage and destruction of buildings.

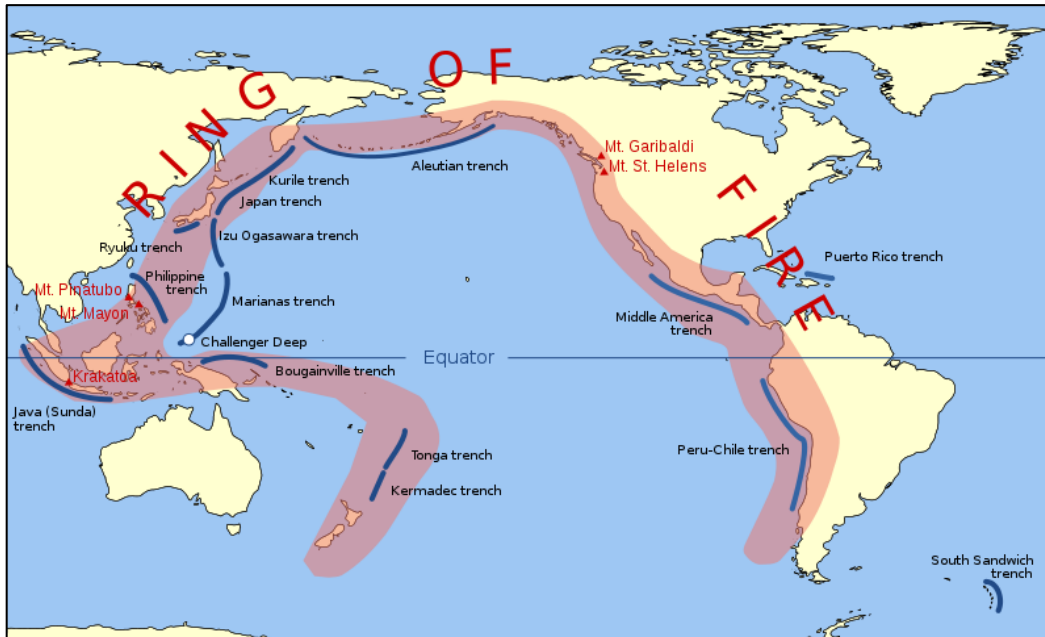


Figure 4.1 Pacific Ring of Fire, Indonesia located along the Sunda trench (http://commons.wikimedia.org/wiki/File%3APacific_Ring_of_Fire.svg)

4.3 Yogyakarta Earthquake, May 2006

On May 27th, 2006, a magnitude M_w 6.3 earthquake hit the Island of Java, Indonesia causing widespread loss of life and property on the island. The epicenter of the earthquake according to USGS (2010b) was 20km south of the city of Yogyakarta, the capital of the Special Region of Yogyakarta (*Daerah Istimewa Yogyakarta*), at a shallow focal depth of 10km. The Central Java and Yogyakarta provinces of Indonesia have experienced little seismicity comparatively and is considered as a seismic gap (Wagner et al. 2007).

Although, the regional tectonic setting is governed by a subduction regime, the shallow depth indicates that the earthquake was associated with local faults stressed as a result of the broader subduction mechanism (Elnashai et al. 2007). In addition to its shallow focal depth, fault plane solutions indicate a left-lateral strike-slip mechanism (Elnashai et al. 2007) located

on the border of a *seismic gap* zone (Wagner et al. 2007). Based on the comparison of aftershock distribution with the geological map of the area, Wagner et al. (2007) suggest that the source is a fault located further east of the Opak River fault contrary to earlier assumptions of the Opak River fault being the source.

The heaviest damage was observed in Bantul and Klaten districts in the Yogyakarta and Klaten provinces, respectively, where 5,700 lives were lost with an estimated 154,000 homes completely destroyed and 260,000 homes suffering some form of damage; in total, the damage is estimated to be around US\$3.1 billion (BAPPENAS et al. 2006; Boen 2010).

4.4 Available Dataset

After the Yogyakarta earthquake of May 27th 2006, the University of Gadjah Mada (UGM) collected damage data through an extensive surveying effort in the Bantul Regency of the Yogyakarta Province. Students and staff of UGM collected the data immediately in the aftermath of the earthquake to ensure the validity of the damage conditions and survey results. It is not clear as to how many actual buildings were surveyed; however, the GIS files obtained have 53,116 buildings recorded out of which, 1,736 data points were recorded as having no data at all or obvious mistakes, and therefore were ignored from the onset. The GIS layers included data such as structure type, roof construction, building function, floors, and damage level sustained. The survey was conducted in ‘rapid’ and ‘detailed’ categories, where the rapid category collected vital information such as building function, number of floors, structure type, roof construction, and level of damage while the detailed category also included the administrative boundary details and additional notes. The dataset presents a substantial wealth of information that could be utilized

to assess the consequences of earthquakes and in particular, seismic performance of structures.

The dataset indicates the dominant construction material in surveyed areas to be clay bricks, with the rest being wood, concrete, bamboo, and mixed/unknown building types (see Figure 4.2). A majority of the buildings were residential dwellings with approximately 95% being single-storey homes (see Figure 4.3 and Figure 4.4). A small number of commercial buildings were also recorded in the survey. The use of clay tiles in residential roof construction is ubiquitous in the region and was highlighted in the surveyed data where 97% of buildings featured clay tiles as the roofing material. Other roofing materials that were noted in the survey included corrugated metal sheeting, asbestos tiles, cement tiles, and bamboo. Many of the homes were identified as mixed dwellings where either the front or the back of the home is used as a storefront, which is quite typical in rural areas of developing countries where the economy is reliant on home-based industries. An overview of the data distribution therefore, indicates that the majority of the surveyed buildings consist of single-storey brick homes with clay tile roofing.

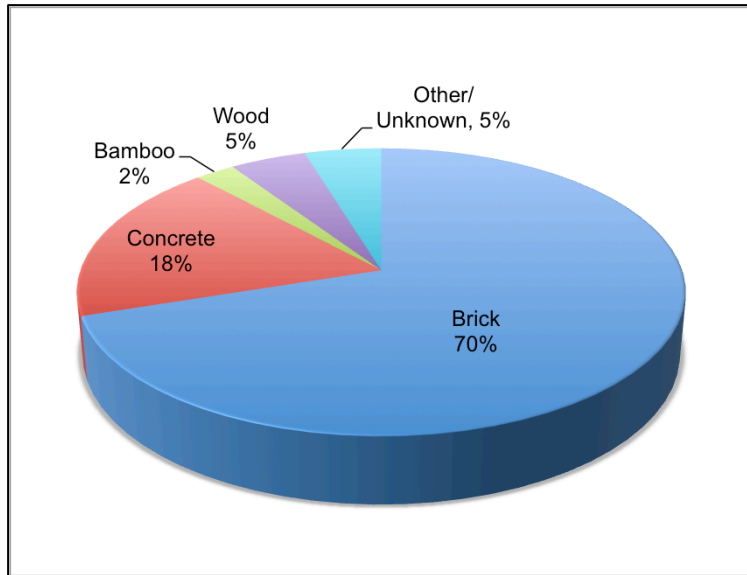


Figure 4.2 Damage data distribution based on building typologies

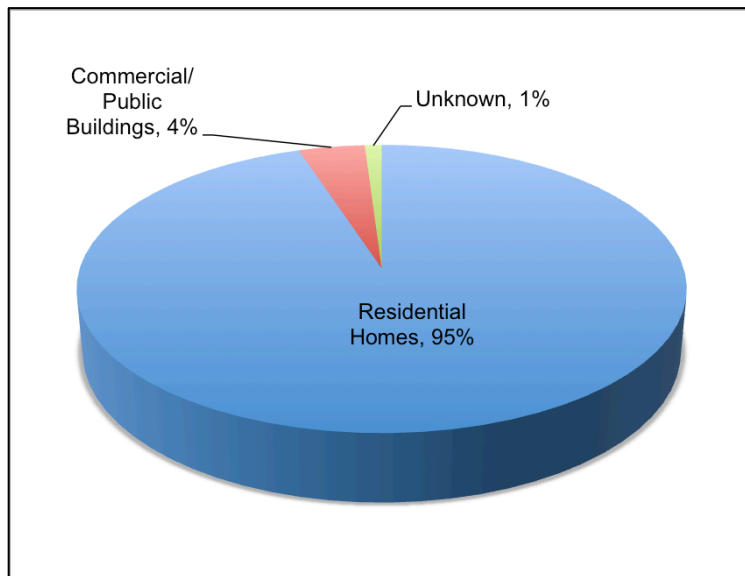


Figure 4.3 Building occupancy distribution

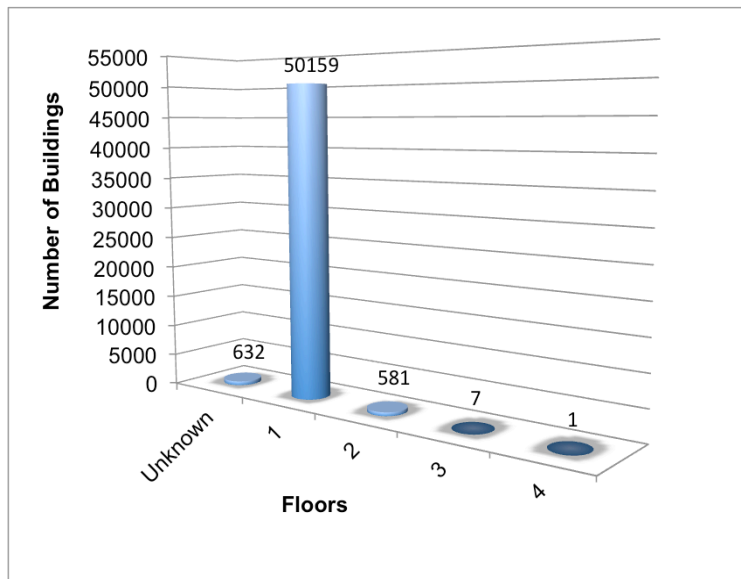


Figure 4.4 Data distribution of storeys

The building construction type recorded in the survey does not specify the brick buildings to be reinforced. However, several reports suggest that most, if not all, single-storey brick homes in the Bantul area were unreinforced (Aswandono 2011; EERI 2006). Most of the damaged or collapsed buildings in Yogyakarta were also non-engineered and primarily consisted of two types: one or one and a half brick thick masonry building without reinforcement (see Figure 4.5) and half brick thick masonry building with and without reinforcement (see Figure 4.6) (Boen 2006). The former category consisted of one or one and a half brick thick masonry walls bounded by brick pilasters while the latter category follows CM construction using half-brick masonry with reinforced concrete frames. However, survey of the damage areas revealed that many of the CM buildings in the Mid Java area lacked reinforcing in the confining ring beams and column elements (Boen 2006). Unreinforced concrete frames together with poor detailing and lack of anchorage tying the walls to the concrete frames will not provide the intended confinement; therefore, both categories can be considered to be essentially of a similar structural

typology and to this effect all brick masonry buildings in the data set are assumed to be unreinforced.



Figure 4.5 One (or One and half) brick thick masonry buildings (Boen 2006)



Figure 4.6 Half brick thick masonry building without reinforcements (Boen 2006)

From the remaining 51,380 data points, 33,324 single-storey URM buildings were then extracted and analyzed to ensure that all relevant metadata required to derive fragility curves were available. Further 18 data points were also removed as they had discrepancies within the metadata. The final processed dataset consisting of 33,306 single-storey URM buildings was combined with ground motion data from ShakeMaps and used to develop fragility curves.

The damage distribution of the URM buildings in the dataset is presented in Figure 4.7 and is dominated by the collapse damage state. This is in

stark contrast to the damage distribution of RC buildings in the dataset shown in Figure 4.8. However, it is important to note that the total number of the RC building type in the collected data is significantly less than the masonry building type as highlighted in Figure 4.2.

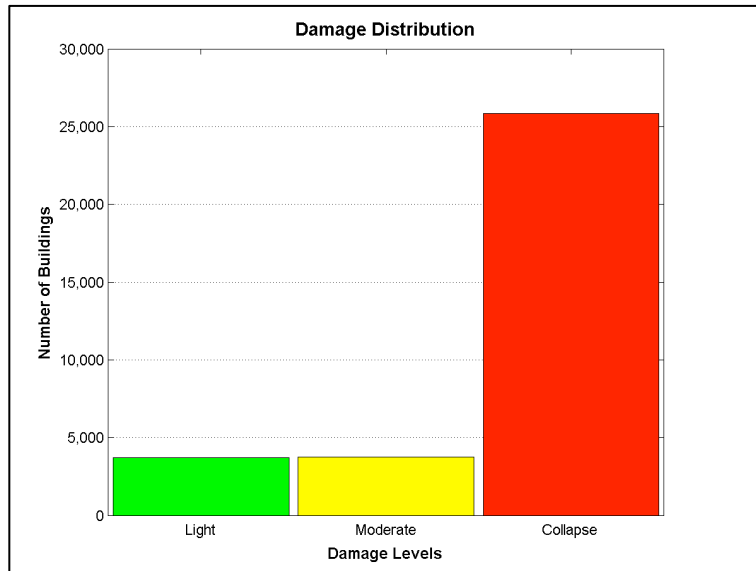


Figure 4.7 Damage distribution of brick masonry buildings

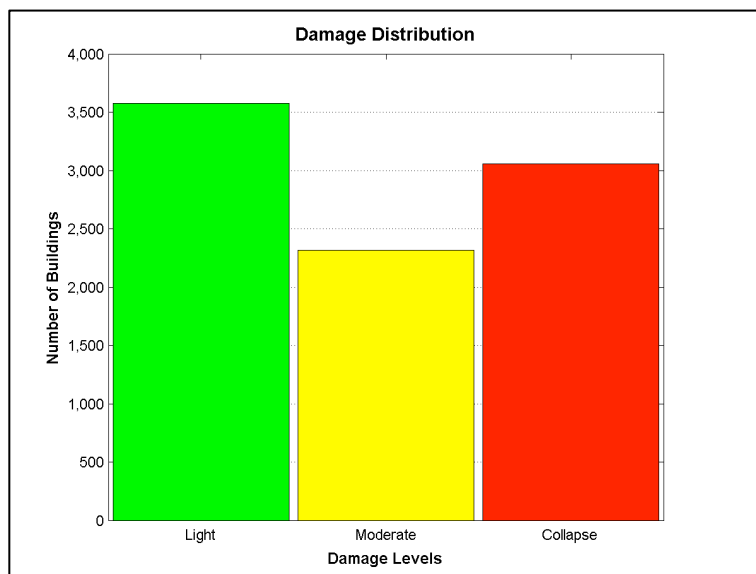


Figure 4.8 Damage distribution of RC buildings

4.5 Damage Classification

The available damage data are broadly labeled as “Light”, “Moderate”, or “Heavy/Collapse” damage states; however, it is not very clear as to what damage classifications were used when surveying the houses. Several other assessments by local agencies also used similar damage states; however, they also lack detailed descriptions. In order to have meaningful fragility curves, it is necessary to have clearly described damage states and the lack of such definitions necessitates the need for adopting a well-defined damage scale and ascribing it to the damage labels in the survey.

For the purpose of this study definitions have been adapted using the damage categories provided in Boen (2010) for non-engineered single-storey URM houses in Indonesia and have been mapped to the labels in the dataset according to Table 4.1. Damage categories provided in Boen (2010) are considered to be an appropriate choice as they have been developed for buildings in Indonesia within the context of non-engineered construction. Six states of damage with their descriptions have been related to three damage labels in the survey data as shown in Table 4.1. The damage descriptions are vital not only for the use of fragility curves in pre-disaster risk assessments and retrofitting of buildings but also in a post-disaster context to understand the behavior of structures, and particularly non-engineered buildings.

Table 4.1 Damage states and definitions (Boen 2010)

Damage States (in dataset)	Damage Category	Definitions
Light	Category 0: No Damage	No Damage Thin cracks (less than 0.075 cm) in plaster, falling of plaster bits in limited parts
	Category I: Slight – Non-structural Damage	Small cracks in walls, falling of plaster in large bits over large areas
	Category II: Slight Structural Damage	Damage to non-structural parts, projecting cornices, etc. The load carrying capacity is not reduced appreciably
Moderate	Category III: Moderate Structural Damage	Large and deep cracks in walls Widespread cracking of walls The load carrying capacity of structure is partially reduced
Heavy/Collapse	Category IV: Severe Structural Damage	Gaps in walls Inner or outer walls collapse
	Category V: Collapse	Approximately 40% main structural components have failed Large portion or whole building collapses

4.6 Ground Motion – USGS ShakeMaps

The numbers of strong ground motion recordings from the Yogyakarta earthquake were limited. The main shock was recorded by one instrument at Mt. Merapi, 55km from the epicenter, and the only other instrument located in region of the earthquake was not turned on during the earthquake (EERI 2006). The lack of seismograph recordings required the development of extensive attenuation relationships to establish the damage-ground motion relationships i.e. fragility curves; however, using

the procedure detailed in Chapter 3, USGS ShakeMaps were used within a GIS framework allowing the extension of the damage dataset to include ground motion values for each building.

GIS files for the most *recent run* of ShakeMaps for the Yogyakarta earthquake were provided by USGS. The historic ShakeMaps are regularly revisited and the ShakeMap generating program is run to include the most recent data for the earthquake. PGA, PGV, and PSA (for 0.3s period) layers were overlaid onto the damage layer in ArcGIS as illustrated in Figure 4.9 and metadata were joined to relate the ground motion measures to each building. Statistical analysis was carried out on the combined damage-ground motion dataset to develop damage probability matrices and subsequently the fragility curves.

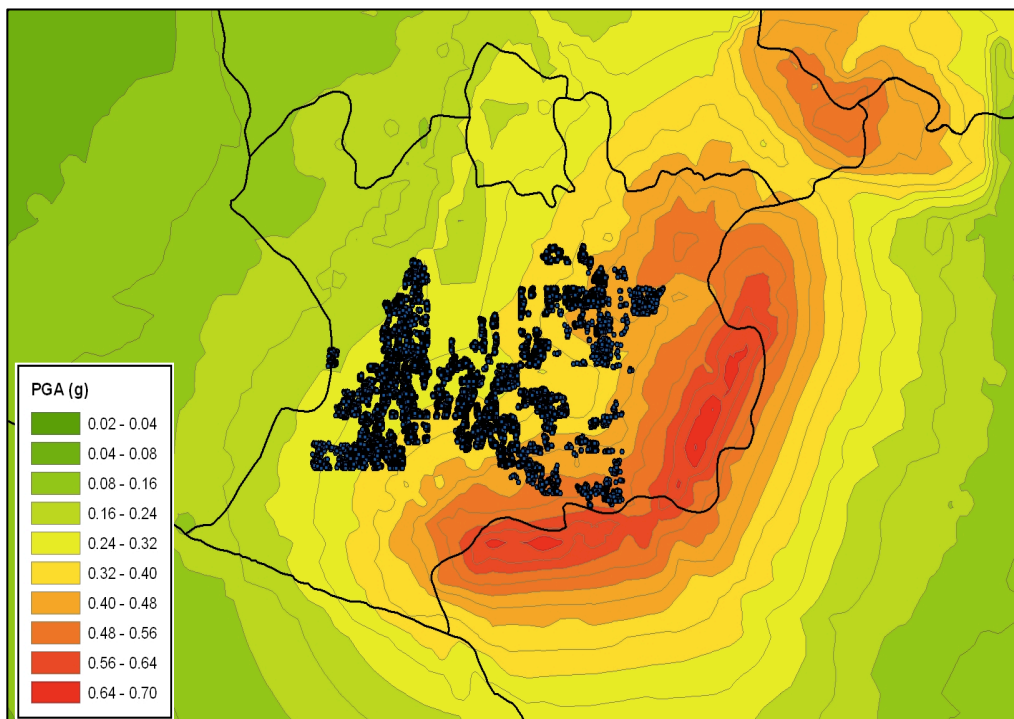


Figure 4.9 Illustration of USGS Shakemap and damage data overlay in ArcGIS (black markers are individual buildings)

4.7 Damage Probability Matrices

Damage distribution of the single-storey URM houses at ground motion intervals (see Figure 4.10 to Figure 4.12) developed from the combined damage-ground motion dataset indicate the severe extent of damage experienced as a result of the earthquake. The bin intervals at either ends of the ground motion range are uneven as there are insufficient samples at lower and higher ground motion amplitudes, and therefore the intervals have been extended to include all valid data.

The distribution trend of the damage states in the highest PGA and PSA interval is considerably different than the lower PGA and PSA intervals as shown in Figure 4.10 and Figure 4.12. The probabilities of light damage and collapse are almost equal at 40% or 0.4, whereas the rest of the PGA and PSA intervals have the collapse damage state dominating the distribution with probabilities over 60%, and even as high as over 80% for some lower intervals. In the case of PGV, the damage distribution trend is consistent for all intervals as shown in Figure 4.11. This discrepancy between the last PGA and PGV, or PSA and PGV intervals, is a result of the difference in spatial variation of ground shaking between acceleration and velocity related variables as illustrated in Figure 4.13 and Figure 4.14. The spatial variation of ground shaking in the USGS ShakeMaps and the availability of damage data in a GIS format allows the determination of ground shaking experienced by each building.

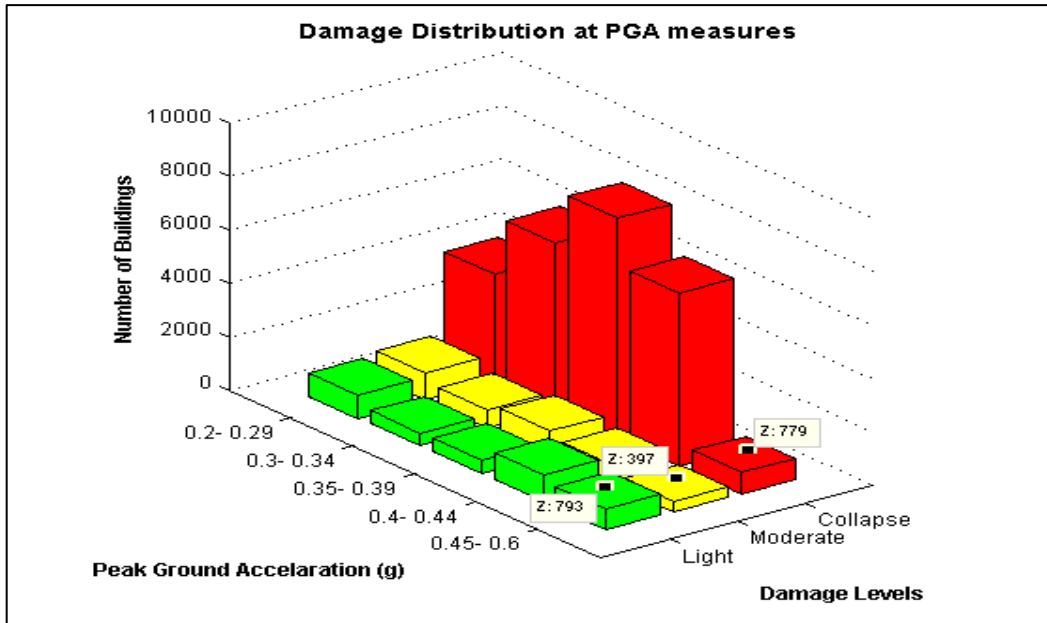


Figure 4.10 Damage Distribution as a function of PGA

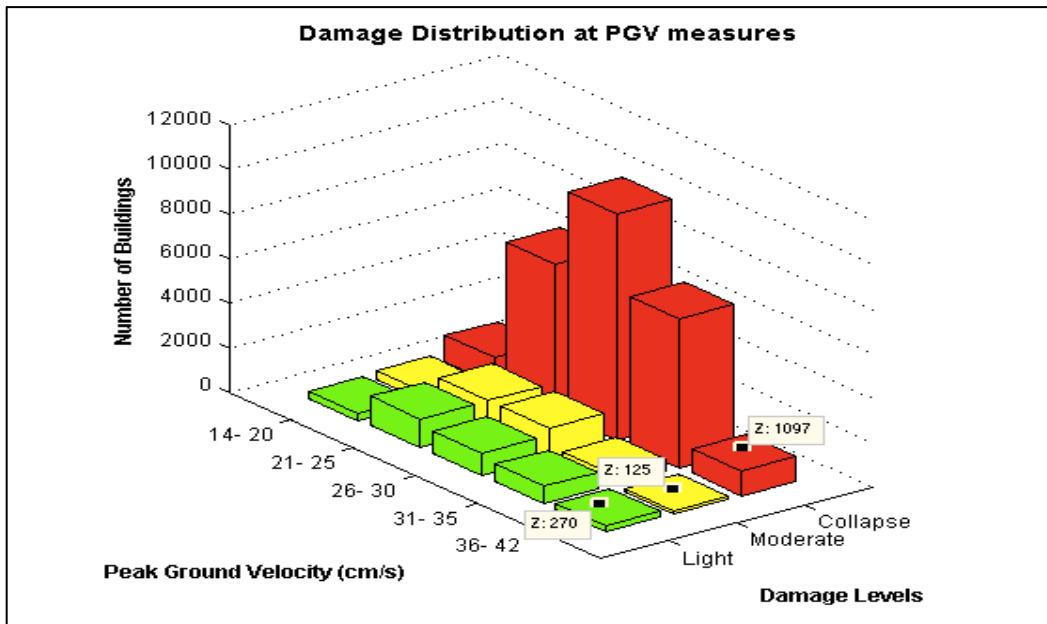


Figure 4.11 Damage distribution as a function of PGV

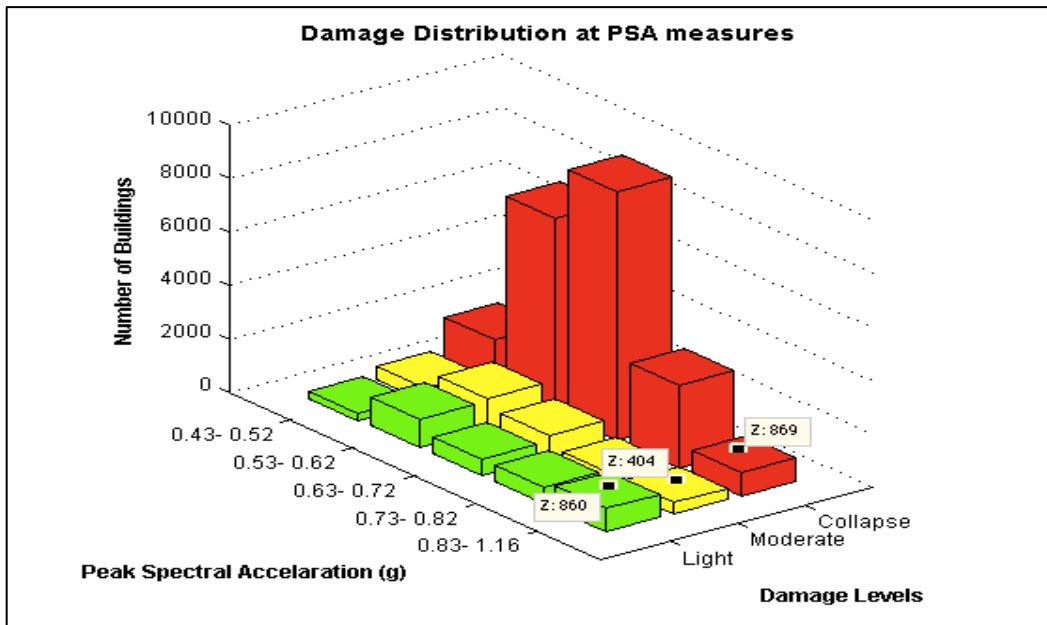


Figure 4.12 Damage distribution as a function of PSA-03

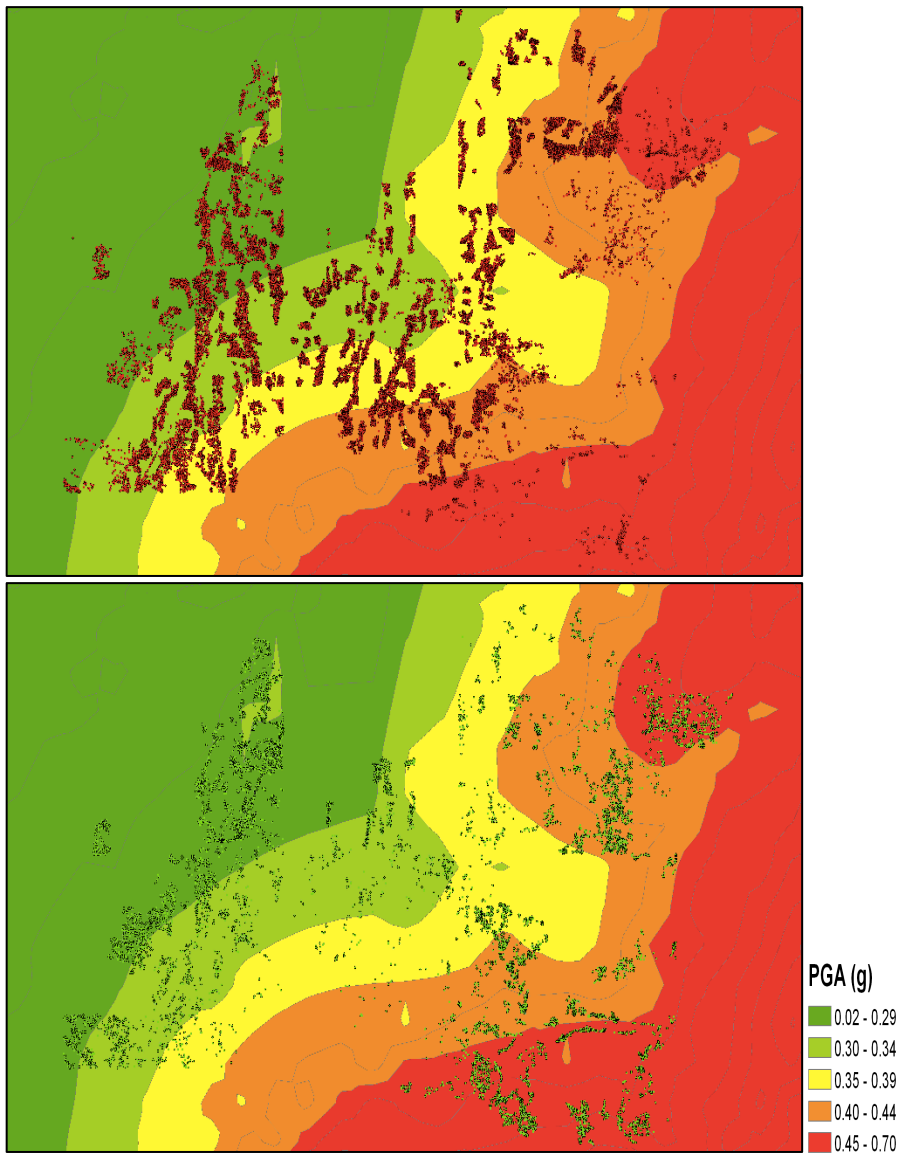


Figure 4.13 Distribution of collapsed (above) and lightly damaged (below) buildings as a function of PGA

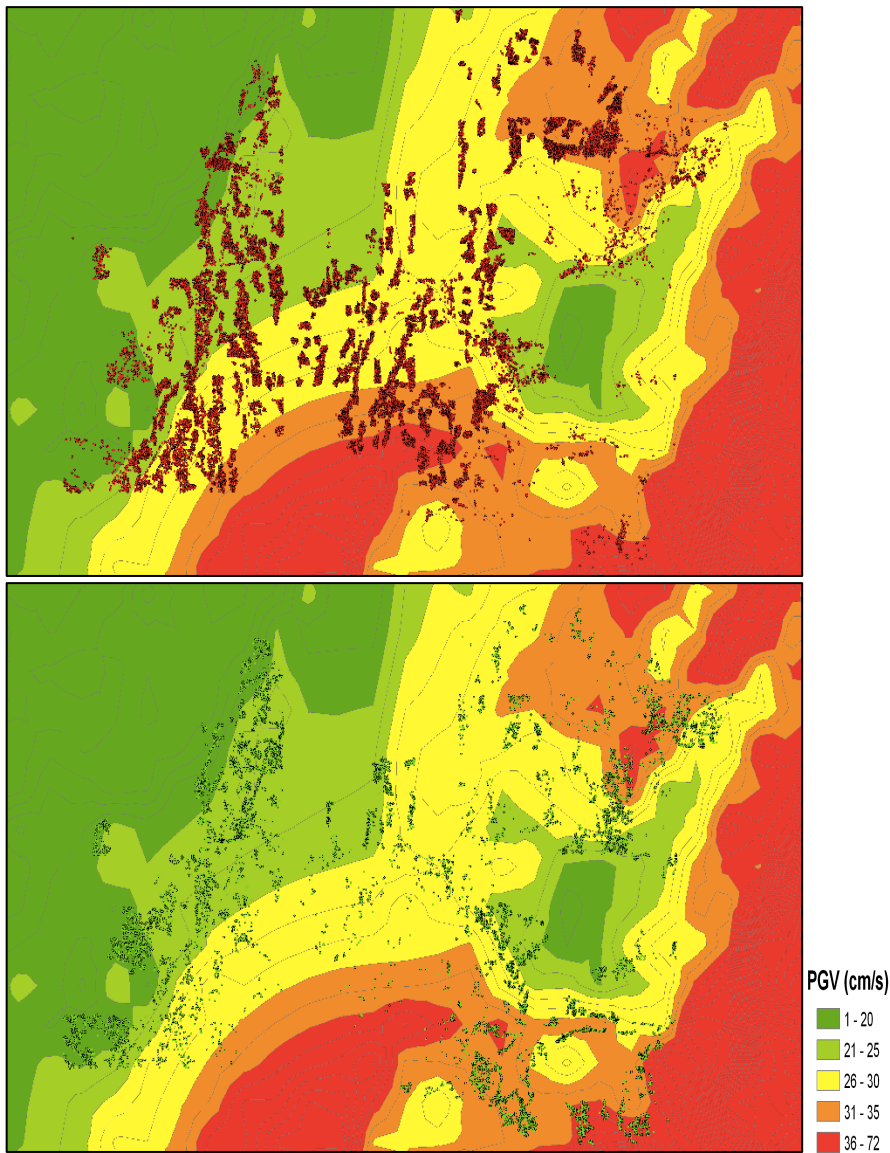


Figure 4.14 Distribution of collapsed (above) and lightly damaged (below) buildings as a function of PGV

Existing empirical fragility curve studies have generally applied attenuation equations to a municipality or similar administrative boundary since the exact positions of the damaged buildings are not available in the data (Rota et al. 2008b; Sabetta et al. 1998) and the actual ground motion experienced by the building can be over- or underestimated depending on the size of the municipality. Even when the exact locations of the damaged

buildings are known, the manual application of attenuation equations to each building can become demanding depending on the number of buildings in the dataset. Therefore, the use of ShakeMaps is evidently favourable in the derivation of empirical fragility curves.

DPMs for PGA, PGV, and PSA are developed from the damage distributions using the procedure illustrated in Chapter 3. The probability of buildings suffering collapse is extremely high in comparison to the light and moderate damage states (see Figure 4.15, Figure 4.16, and Figure 4.17), for all ground motion intervals. This is contrary to what is expected, which is that buildings would suffer less damage at lower ground shaking intensities, and the extent of damage would increase as the intensity of ground shaking increases. However, DPMs from several other studies developed using post-earthquake damage data are also observed to deviate from this expectation (Eleftheriadou and Karabinis 2011; Rota et al. 2008b). Sarabandi et al. (2004) notes that the DPMs derived in the ATC-13 (1985) using expert-opinion show probabilities of higher damage levels increasing significantly with the higher ground shaking intensities, while those derived empirically for the same building indicate only a slight increase. DPMs developed using analytical methods also show an increase in the probabilities of damage levels at higher ground shaking intensities (Dumova-Jovanoska 2000; Singhal and Kiremidjian 1996a). This observation is significant as it highlights the data source's (i.e. empirical, analytical or expert-opinion) influence on the damage assessment results. The simplification and assumptions of analytical models and the subjectivity of expert opinions tend to develop DPMs that are in line with the notion of increasing probabilities of damage with increasing ground shaking; however, they fail to account for many variables such as the use of specific construction details and variation in

material quality (Rossetto and Elnashai 2003). These variables are inherently captured in the empirical dataset.

The probability of reaching or exceeding a specific damage state are expressed in the cumulative DPMs presented in Figure 4.19 to Figure 4.20. As a result of the damage distribution in the highest interval discussed earlier, the cumulative probabilities for PGA and PSA are significantly lower than the other intervals. The cumulative probabilities are subsequently fitted with curves using cumulative lognormal distribution, cumulative beta distribution, and exponential functions.

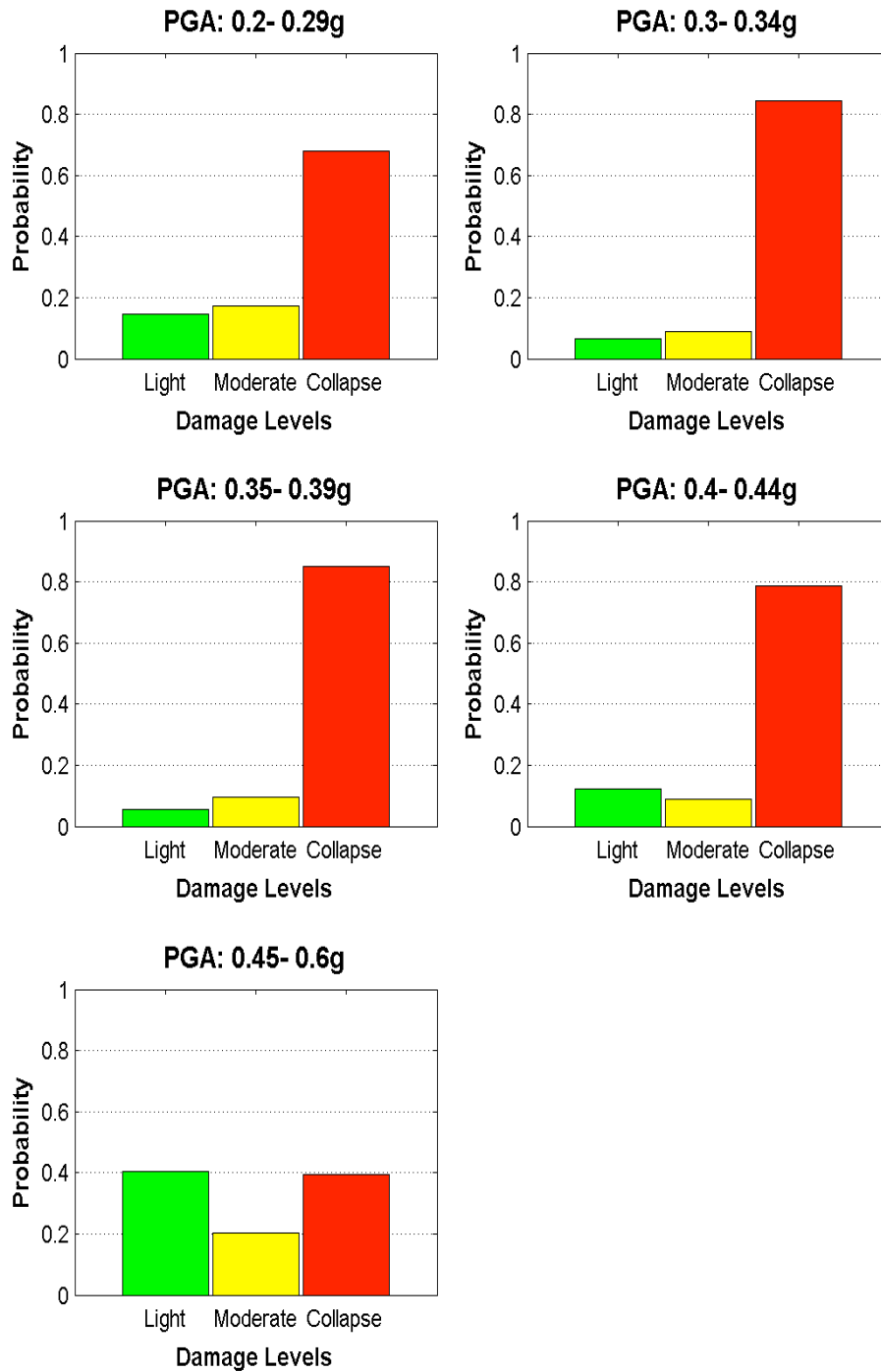


Figure 4.15 Damage Probability Matrices in PGA

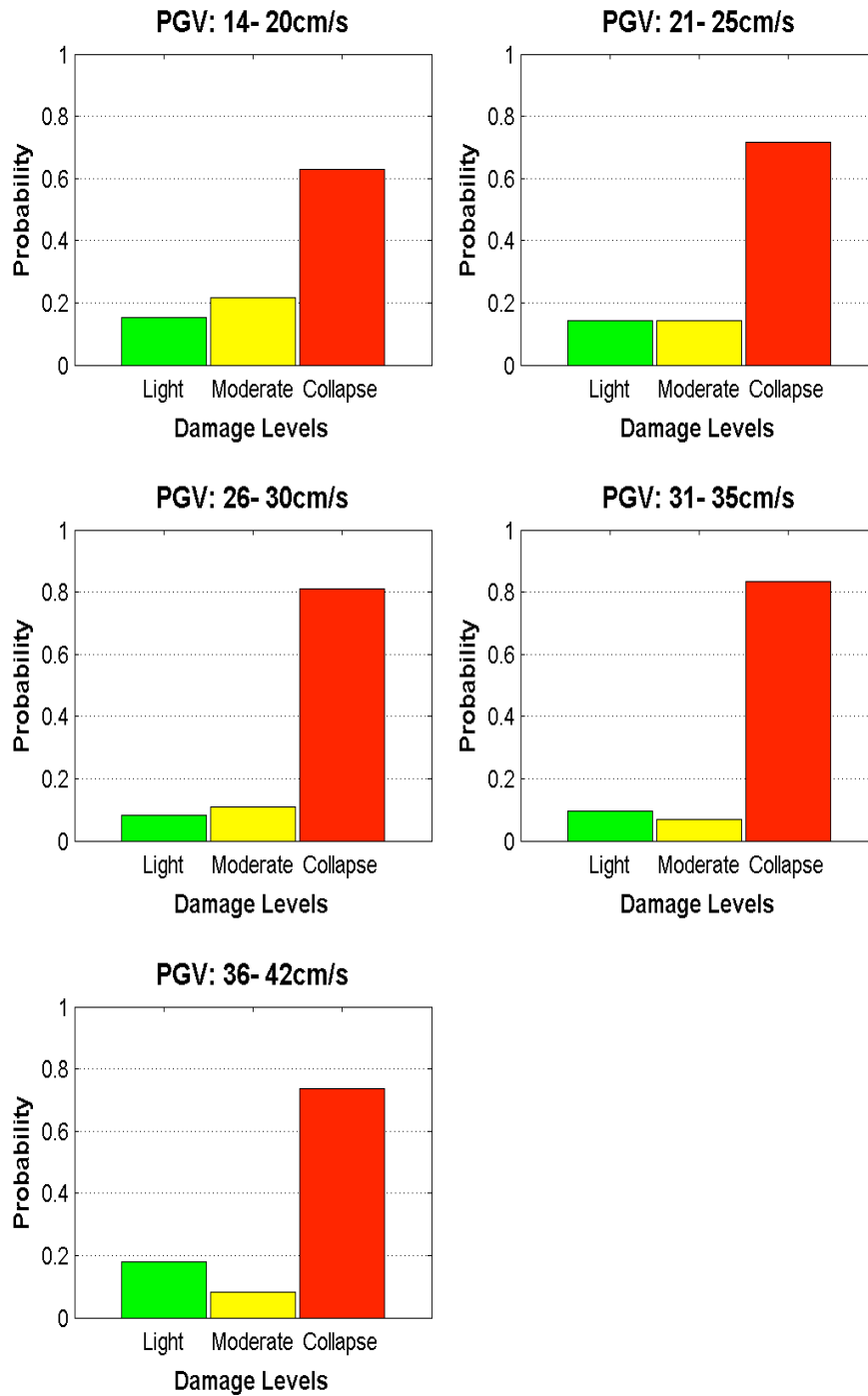


Figure 4.16 Damage Probability Matrices in PGV

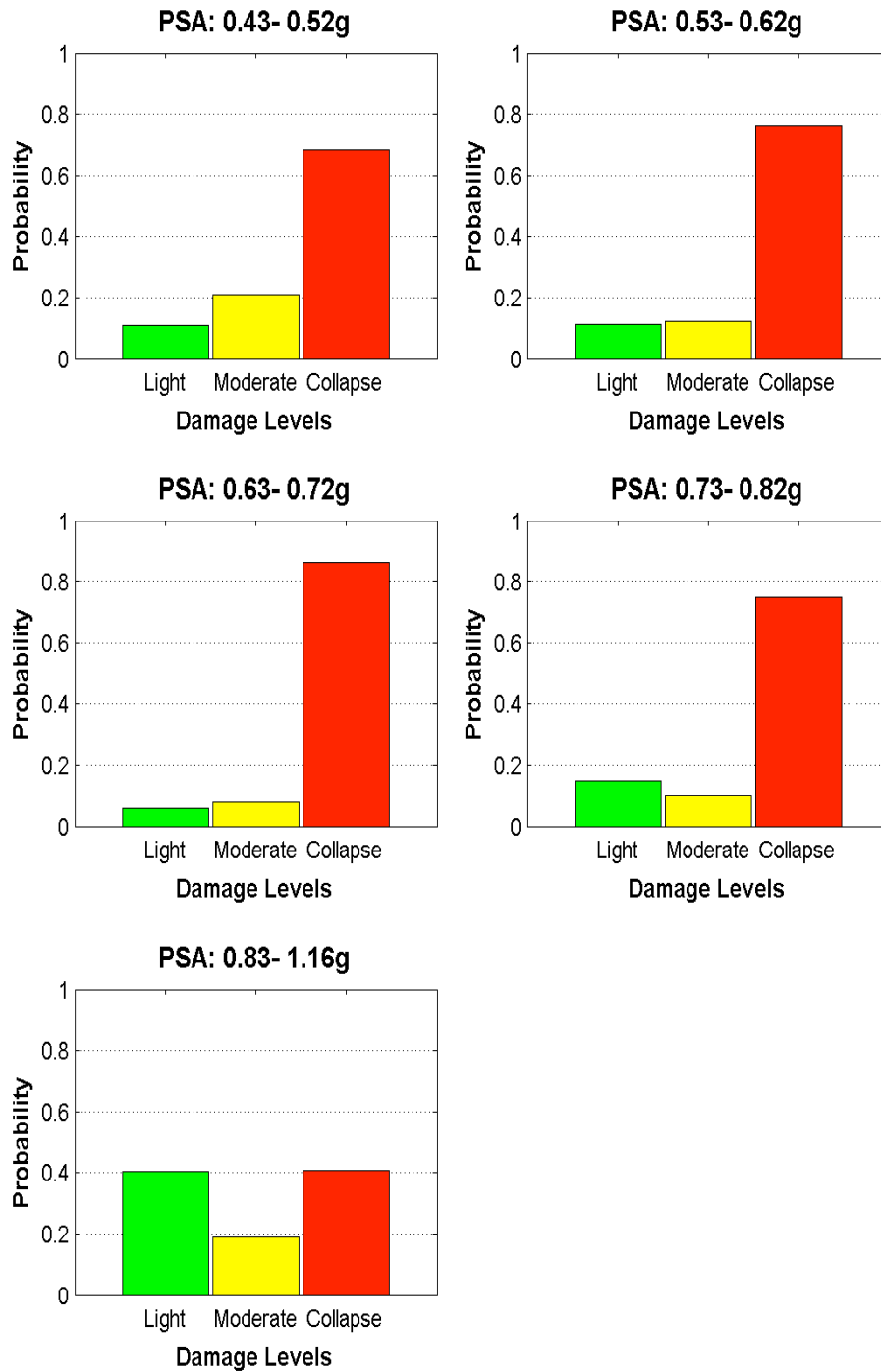


Figure 4.17 Damage Probability Matrices in PSA

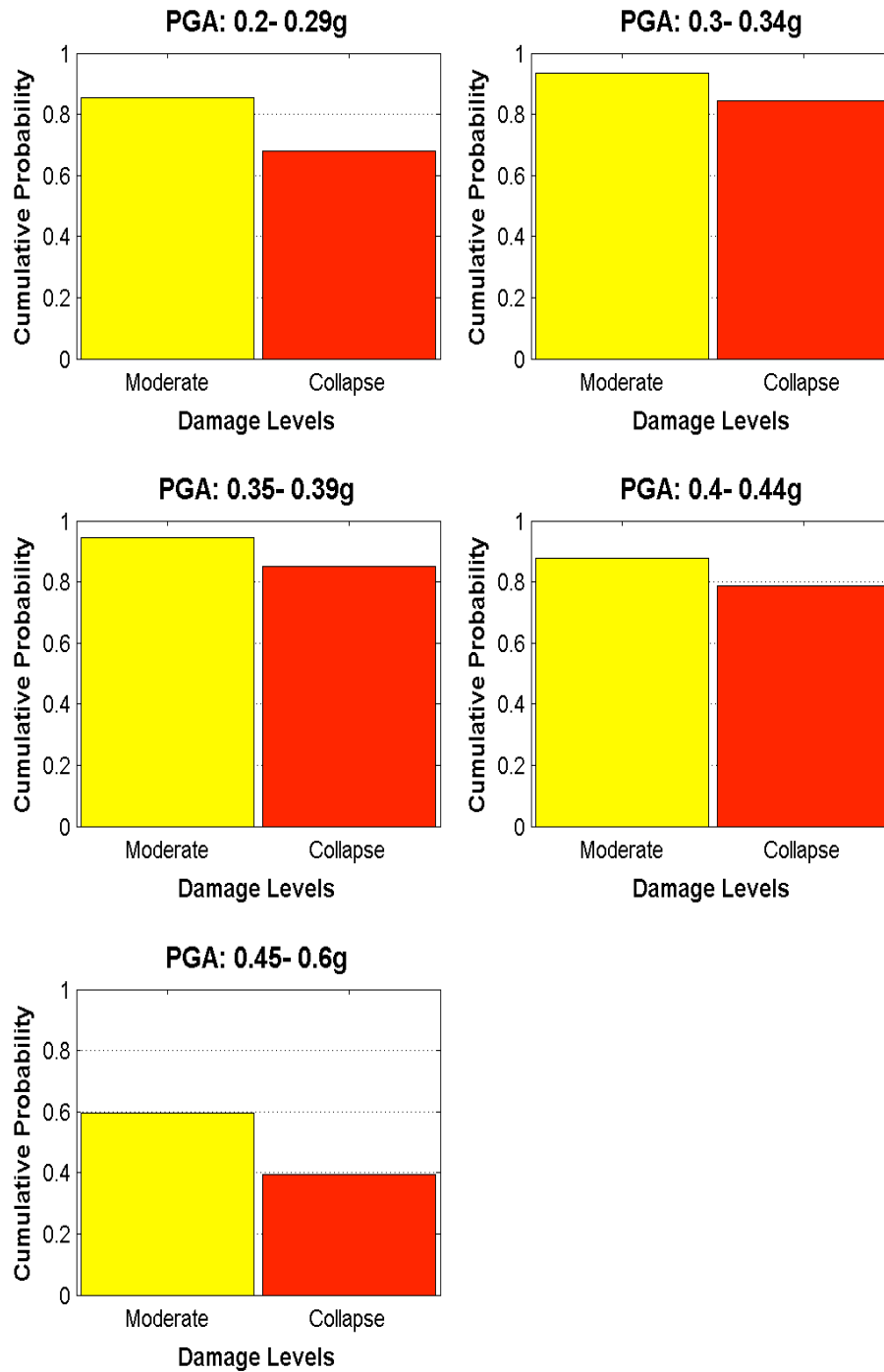


Figure 4.18 Cumulated DPMs for PGA intervals

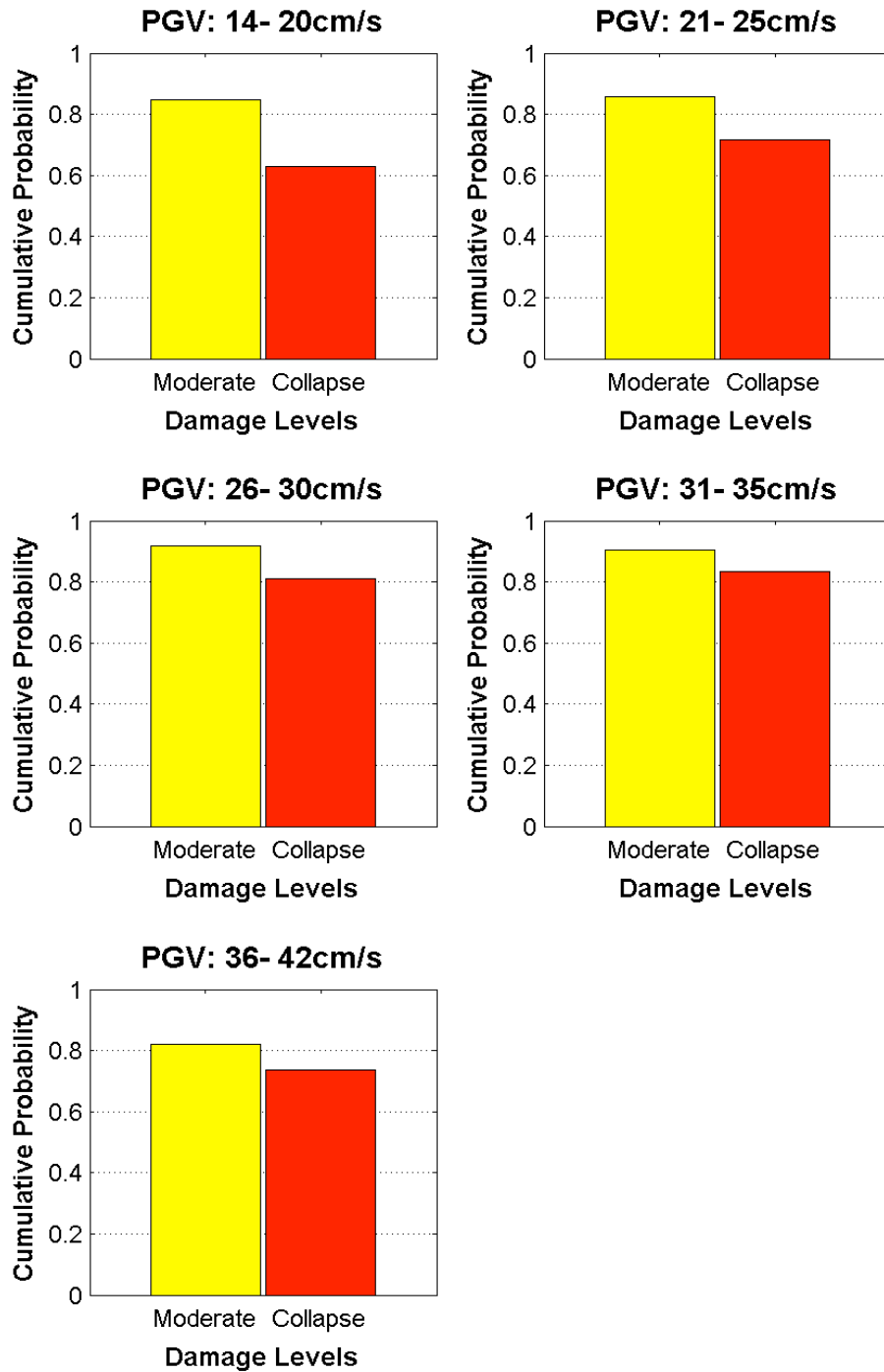


Figure 4.19 Cumulated DPMs for PGV intervals

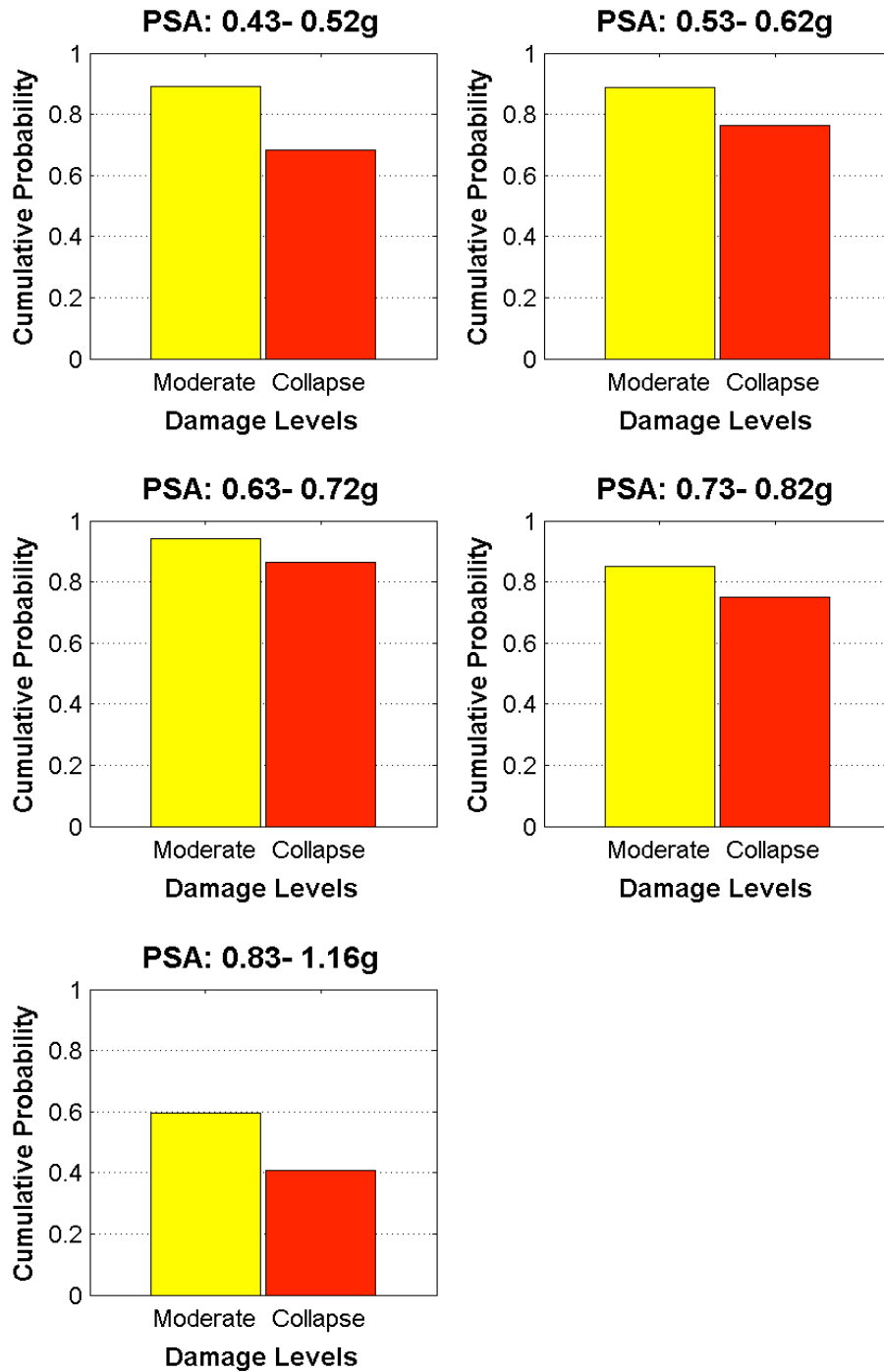


Figure 4.20 Cumulated DPMs for PSA (0.3s Period, 5% damping) intervals

4.8 Derivation of Fragility Curves

Fragility curves derived in this study are presented in this section. The curves have been obtained by fitting them to the cumulative probabilities calculated in the previous section using the cumulative lognormal distribution, cumulative beta distribution, and exponential functions. The fragility curves in Figure 4.21 to Figure 4.23 express the probability of a single-storey URM building described in this study reaching or exceeding the damage states as a function of PGA. The shapes of the curves obtained from the fitted functions are quite similar, particularly at higher values of PGA as shown in Figure 4.24. The beta cumulative function showed an overall better fit to the case study data in comparison to the cumulative lognormal and exponential functions considering the R-square values in Table 4.2. About 80% of the buildings would have suffered or exceeded the moderate damage state and just over 50% of the buildings would have collapsed at just 0.1g. The cumulative lognormal curves give the lowest estimates of probability of reaching or exceeding both the damage states followed by the exponential and cumulative beta, respectively.

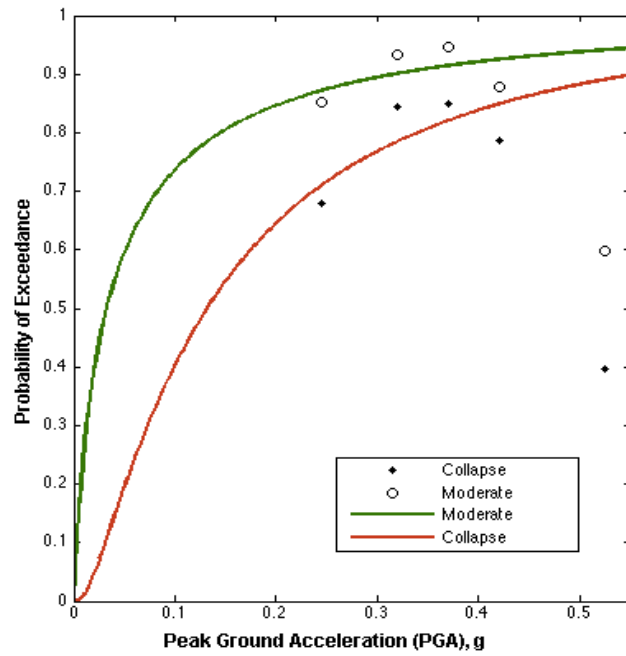


Figure 4.21 Cumulative lognormal distribution fragility curves in PGA

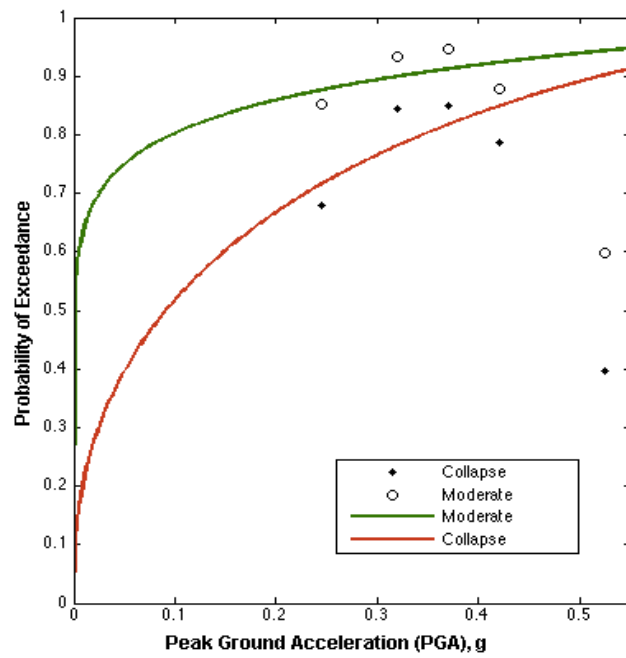


Figure 4.22 Cumulative beta distribution fragility curves in PGA

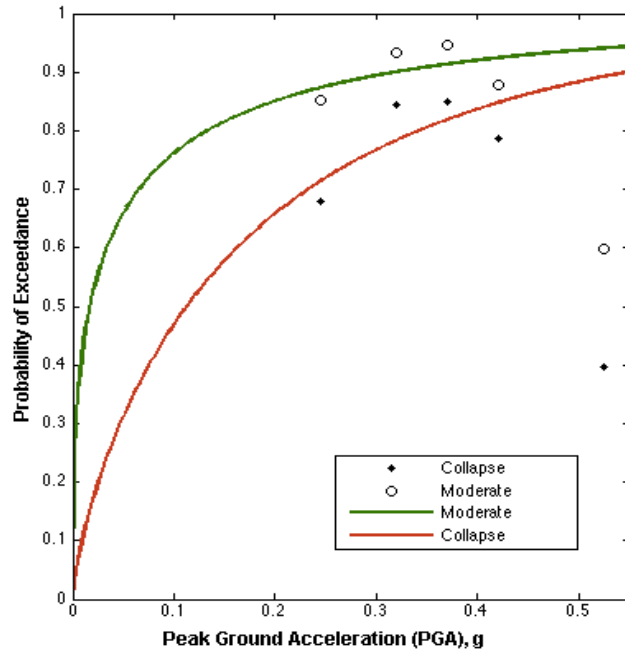


Figure 4.23 Exponential fragility curves in PGA

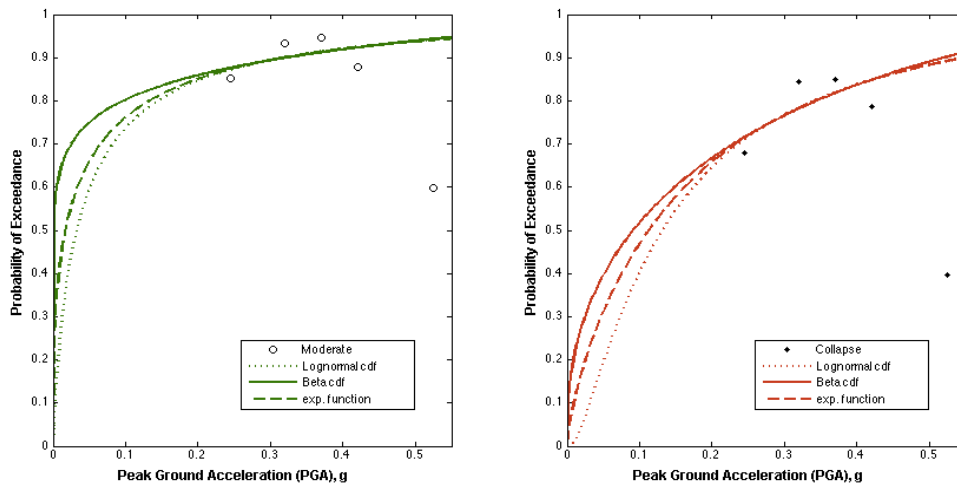


Figure 4.24 Comparison of fitted functions in PGA

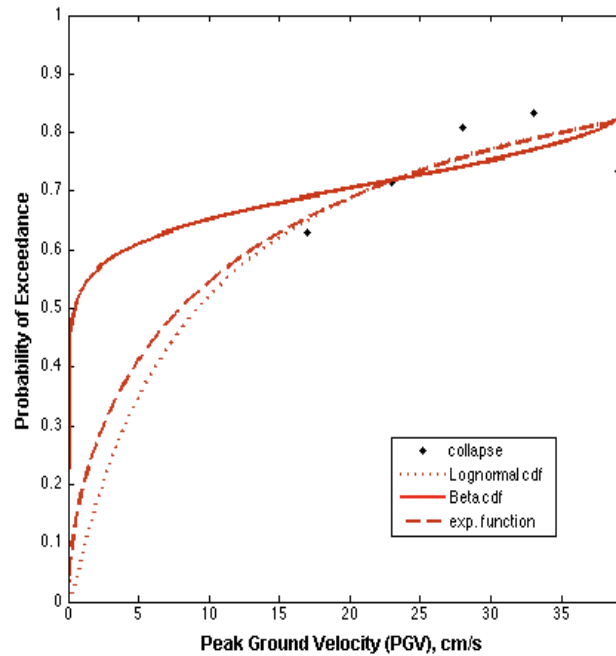


Figure 4.25 Comparison of fitted functions in PGV

Fragility curves developed as a function of PGV for the collapse damage state are presented in Figure 4.25. The independent variate in the beta distribution is bound between 0 and 1; therefore, the PGV values are scaled using Eq. (4.1) as suggested by Hahn and Shapiro (1994) and the curve fitting procedure for a 2-parameter cumulative beta distribution discussed in Chapter 3 is then applied to obtain the fragility curves.

$$x' = \frac{x - a}{b - a}; \text{ where } a \leq x \leq b \quad (4.1)$$

Curves for the moderate damage state have not been shown as all three functions were found to fit poorly to the cumulative probabilities and they do not provide any meaningful explanation of the damage. The cumulative lognormal and exponential curves have similar shapes while the cumulative beta curve has a steeper rise. The extent of damage can again

be observed as a function of PGV where over 50% of the buildings are estimated to reach or exceed the collapse damage state at a PGV of 10 cm/s.

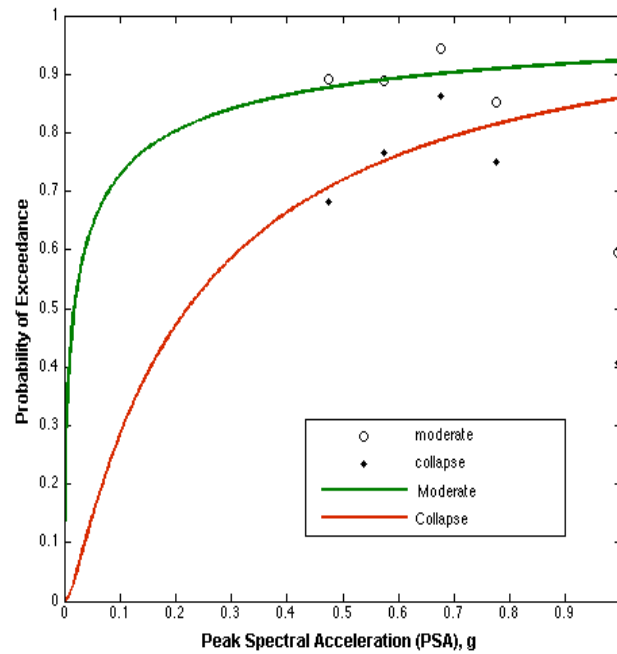


Figure 4.26 Cumulative lognormal distribution fragility curves in PSA (0.3s period, 5% damping)

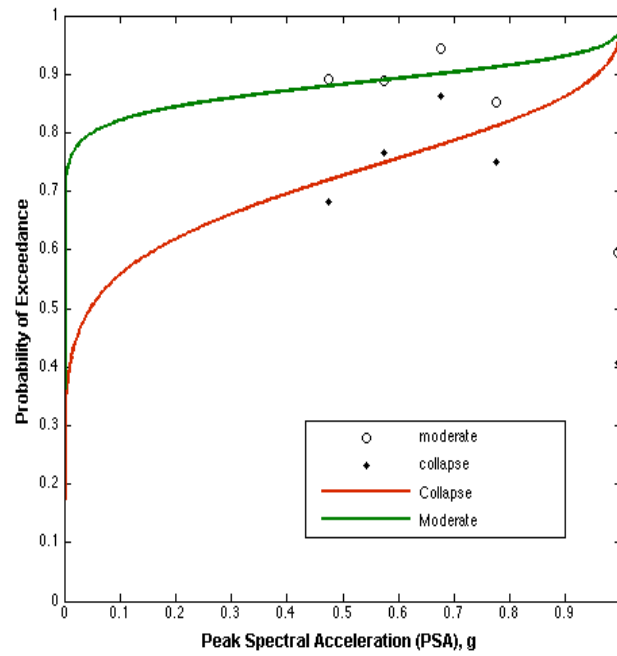


Figure 4.27 Cumulative beta distribution fragility curves in PSA (0.3s period, 5% damping)

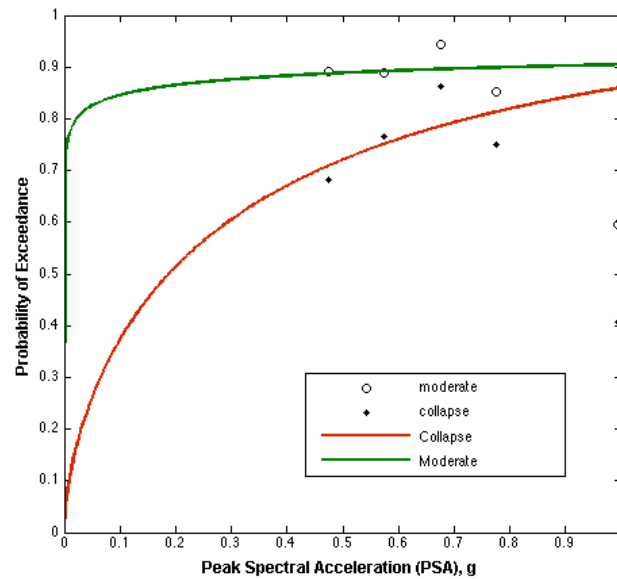


Figure 4.28 Exponential fragility curves in PSA (0.3s period, 5% damping)

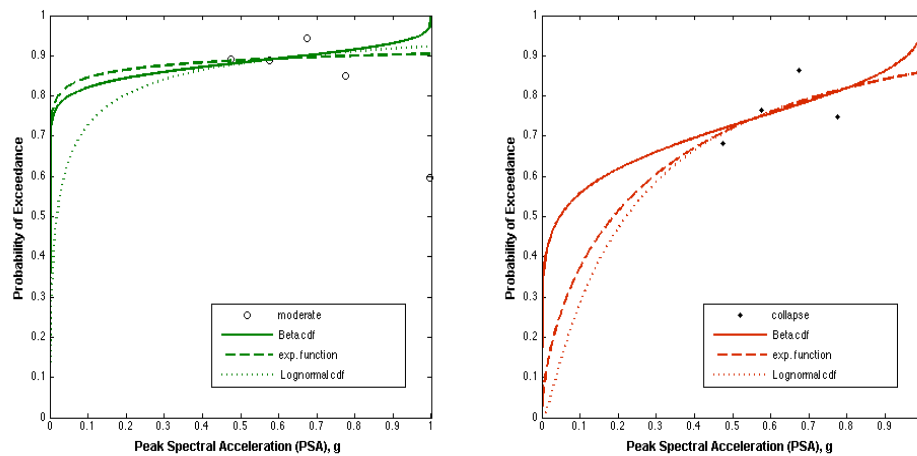


Figure 4.29 Comparison of fitted functions in PSA

The final group of fragility curves developed as a function of PSA at a period of 0.3s with 5% damping are shown in Figure 4.26 to Figure 4.28. The curves estimate that 80% of the buildings would have suffered moderate damage or 50% of the buildings would have collapsed at a spectral acceleration of 0.2g. A comparison of the curves in Figure 4.29 indicates that the cumulative lognormal and exponential curves are particularly similar in contrast to the cumulative beta curve for the collapse damage state. However, for the moderate damage states, the cumulative beta curve agrees, in term of the overall shape, with the exponential curve for PSA values less than 0.6g, and higher values show that the cumulative lognormal and exponential curves are almost identical. The R-square values in Table 4.2 suggest that the exponential function provides an overall better fit to the cumulative probabilities for both damage states derived from the case study damage data.

Table 4.2 Fragility curve results

	DS ¹	Analytical Function	SSE ²	R-square ³	Adjusted R-square ⁴	RMSE ⁵	Parameters (with 95% confidence bounds)
PGA	M	Cumulative Lognormal	0.0476	0.4080	0.2106	0.1259	$\mu = -3.425$ (-21.57, 14.72) $\sigma = 1.777$ (-12.06, 15.61)
	C	Cumulative Lognormal	0.0817	0.4283	0.2377	0.1651	$\mu = -2.028$ (-5.803, 1.748) $\sigma = 1.124$ (-3.339, 5.587)
	M	Cumulative Beta	0.0423	0.4729	0.2972	0.1188	$\alpha = 0.09909$ (-1.118, 1.316) $\beta = 1.06$ (-10.43, 12.55)
	C	Cumulative Beta	0.0762	0.4672	0.2896	0.1593	$\alpha = 0.4012$ (-2.353, 3.155) $\beta = 1.801$ (-8.977, 12.58)
	M	Exponential	0.0420	0.4774	0.3033	0.1183	$\alpha = 3.681$ (-8.994, 16.36) $\beta = 0.41$ (-2.679, 3.499)
	C	Exponential	0.0829	0.4200	0.2267	0.1662	$\alpha = 3.635$ (-8.746, 16.02) $\beta = 0.7586$ (-2.328, 3.845)
PGV	M	Cumulative Lognormal	-	-	-	-	-
	C	Cumulative Lognormal	0.0157	0.4074	0.2098	0.0723	$\mu = 2.221$ (0.379, 4.063) $\sigma = 1.58$ (-1.207, 4.367)
	M*	Cumulative Beta	-	-	-	-	-
	C*	Cumulative Beta	0.0216	0.1850	-0.0867	0.0848	$\alpha = 0.0577$ (-0.104, 0.219) $\beta = 0.1698$ (-0.309, 0.649)
	M	Exponential	-	-	-	-	-
	C	Exponential	0.0166	0.3738	0.1651	0.0743	$\alpha = 0.2123$ (-0.531, 0.956) $\beta = 0.5692$ (-0.502, 1.64)
PSA - 03	M	Cumulative Lognormal	0.0469	0.3710	0.1614	0.1250	$\mu = -4$ (-45.35, 37.35) $\sigma = 2.807$ (-29.78, 35.39)
	C	Cumulative Lognormal	0.0735	0.3826	0.1768	0.1565	$\mu = -1.506$ (-6.314, 3.301) $\sigma = 1.4$ (-4.869, 7.67)
	M	Cumulative Beta	0.0692	0.0712	-0.2384	0.1519	$\alpha = 0.03605$ (-0.461, 0.533) $\beta = 0.26$ (-2.676, 3.196)
	C	Cumulative Beta	0.0682	0.4269	0.2359	0.1508	$\alpha = 0.1387$ (-0.756, 1.034) $\beta = 0.3502$ (-1.435, 2.136)
	M	Exponential	0.0416	0.4416	0.4416	0.1020	$\alpha = 2.351$ (1.088, 3.614) $\beta = 0.1$ (fixed at bound)
	C	Exponential	0.0701	0.4112	0.2149	0.1528	$\alpha = 1.966$ (-0.711, 4.644) $\beta = 0.6241$ (-2.117, 3.365)

¹ DS = Damage State; M = Moderate, C = Collapse

² Sum of Square due to Errors (SSE) measures the discrepancy between the values obtained from the fitted curve and the data

³ R-square (r^2) also known as the coefficient of determination measures the success of the fit in explaining the variation of the data

⁴ Adjusted R-square is the R-square adjusted for the residual degrees of freedom calculated as number of data points (n) minus the number of fitted parameters (m) giving residual degrees of freedom (v); $v=n-m$

⁵ Root Mean Square Error (RMSE) is the standard deviation of the residuals

* Generalized cumulative beta distribution function

4.9 Discussion on the Derived Fragility Curves

4.9.1 Data Points and Fragility Curves

Fragility curves have been derived for non-engineered URM single-storey homes in Bantul, Indonesia using post-earthquake damage data and USGS ground motion ShakeMaps. The damage distribution trends discussed earlier, in particular the highest ground motion intervals have been explored further to assess their influence on the fragility curves. A summary of fragility curve parameters and statistical measures presented in Table 4.2 are used to draw observations on the adequacy of the fragility curves. Furthermore, the shapes of the curves and the probabilistic interpretations have also been examined.

The final data point in the fragility curves in terms of PGA and PSA found in Figure 4.21 to Figure 4.23 and Figure 4.26 to Figure 4.28, are observed to be considerably lower in contrast to the rest of the points. As discussed in Section 4.7, the probabilities of the light and collapse damage states are almost equal and significantly lower for the highest PGA and PSA intervals as a result of the damage distribution within these intervals. Consequently, this divergent trend is then carried over when cumulating the probabilities that are used to fit the data. The overall damage distribution strongly suggests that with more data collected in areas experiencing higher ground shaking, this divergent data point would follow the damage trends exhibited in the lower ground motion intervals.

The last data point is considered as an outlier; however, not as a result of an experimental error but rather as a consequence of deviation of the damage distribution as discussed above. The influence of this data point has been reduced by applying a robust weighted minimized sum of squares error method called bisquares weights, which is discussed in

Chapter 3. Exclusion of the last data point during a trial curve fitting exercise yielded no changes to the shape of the fragility curves. The trial curve fitting exercise also served as verification to the bisquares weights method. Figure 4.30 presents the cumulative lognormal fragility curves in terms of PGA fitted with and without the last data point on the same plot. The plot shows negligible change in the shape from the exclusion of the highest PGA interval. Similar results were obtained for all other PGA and PSA curves and have been attached in Appendix A. Therefore, the last data point was included in the derivation of the final fragility curves as it had insignificant influence on the shape of the curve.

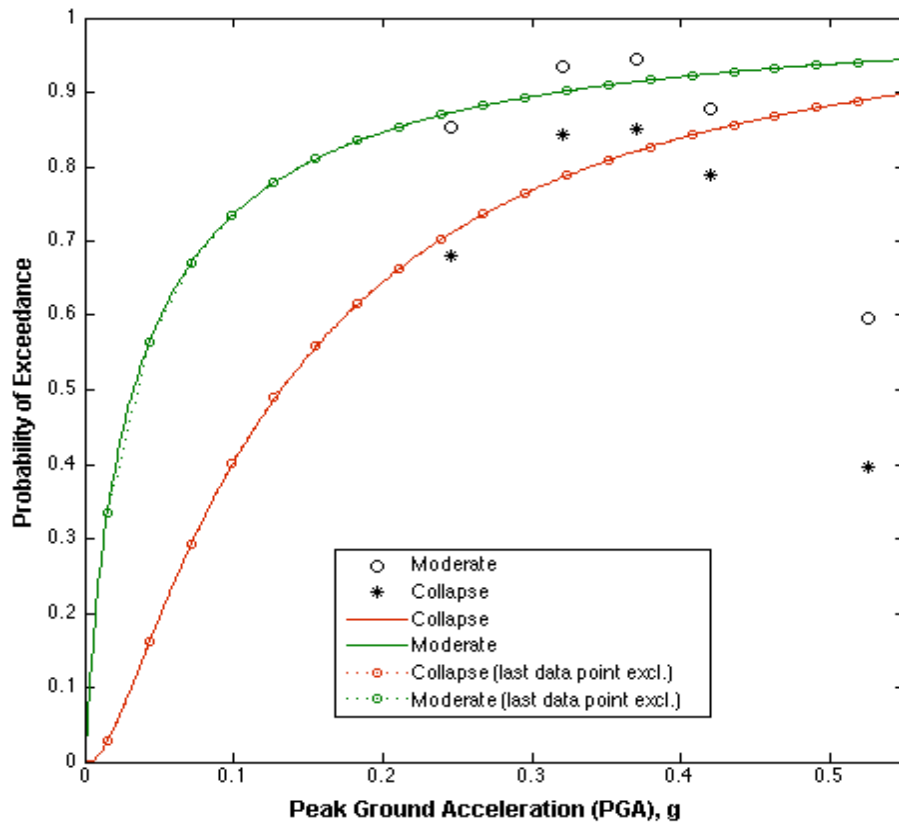


Figure 4.30 Fragility curves fitted with and without the last data point (cumulative lognormal fragility curve in terms of PGA)

The extent of damage exhibited by the fragility curves is not surprising in the context of the reported damage statistics. Over 142,000 buildings were reported to have been heavily damaged or destroyed in the Bantul Regency (OCHA 2006) as a result of the Yogyakarta earthquake. This number represents over 78% of the total housing stock in the area before the earthquake (BAPPENAS et al. 2006). A breakdown of the damage according to the construction types is not available, however, several reports indicate that the most common form of housing found in the area was of brick construction (EERI 2006, Elnashai et al. 2007). Therefore, the distribution of the damage data used in the derivation of the fragility curves is representative of the damage proportions experienced during the earthquake.

In addition to the high vulnerability observed in the fragility curves for Indonesian URM buildings, it is important to assess the shapes of the curves. All the fragility curves in this study exhibit a steep rise, almost vertical at the origin for some instances, at lower ground motion intensities. Similar features were noted by Rota et al. (2008b) in the derivation of empirical fragility curves for Italian structures illustrated in Figure 4.31. It is commonly assumed that fragility curves will follow an S-shape, however this is not always that case. Rota et al. (2008b) suggests that the shapes of the curves depend on the form of the distribution that is fitted to the data and the steep rise was attributed partly to the lognormal distribution expression and in particular, to the low and often negative mean parameter values. Likewise, the mean parameter values (μ) for cumulative lognormal distribution function given in Table 4.2 are also primarily negative. Rota et al. (2008b) further explains that the parameters of the functions are directly derived from the damage data, and they reflect the distribution of the damage where damage is present even for very low

values of PGA. However, in the present study, all three analytical expressions used to fit curves to the cumulative probabilities were found to exhibit the steep branch suggesting the influence of the consistently high levels of damage across all ground motion intervals in the damage distributions in Figure 4.10 to Figure 4.12. It is also possible that damage data for the lower ground motion ranges, which is lacking in the present study, would influence the shape of the curve. However it is expected to be minimal as the proportions of collapse are significantly high across the ground motion ranges resulting in high cumulative probabilities.

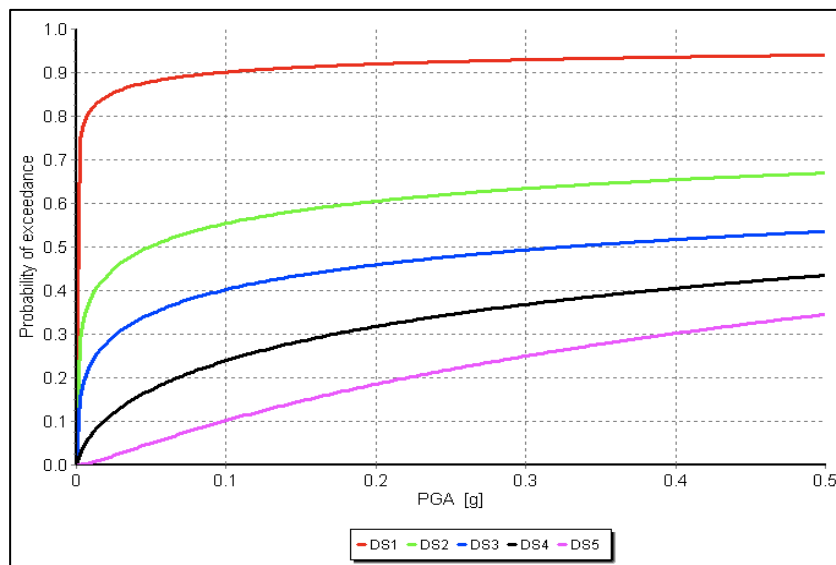


Figure 4.31 Fragility curves for building typology IMA2 (Rota et al. (2008b) found in: Crowley et al. (2011a))

4.9.2 Curve Fitting Statistics

Furthermore, the lack of data for the lower ranges of ground motion also reduces the R-square values for the fitted curves. R-square values given in Table 4.2 are often interpreted as a measure for goodness of fit of the curve to the data. However, more specifically, it expresses the adequacy of the fitted curve in explaining the variation present in the data. R-square is a ratio of the variation of the fitted values around the mean to the

variation of the observed values around the mean, and is mathematically defined as the ratio of sum of squares of regression (SSR) to the total sum of squares (SST) as shown in Eq. (4.2). The R-square value can also be related to the variation of the observed values around the fitted curve defined as summed squares of residuals or sum of squares due to error (SSE) as in Eq. (4.3).

$$R^2 = \frac{SSR}{SST};$$

$$SSR = \sum_{i=1}^n w_i (\hat{y}_i - \bar{y}_i)^2, \text{ and} \quad (4.2)$$

$$SST = \sum_{i=1}^n w_i (y_i - \bar{y})^2$$

$$R^2 = 1 - \frac{SSE}{SST}; \text{ where} \quad (4.3)$$

$$SSE = SST - SSR = \sum_{i=1}^n w_i (y_i - \hat{y}_i)^2$$

R-square is often evaluated between 0 and 1, with closer to unity indicating a good fit, and closer to 0 indicating a poor fit. However, it has been argued that the R-square is an inadequate measure of goodness of fit and can often be misleading (Fonticella 1998; Legates and McCabe 1999). Evaluation of R-square as a measure of goodness of fit is beyond the scope of this report; however, it is sufficient to recognize that the goodness of fit cannot be evaluated solely based on the R-square value. It is more appropriate to use the R-square value to evaluate the amount of

variation present in the data that is explained by the curve and the R-square values for the fragility curves fitted given in Table 4.2 have been evaluated considering this definition.

R-square values for the fragility curves in this study are fairly low and can be attributed to the lack of data coverage particularly at lower ground motion intensities (Mac Berthouex and Brown 2002). This is a common concern with empirical derivations and is resolved by using damage data from multiple earthquakes (Rossetto and Elnashai 2003). However, as discussed in Section 2.2.1, the use of damage data from different earthquakes can induce additional uncertainty among other complications. Therefore, this study utilized data from a single earthquake only, and found that the R-square values were comparable to those reported by Rossetto and Elnashai (2003) that employed a large dataset from several earthquakes. The R-square values in Table 4.2 for fragility curves derived using the exponential functions in terms of PGA range between 0.42 and 0.48, and those in Rossetto and Elnashai (2003) range between 0.28 and 0.39. Similarly, R-square values for exponential functions in terms of spectral acceleration range between 0.41 and 0.44 compared to Rossetto and Elnashai (2003) which range between 0.37 and 0.52. The R-square values indicate that less than 50% of the variation present in the data can be explained for most of the fragility curves. Comparison of R-square values with additional existing empirical fragility studies was not possible, as they are often not reported in literature. The R-square values obtained in this fragility curve are considered reasonable considering the unpredictable nature of earthquakes, inconsistencies in data collection methods, and small datasets lacking sufficient coverage of ground motion intensities, ultimately contribute to the quality of empirical fragility curves.

R-square will tend to inflate as the number of coefficients in a model or function is increased and to account for this, an *adjusted* R-square in Eq. (4.4) is used. This value is particularly important when comparing several models with different number of coefficients; however, this is not the case with the functions used in this study, as the number of parameters is consistent.

$$\text{adjusted } R^2 = 1 - \frac{SSE(n-1)}{SST(v)}; \text{ where}$$

$$n = \text{number of data points or response values} \quad (4.4)$$

$$v = \text{degrees of freedom} = n - m$$

$$m = \text{number of fitted coefficients}$$

The root mean square error (RMSE) in Eq. (4.5) is another measure that is used to assess the goodness of fit of the fitted curve. It is defined as the standard error of the model or the standard deviation of the model and is in the units of the dependent variable. The RMSEs for the fragility curves indicating the standard deviation in prediction of the probability of exceedance, in terms of PGA, ranges between 0.11 and 0.17, and in terms of PSA, ranges between 0.10 and 0.16. PGV has not been considered in discussion, as several of the curves could not be fit to the data.

$$RMSE = \sqrt{MSE}; \quad MSE = \frac{SSE}{v} \quad (4.5)$$

4.9.3 Comparable Fragile Structures

The probabilities of exceedance for both damage states are considerably high at even lower ground motion intensities for all fragility curves developed in this study. Moderate damage or worse can be expected with a probability of almost 0.8 or 80% at a PGA of only 0.1g, and the curves present very steep slopes at low ground motion intensities. Similar observations can be made of the fragility curves in terms of PSA. The extreme form of damage expectation is quite alarming and requires some further assessment. An effort has been made to review existing fragility studies to find fragility curves exhibiting similar high probabilities of damage.

A study on the vulnerability of adobe dwellings in Peru by Tarque et al. (2010) predicts from their fragility curves reproduced in Figure 4.32, that almost 98% of the buildings will sustain or exceed LS3, and over 90% of the buildings will reach LS4. LS3 corresponds to in-plane failure resulting in significant structural damage characterized by beginning of horizontal cracking and significant loss in original stiffness. Collapsed or almost collapsed damage state is categorized as LS4 corresponding with the inability to repair the damage and posing danger to occupants. The curves highlight the high seismic vulnerability associated with such non-engineered structures in developing countries.

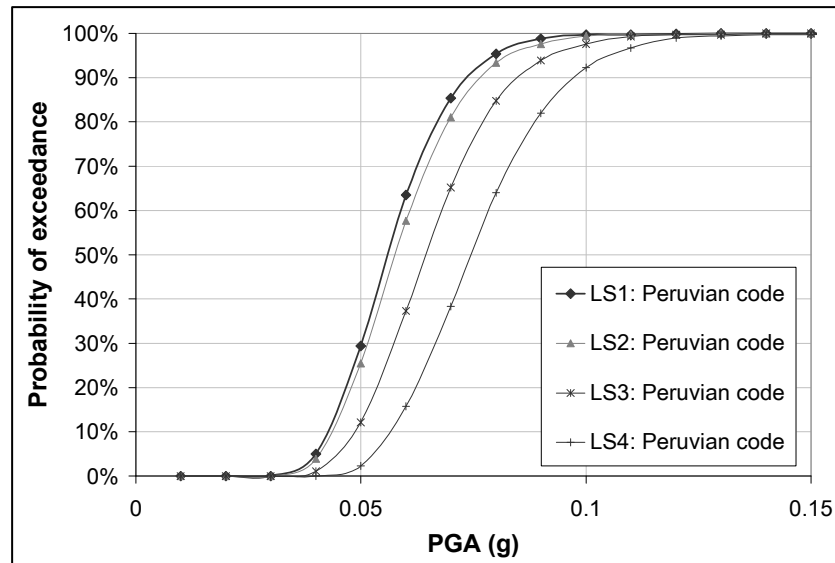


Figure 4.32 In-plane failure fragility curves (Tarque et al. 2010)

4.10 Comparison with existing fragility curves

The main purpose of this section is compare the performance of the single-storey URM buildings discussed in the context of developing countries in this study to similar structures in other regions. It is an arduous task to find appropriate fragility studies to carry out comparisons, as fragility curves are inherently a function of the tectonic characteristics of earthquakes and diversity of regional construction techniques and materials. The various components of the fragility curves, such as number of damage states used, the range of ground motions, and the analytical functions used to describe the curves also need to be considered in any meaningful comparisons. A set of criteria is established to select a study that requires a suitable level of manipulation to carry out some direct comparisons with the fragility curves developed within this report.

Fragility curves selected for comparison are to meet the following criteria:

- Derived using the empirical method

- Two damage states
- Single-storey URM brick buildings or similar structural typology
- Ground motion parameter in terms of PGA, PGV, or PSA
- Analytical functions describing the fragility curves to be cumulative lognormal, cumulative beta, or exponential function

A review of existing fragility curves found no study that met all of the above criteria; however, fragility curves for Turkish masonry structures developed by Erberik et al. (2008) that were discussed in Chapter 2 were found to satisfy most of the requirements. The cumulative lognormal fragility curves were derived using an analytical approach as a function of PGA using structural parameters observed in existing earthquake compiled in a database for the region. The primary concerns in carrying out comparison with fragility curves developed using a different approach are the assumptions and methods used to develop the damage database. However, in the absence of other adequate empirical fragility studies, the analytical fragility curves are used and the challenges arising as a result are discussed below.

While not all fragility curves in the Turkish fragility study are accessible, thirteen sub-classes of structural typologies that are commonly found in Europe have been collected as part of the Syner-G project (Crowley et al. 2011a). Three fragility curves for URM buildings denoted as M1EU, M1NR and M1NU are relevant to the criteria established and have been extracted using the Fragility Function Manager tool developed by the Syner-G project team. These building classes are considered to be non-engineered by Erberik (2008) and are described briefly in Table 4.3. Fragility curves for the Indonesian structures derived in this study are labeled as “*Bantul*” in Figure 4.33 and Figure 4.34.

Table 4.3 Descriptions of Turkish building sub-classes (Erberik 2008)

M1EU	<ul style="list-style-type: none"> • URM – Fired brick with cement mortar • Average compressive strength – 4 MPa to 8 MPa • Regular plan with regular elevation • Moderate code level
M1NR	<ul style="list-style-type: none"> • URM – Adobe, rubble, stone, with mud mortar • Average compressive strength – 2 MPa to 4 MPa • Regular plan, with regular and irregular elevation • Thatch or corrugated metal sheet roof • No code
M1NU	<ul style="list-style-type: none"> • URM – Concrete masonry unit, hollow clay tile, with lime mortar • Average compressive strength – 2 MPa to 4 MPa • Irregular plan, with regular and irregular elevation • Low code level

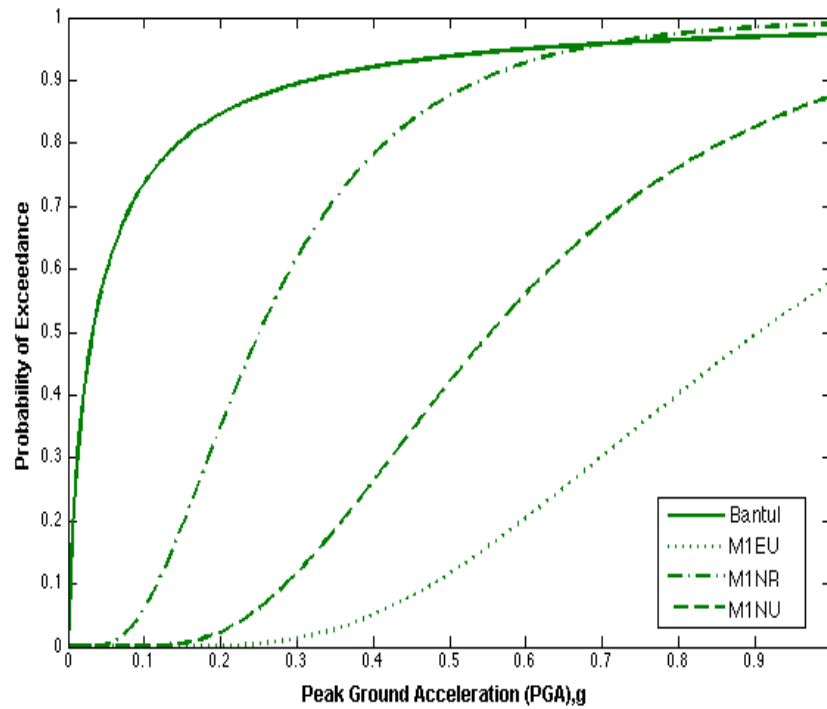


Figure 4.33 Comparison with Turkish fragility curves (moderate damage state)

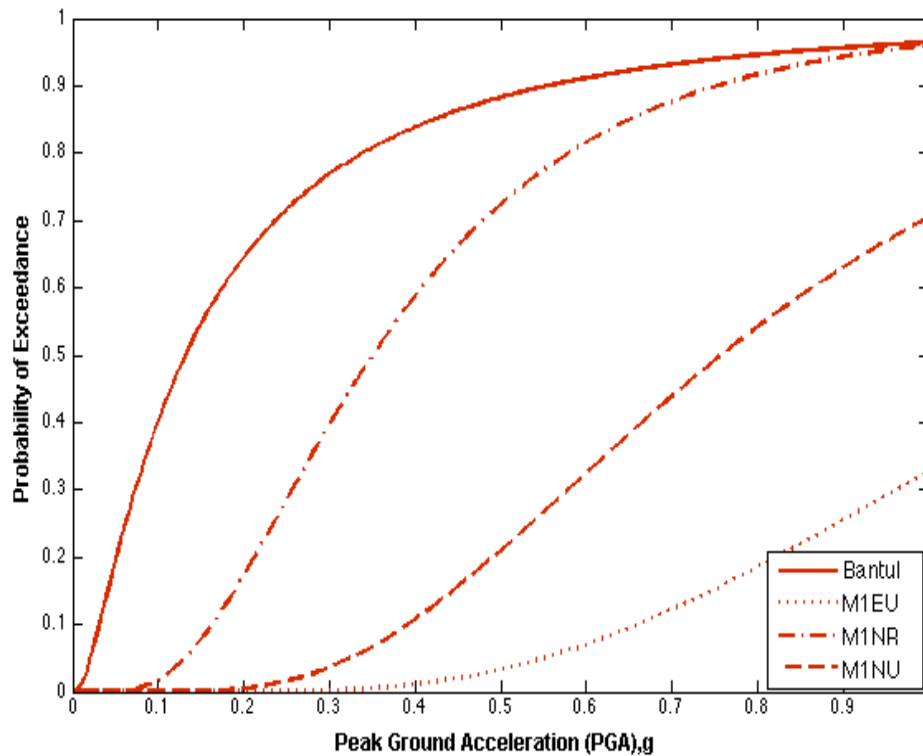


Figure 4.34 Comparison with Turkish fragility curves (collapse damage state)

The fragility curves for the Indonesian and Turkish buildings in Figure 4.33 and Figure 4.34 are significantly different. The non-engineered Indonesian structures are considerably more fragile than presumably the weakest of the three Turkish structural typologies, M1NU, particularly at lower PGA values. M1EU is the most comparable construction to the Indonesian URM buildings with its use of fired-clay bricks; however, the average compressive strength and mortar quality of the M1EU category summarized in Table 4.3 are higher. The URM brick masonry homes in Indonesia are generally constructed using sand-clay mortar or weak cement-sand-lime mortar (Build Change 2008) that is often brittle. The brittleness of the mortar is attributed to the application of acrylic based and weather shield paints that prevent moisture from penetrating the wall

surface (Boen 2006). The compressive strength of the clay bricks used for construction in Indonesia vary between 2 MPa and 6 MPa (Elnashai et al. 2007). The improved performance of the M1EU category can be associated with the quality of materials used since in-plane failure of URM buildings is generally governed by the compressive strength of the brick, and the quality of mortar. However, in comparison, the Canadian and American material standards, CSA A82-06 (2006) and ASTM C216-12 (2012), respectively, require a minimum compressive strength of 20.7 MPa for exterior grade fired clay bricks. This further illustrates the disparity of material quality between code-enforced construction in developed countries and non-engineered buildings in developing countries.

The M1NR and M1NU categories belong to a similar structural typology and have been included in the comparison to show the extent of vulnerability involved with non-engineered houses in Indonesia. These two categories are constructed from inferior materials, and meet very few seismic design criteria set by the local design codes, or none at all. The fragility of structures resulting from a lack of engineering input or code compliance is clearly evident in the comparison of the fragility curves above. The Indonesian structures and the two weaker categories of Turkish buildings would be expected to perform comparably; however, as highlighted in Figure 4.33 and Figure 4.34, the single-storey houses in Indonesia are much more vulnerable. This observation suggests that there may be other factors that influence the curves besides the known structural and material variations.

One possible factor that considerably impacts the fragility curve is the method used in deriving the fragility curve, in particular, the analytical method. The fragility curves for buildings in Turkey have been derived considering in-plane failure modes only. However, Bothara et al. (2011)

have observed that for stone masonry as that used in category M1NR, the in-plane failure is less dominant than the out-of-plane failure modes. Similarly, out-of-plane failure in adobe buildings and stone masonry buildings has commonly been observed during earthquakes (Kaplan et al. 2008; Ural et al. 2012). The simplification of analytical model to evaluate damage often leads to an underestimation of the potential damage. Depending on the construction methods employed, several other failure modes can govern the damage states that might not be considered in the analytical model. In contrast, the empirical damage data used to develop fragility curves inherently includes all failure modes as the level of damage is recorded visually. In particular, the fragility of the URM buildings during the Yogyakarta earthquake were attributed mainly to weak and brittle mortar, inadequate connections between primary building elements, and poor diaphragm action (Bali et al. 2006; Boen 2006; Elnashai et al. 2007). This observation is pertinent for non-engineered buildings in developing countries as the construction quality and techniques vary significantly, and it is impossible to account for all these variations in analytical models.

Fragility curves derived using empirical methods can significantly vary from those derived using analytical methods, for the same structure. Several other factors such as local construction knowledge and techniques, and local material quality that are influenced by socioeconomic conditions of the population or region can also contribute to the differences observed in the fragility curves. However, the influence of these factors on the fragility curves requires substantial investigation and is beyond the primary scope of this study. In general, the observations discussed can be considered as an impetus to carry out additional fragility studies with the intention of understanding and assessing the influence of different factors influencing the fragility curves. Finally, the comparison

between the fragility curves highlights the influence of the key components of fragility curves, and the challenges involved in assessing structural performance of buildings through comparative analysis.

4.11 Conclusion

Fragility curves derived using empirical damage data indicate the high seismic vulnerability of non-engineered URM single-storey homes, particularly in developing countries. The exceedance of moderate and heavy/collapse damage states is significantly probable at all ground shaking intensities. Moderate damage or worse can be expected with a probability of almost 0.8 or 80% at a PGA of only 0.1g. Such high levels of probable damage have also been indicated for other non-engineered structures including adobe homes in Peru (Tarque et al. 2010). The fragility curves presented in this study supplement the limited collection of fragility curves for developing countries, particularly those derived using the empirical approach.

It is obvious that the damage data collected after the 2006 Yogyakarta earthquake was not intended for the derivation of fragility curves; however, a substantial effort has been made to utilize and apply the available data in a fragility study. Furthermore, the lack of ground motion data in the region was addressed through the use of USGS ShakeMaps for PGA, PGV, and PSA. Three analytical expressions were explored in fitting the empirical data with fragility curves, and the shapes were found to be very similar. In addition, fragility curves were derived as a function of three ground motion parameters. The correlations obtained in the curve fitting are fairly low for all three parameters, with the PGV curves yielding the worst fit. Overall, minimal variation in quality of fit was observed between the choices of analytical functions, however the exponential function used

as a function of PSA provided the best fit to the observed data. The R-square values for the fitted curves were found to be comparable to existing empirical fragility curves even with a smaller dataset that lacked sufficient coverage of ground motion intensities. Overall, the fragility curves derived can be considered to be reasonable given the size and quality of data; however the direct use of these curves to assess seismic risk is not recommended without further investigation.

A comparison of the fragility curves in the present study with existing fragility curves derived by Erberik (2008) suggests that there are several factors that can influence the curves. The most significant factor is the type of method used to derive the fragility curves. Analytical method utilizes mechanical parameters of an idealized structure to assess the damage in contrast to the visual observation of damage in the empirical method. It was found that the existing fragility curves were significantly less vulnerable as the analytical model only considered in-plane failure modes. Therefore, it is recommended that the use of simplified or idealized analytical models for deriving fragility curves is limited only for verification purposes in the case of developing countries because of the rich diversity in construction techniques and material quality.

5 Conclusions and Recommendations

5.1 Summary

The impact of natural disasters is far greater on developing countries than developed countries as a result of lower socioeconomic conditions. Socioeconomic conditions significantly influence the construction methods, quality of materials, and in general, public awareness of structural safety. Poorly constructed structures lacking adequate resistance to earthquakes are the major cause of deaths in developing countries during earthquakes. Global disaster risk reduction agreements such as the Yokohama Strategy and Hyogo Framework have recognized the need to develop disaster risk reduction strategies specifically addressing developing countries. Fragility of structures is a key component in assessing seismic risk and is defined by its potential to suffer damage as a result of a given seismic force on the structure. Fragility curves are therefore used to express this concept probabilistically by describing the probability of reaching or exceeding specific damage states as a function of the seismic intensity parameter.

Fragility curves are generally derived using empirical, analytical, expert-opinion, and hybrid approaches. The important difference between these methods is the source of the building damage data. Damage data sources include post-earthquake damage surveys, analytical models, expert opinions, and a combination of these methods. A methodology for deriving fragility curves using an empirical approach has been presented in this study. The methodology specifically addressed the lack of ground motion recordings typically encountered in developing countries through the use of USGS ShakeMaps. Empirical damage data available in GIS format is overlaid onto the ShakeMaps. The merged database provides a ground motion intensity and damage state for each building. DPMs and

cumulative DPMs are then developed from this database, which are subsequently used to derive fragility curves. The methodology was then applied to a case study comprising of damage data from the 2006 Yogyakarta earthquake in Indonesia. Fragility curves were developed for single-storey URM houses as a function of PGA, PGV, and PSA. This type of housing is pervasive in developing countries and is categorized as non-engineered since they are constructed without the input of engineers or design codes. The fragility curves were derived using three analytical functions: cumulative lognormal, cumulative beta, and exponential. Finally, the fragility curves were compared to an existing fragility study on non-engineered Turkish buildings carried out by Erberik (2008).

5.2 Conclusions

Literature review conducted in this research presented very few fragility studies for structures in developing countries considering the great impact of earthquakes on these countries. Lack of data, both, ground motion and damage data, are frequently cited as key obstacles. While there are efforts in progress to create global tools, existing seismic risk assessment tools do not necessarily account for the structural diversity present in developing countries. Furthermore, many parts of the developing world lack ground motion data and as a result, the tools incorporate records from other regions. Therefore, it is necessary to assess and integrate the fragility of structural typologies found in developing countries into future risk assessment tools.

There are several methods of deriving fragility curves and the primary difference between the methods is the data source. The analytical method is preferred for deriving fragility curves for developing countries, as it does not require damage data that is often not available. However, the diversity

of construction techniques and details in non-engineered structures commonly found in developing countries make it difficult for an analytical model to idealize all possible variations. Model simplifications can lead to an over- or under-estimation of vulnerability. Empirical data inherently include the variations in a structural typology and give a better representation of the damage. It is therefore imperative to utilize any post-earthquake data when available to empirically derive fragility curves for developing countries.

The damage data used in the case study was collected by the UGM located in D.I. Yogyakarta, in the immediate aftermath of the May 2006 Yogyakarta earthquake. The total number of houses in the Bantul region that experienced some kind of damage during the Yogyakarta earthquake is reported to be around 208,697 (OCHA 2006). Fragility curves derived for single-storey URM brick houses represent almost 16% of the total homes that were either damaged or destroyed. This is a significant sample; however, the dataset was still lacking sufficient details, particularly about the descriptions or definitions of the damage states. It is also not clear as to whether all buildings in the regency were surveyed or only those that were observed to have a specific level of damage were recorded. In addition, it is obvious from the damage dataset that it was not collected to develop fragility curves as the metadata is not standardized and several different terms are used to describe similar observations. Despite these limitations, the use of the available dataset has been exhausted with the aid of several assumptions, as it was difficult to find such a large dataset from a single earthquake without any deficiencies. Post-earthquake surveys are also frequently carried out for purposes other than fragility studies, and are often not easily accessible as they are considered to be proprietary or sensitive information (EERI 2003). Further

details and recommendations on the collection and management of seismic damage data are provided by EERI (2003).

The DPMs for the case study dataset indicate extensive damage at all ground motion intervals and the fragility curves show high probability of damage at very low values of all three ground motion parameters i.e. PGA, PGV, and PSA. The fragility curves exhibited a steep rise at low ground motion intensities as a result of the high damage probabilities. For example, the fragility curves indicate that there is probability of 80% that damage to a single-storey URM house will include significant cracking of the walls resulting in a reduced load carrying capacity of the structure, or worse, at a PGA of only 0.1g. Similarly, the probability of exceedance of the Heavy/Collapse damage state is also high. This trend is observed for all analytical functions used in describing the fragility curves in this study. It is important to note that the results and observations presented in the case study are limited to the specific damage levels identified and the dataset used. This dataset included several parameters that are specific to the case study including, but not limited to, the building topography, seismic hazard level, and construction techniques. As such, the application of the derived fragility curves as a general damage prediction tool to what may be perceived to be similar scenarios is strictly not recommended due to the significant variation in parameters relating to each particular situation.

All the fitted curves have low R-square values; however, the PGA and PSA curves using the cumulative lognormal and exponential functions provided better representation of the data. The RMSEs indicate that the curves predict at an average, within 7% to 17% of the actual probability of exceedance from the data. The statistics for the fragility curves obtained

are reasonable considering the limitations of the data used in the case study discussed earlier.

5.3 Recommendations

This section outlines recommendations in general, and for future work, based on the observations made in this study. The recommendations address the study of fragility curves in the area of seismic risk assessments, and in the derivation of fragility curves. The recommendations are as follows:

- Cumulative lognormal function is most commonly used for fragility curves; however, other analytical expressions should be reviewed as some of them have shown to give reasonable results. In this study, the exponential function used by Rossetto and Elnashai (2003) was applied and was observed to produce slightly better fitting curves for the case study damage data.
- Detailed analytical models representing single-storey URM brick buildings such as those in the dataset should be developed for comparison and verification purposes. The model should consider the damage descriptions used in post-earthquake surveys and adapt them to mechanical properties such as the ISD. The results should be used to derive fragility curves and compared to those in this study.
- Further research is required in the field of seismic risk assessment, and particularly in the development of additional fragility curves for non-engineered structures in developing countries.
- Empirical method of deriving fragility curves is generally preferred over the other methods; however, a common concern with this

approach is the lack of post-earthquake damage data. A concerted effort should be made by multinational organizations to encourage and provide incentives for local agencies to collect damage data after earthquakes that include sufficient information about the damaged buildings. The data should also be collected using GPS technology and presented in a GIS format. Furthermore, the data should be made publicly available for research studies.

- An effort to develop a global taxonomy of engineered and non-engineered building typologies is being carried out by GEM (Crowley, Colombi, et al. 2010). However, there is an urgent need to standardize post-earthquake surveys that incorporate the global building taxonomies, and to develop consistent building damage states. This will allow the development of seismic risk assessments that can utilize a combination of fragility curves from different regions with a level of consistency. It will also enable a direct comparison of fragility curves for different building typologies.

Bibliography

- Abrams, D. P. (2000). "Damage and Performance of Unreinforced Masonry Buildings in Earthquakes." *Proceedings of the 2nd Multi-lateral Workshop on Development of Earthquake and Tsunami Disaster Mitigation Technologies and Their Integration for the Asia-Pacific Region*, Kobe, Japan, 163–166.
- Ahari, M. N., and Azarbakht, A. (2005). "Report No. 114: Stonework Building with Wooden Timber Roof." *World Housing Encyclopedia*, <<http://world-housing.net/wherereport1view.php?id=100111>> (May. 2011).
- Ahmad, N., Crowley, H., Pinho, R., and Ali, Q. (2010a). "Derivation of Displacement-Based Fragility Functions for Masonry Buildings." *Proceedings of the 14th European Conference on Earthquake Engineering*, Ohrid, Macedonia.
- Ahmad, N., Crowley, H., Pinho, R., and Ali, Q. (2010b). "Simplified Formulae for the Displacement Capacity, Energy Dissipation, and Characteristic Vibration Period of Brick Masonry Buildings." *Proceedings of the 8th International Masonry Conference*, Dresden, Germany, 11(2), 1385–1394.
- Ali, Q. (2006). "Report No. 112: Unreinforced Brick Masonry Residential Building." *World Housing Encyclopedia*, <<http://www.world-housing.net/wherereport1view.php?id=100109>> (May. 2011).
- Ali, Q., and Muhammad, T. (2007). "Report No. 138: Stone Masonry Residential Buildings." *World Housing Encyclopedia*, <<http://www.world-housing.net/wherereport1view.php?id=100145>> (May. 2011).
- Allen, T. I., Wald, D. J., Hotovec, A. J., Lin, K., Earle, P. S., and Marano, K. D. (2008). "An Atlas of ShakeMaps for Selected Global Earthquakes: U.S. Geological Survey Open-File Report 2008–1236." *United States Geological Survey*, Reston, Virginia.
- Anagnos, T., Rojahn, C., and Kiremidjian, A. S. (1995). *NCEER-ATC Joint Study on Fragility of Buildings*. National Center for Earthquake Engineering Research (NCEER), Buffalo, NY.
- Ansary, M. (2003). "Report No. 91: Single-Storey Brick Masonry House." *World Housing Encyclopedia*, <<http://www.world-housing.net/wherereport1view.php?id=100098>> (May. 2011).
- ASTM, International. (2012). *ASTM C216-12, Standard Specification for Facing Brick (Solid Masonry Units Made from Clay or Shale)*. West Conshohocken, PA, USA.
- Astroza, M., Moroni, O., Brzev, S., and Tanner, J. (2012). "Seismic Performance of Engineered Masonry Buildings in the 2010 Maule

- Earthquake.” *Earthquake Spectra*, 28(S1), S385–S406.
- Aswandono, B. (2011). “Building Replacement Cost for Seismic Risk Assessment in Palbapang Village, Bantul Sub-District, Yogyakarta Indonesia.” Masters Thesis, University of Gadjah Mada, Indonesia and Faculty of Geo-Information Science and Earth Observation (ITC), University of Twente, Netherlands.
- ATC, Applied Technology Council. (1985). *Earthquake Damage Evaluation Data for California (ATC-13)*. Federal Emergency Management Agency, Washington D.C., USA.
- ATC, Applied Technology Council. (2011). *Seismic Performance Assessment of Buildings: Volume 1 – Methodology*. Federal Emergency Management Agency, Washington D.C., USA.
- Bakhshi, A., and Karimi, K. (2006). “Method of Developing Fragility Curves - a Case Study for Seismic Assessment of Masonry Buildings in Iran.” Tehran, Iran.
- Bakhshi, A., Bozorgnia, Y., Ghannad, M., Khosravifar, A., Mousavi Eshkiki, S., Rahimzadeh Rofooei, F., and Taheri Behbahani, A. (2005). “Seismic Vulnerability of Traditional Houses in Iran.” *Proceedings of the 1st International Conference on Seismic Adobe Structures*, Lima, Peru.
- Bali, I., Kuo, W., Lesmana, C., Suswanto, B., Lin, K., Chen, C.-C., Ko, J.-W., and Hwang, S.-J. (2006). “Structural damage observation and case study of 2006 Yogyakarta earthquake.” *International Seminar and Symposium on Earthquake Engineering and Infrastructure & Building Retrofitting*, Yogyakarta, Indonesia.
- BAPPENAS. (2010). *Report on the Achievement of Millennium Development Goals Indonesia, 2010*. Ministry of National Development Planning/ National Development Planning Agency (BAPPENAS), Jakarta, Indonesia.
- BAPPENAS, Government of D.I. Yogyakarta, Government of Central Java, International Partners. (2006). *Preliminary Damage and Loss Assessment - Yogyakarta and Central Java Natural Disaster*. Jakarta, Indonesia, 1–141.
- Bird, J. F., and Bommer, J. J. (2004). “Earthquake Losses Due to Ground Failure.” *Engineering Geology*, 75(2), 147–179.
- Blondet, M., and Villa-Garcia, G. (2004). *Adobe Construction*. Earthquake Engineering Research Institute (EERI), Oakland, CA.
- Blondet, M., Villa-Garcia, G., Brzev, S., and Rubinos, A. (2011). *Earthquake-Resistant Construction of Adobe Buildings: A Tutorial*. Earthquake Engineering Research Institute (EERI), Oakland, CA.
- Boen, T. (2006). *Yogya Earthquake 27 May 2006, Structural Damage Report*. Earthquake Engineering Research Institute (EERI), Oakland, CA.

- Boen, T. (2010). *Retrofitting Simple Buildings Damaged by Earthquakes*. World Seismic Safety Initiative.
- Bommer, J. J., and Crowley, H. (2006). "The Influence of Ground-Motion Variability in Earthquake Loss Modelling." *Bulletin of Earthquake Engineering*, 4, 231–248.
- Bothara, J., and Brzev, S. (2011). *A TUTORIAL: Improving the Seismic Performance of Stone Masonry Buildings*. Earthquake Engineering Research Institute (EERI), Oakland, CA.
- Branch, M. A., Coleman, T. F., and Li, Y. (1999). "A Subspace, Interior, and Conjugate Gradient Method for Large-Scale Bound-Constrained Minimization Problems." *SIAM Journal on Scientific Computing*, 21(1), 1–23.
- Brzev, S. (2007). *Earthquake-Resistant Confined Masonry Construction*. National Information Center of Earthquake Engineering, Kanpur, India.
- Build Change. (2008). *Preliminary Observations of the 27 May 2006 Central Java Earthquake*. Build Change.
- Byrd, R. H., Schnabel, R. B., and Shultz, G. A. (1988). "Approximate solution of the trust region problem by minimization over two-dimensional subspaces." *Mathematical Programming*, 40(1), 247–263.
- Calvi, G., Pinho, R., Magenes, G., Bommer, J. J., Restrepo-Velez, L., and Crowley, H. (2006). "Development of Seismic Vulnerability Assessment Methodologies Over the Past 30 Years." *ISET journal of Earthquake Technology*, 43(3), 75–104.
- Clarke, R. P. (2010). "Seismic Fragility Functions for Typical URM Single-Story Residential Structures in Trinidad and Tobago." *Proceedings of the 9th U.S. National and 10th Canadian Conference on Earthquake Engineering*, Toronto, Ontario, Canada.
- Clarke, R. P., and Ramnath, R. (2009). "Report No. 156: Typical Single-Story Residential Construction Practices in Trinidad and Tobago." *World Housing Encyclopedia*, <<http://www.world-housing.net/whereport1view.php?id=100174>> (May. 2011).
- Colombi, M., Borzi, B., Crowley, H., Onida, M., Meroni, F., and Pinho, R. (2008). "Deriving Vulnerability Curves Using Italian Earthquake Damage Data." *Bulletin of Earthquake Engineering*, 6(3), 485–504.
- Crowley, H., Cerisara, A., Jaiswal, K., Keller, N., Luco, N., Pagani, M., Porter, K., Silva, V., Wald, D. J., and Wyss, B. (2010). *GEM1 Seismic Risk Report: Part 2*. GEM Foundation, Pavia, Italy.
- Crowley, H., Colombi, M., Crempien, J., Enduran, E., Lopez, M., Liu, H., Mayfield, M., and Milanesi, M. (2010). *GEM1 Seismic Risk Report: Part 1*. GEM Foundation, Pavia, Italy.
- Crowley, H., Colombi, M., Silva, V., Ahmad, N., Fardis, M., Tsionis, G., Karantoni, T., Lyrantzaki, F., Taucer, F., Hancilar, U., Yakut, A., and Erberik, M. A. (2011a). *D3.2 Deliverable: D3.2 - Fragility functions for*

- common masonry building types in Europe*. SYNER-G 2009/2012.
- Crowley, H., Colombi, M., Silva, V., Ahmad, N., Fardis, M., Tsionis, G., Papailia, A., Taucer, F., Hancilar, U., Yakut, A., and Erberik, M. A. (2011b). *D3.1 Deliverable: D3.1 - Fragility functions for common RC building types in Europe*. SYNER-G 2009/2012.
- Crowley, H., Monelli, D., Pagani, M., Silva, V., and Weatherill, G. (2011). *OpenQuake Book*. GEM Foundation, Pavia, Italy.
- Crowley, H., Pinho, R., and Bommer, J. J. (2004). "A Probabilistic Displacement-Based Vulnerability Assessment Procedure for Earthquake Loss Estimation." *Bulletin of Earthquake Engineering*, 2(2), 173–219.
- CSA, Canadian Standards Association. (2006). *Fired Masonry Brick Made from Clay Or Shale*. Canadian Standards Association, Mississauga, Ontario, Canada.
- D'Ayala, D., Jaiswal, K., Wald, D. J., Porter, K., and Greene, M. (2010). "Collaborative Effort to Estimate Collapse Fragility for Buildings Worldwide: the Whe-Pager Project." *Proceedings of the 9th U.S. National and 10th Canadian Conference on Earthquake Engineering*, Toronto, Ontario, Canada.
- DesRoches, R., Comerio, M., Eberhard, M., Mooney, W., and Rix, G. J. (2011). "Overview of the 2010 Haiti Earthquake." *Earthquake Spectra*, 27(S1), S1–S21.
- Dumova-Jovanoska, E. (2000). "Fragility curves for reinforced concrete structures in Skopje (Macedonia) region." *Soil Dynamics and Earthquake Engineering*, 19(6), 455–466.
- EERI. (1996). "Post-Earthquake Investigation Field Guide." Earthquake Engineering Research Institute (EERI), Oakland, CA, <<http://www.eeri.org/site/lfe-field-guide>> (Mar. 2012).
- EERI. (2003). "Collection & Management of Earthquake Data: Defining Issues for an Action Plan." Earthquake Engineering Research Institute (EERI), Oakland, CA.
- EERI. (2006). "The Mw 6.3 Java, Indonesia, Earthquake of May 27, 2006." Earthquake Engineering Research Institute (EERI), <https://www.eeri.org/lfe/pdf/indonesia_java_eeri_prelim_report.pdf> (Jul. 13, 2011).
- Eleftheriadou, A. K., and Karabinis, A. I. (2011). "Development of damage probability matrices based on Greek earthquake damage data." *Earthquake Engineering and Engineering Vibration*, 10(1), 129–141.
- Elnashai, A., Jig, K. S., Jin, Y. G., and Djoni, S. (2007). *The Yogyakarta Earthquake of May 27 2006*. Mid-America Earthquake Center.
- Erberik, M. A. (2008). "Generation of Fragility Curves for Turkish Masonry Buildings Considering in-Plane Failure Modes." *Earthquake Engineering & Structural Dynamics*, 37(3), 387–405.

- ESRI. (2011). "ArcGIS - Mapping and Spatial Analysis for Understanding Our World." *Environmental Systems Research Institute, Inc.*, <<http://www.esri.com/arcgis>> (Mar. 2012).
- FEMA, Federal Emergency Management Agency. (2003). *HAZUS MH MR4 - Earthquake Model Technical Manual*. Department of Homeland Security, Federal Emergency Management Agency, Washington D.C.
- FEMA, Federal Emergency Management Agency. (2012a). *Hazus MH 2.1 Earthquake Model Technical Manual*. Department of Homeland Security, Federal Emergency Management Agency, Washington D.C.
- FEMA, Federal Emergency Management Agency. (2012b). *Hazus MH 2.1 Earthquake Model User Manual*. Department of Homeland Security, Federal Emergency Management Agency, Washington D.C.
- Fonticella, R. (1998). "The Usefulness of the R^2 Statistic." *Casualty Actuarial Society Forum*, Maryland, USA.
- French, M. A. (2007a). "Report No. 134: Adobe with Timber and Clay Tile Roof." *World Housing Encyclopedia*, <<http://www.world-housing.net/whereport1view.php?id=100147>> (May. 2011a).
- French, M. A. (2007b). "Report No. 136: Adobe with Sawn Timber Roof Framing and Corrugated Iron Sheeting." *World Housing Encyclopedia*, <<http://www.world-housing.net/whereport1view.php?id=100149>> (May. 2011b).
- French, M. A. (2007c). "Report No. 137: Adobe Walls Supporting Rough Timber Framed Roof with Corrugated Iron Sheeting ." *World Housing Encyclopedia*, <<http://www.world-housing.net/whereport1view.php?id=100150>> (May. 2011c).
- GEM Foundation. (2010). *GEM1 Executive Summary, GEM Technical Report 2010-1*. GEM Foundation, Pavia, Italy.
- Goretti, A., and Di Pasquale, G. (2002). *An Overview of Post-Earthquake Damage Assessment in Italy*. Earthquake Engineering Research Institute, Oakland, CA.
- Grünthal, G. (Ed.). (1998). *European Macroseismic Scale 1998*. Cahiers du Centre Européen de Géodynamique et de Séismologie Volume 15, Centre Européen de Géodynamique et de Séismologie.
- Guha-Sapir, D., Vos, F., Below, R., and Ponserre, S. (2011). *Annual Disaster Statistical Review 2010: The Numbers and Trends*. Centre for Research on the Epidemiology of Disasters (CRED), Brussels.
- Gulati, B. (2006). "Earthquake Risk Assessment of Buildings: Applicability of HAZUS in Dehradun, India." Masters Thesis, International Institute of Geoinformation Science and Earth Observation (ITC), University of Twente, Netherlands.
- Hahn, G. J., and Shapiro, S. S. (1994). *Statistical Models In Engineering*. John Wiley & Sons, Inc, New York.
- Hill, M., and Rossetto, T. (2008). "Comparison of building damage scales

- and damage descriptions for use in earthquake loss modelling in Europe.” *Bulletin of Earthquake Engineering*, 6(2), 335–365.
- Husein, S., Pramumijoyo, S., Thant, M., Naing, T., and Murjaya, J. (2007). “A Short History on the Seismic History of Yogyakarta Prior to the May 27, 2006 Earthquake.” *The Yogyakarta Earthquake of May 27, 2006*, D. Karnawati, S. Pramumijoyo, R. Anderson, and S. Husein, eds. Star Publishing, Belmont, California.
- IDNDR, International Decade for Natural Disaster Reduction. (1994). “Yokohama Strategy and Plan of Action for a Safer World: Guidelines for Natural Disaster Prevention, Preparedness and Mitigation.” World Conference on Natural Disaster Reduction, Yokohama, Japan.
- IMF, International Monetary Fund. (2011). *World Economic Outlook April 2011*. International Monetary Fund, Washington D.C.
- ISDR, International Strategy for Disaster Reduction. (2005). *Hyogo Framework for Action 2005-2015: Building the Resilience of Nations and Communities to Disasters*. World Conference on Disaster Reduction, International Strategy for Disaster Reduction, Kobe, Hyogo, Japan.
- ISDR, International Strategy for Disaster Reduction. (2009). *UNISDR Terminology on Disaster Risk Reduction*. United Nations International Strategy for Disaster Reduction (UNISDR), Geneva, Switzerland.
- Jaiswal, K., and Wald, D. J. (2009). “Analysis of Collapse Fragilities of Global Construction Types Obtained During WHE-PAGER Phase I Survey.” World Housing Encyclopedia (WHE) and Prompt Assessment of Global Earthquakes for Response (PAGER), <<http://www.world-housing.net/wp-content/uploads/pager/2009/06/JaiswalWald2009Analysis-of-Phase-I1.pdf>> (Nov. 3, 2011).
- Jaiswal, K., Wald, D. J., and D'Ayala, D. (2011). “Developing Empirical Collapse Fragility Functions for Global Building Types.” *Earthquake Spectra*, 27(3), 775–795.
- Kahn, M. E. (2005). “The Death Toll from Natural Disasters: The Role of Income, Geography, and Institutions.” *The Review of Economics and Statistics*, 87(2), 271–284.
- Kaplan, H., Yilmaz, S., Akyol, E., Sen, G., Tama, Y. S., Cetinkaya, N., Nohutcu, H., Binici, H., Atimtay, E., and Sarisin, A. (2008). “29 October 2007, Çameli earthquake and structural damages at unreinforced masonry buildings.” *Natural Hazards and Earth System Sciences*, 8, 919–926.
- Kappos, A. J., and Panagopoulos, G. (2010). “Fragility Curves for Reinforced Concrete Buildings in Greece.” *Structure and Infrastructure Engineering*, 6(1-2), 39–53.
- Kappos, A. J., Panagopoulos, G., Panagiotopoulos, C., and Penelis, G.

- (2006). "A Hybrid Method for the Vulnerability Assessment of R/C and URM Buildings." *Bulletin of Earthquake Engineering*, 4(4), 391–413.
- Kenny, C. (2009). *Why Do People Die in Earthquakes? The Costs, Benefits and Institutions of Disaster Risk Reduction in Developing Countries*. World Bank, Washington D.C.
- Khater, M., Scawthorn, C., and Johnson, J. J. (2003). "Loss Estimation." *Earthquake Engineering Handbook*, W.-F. Chen and C. Scawthorn, eds. CRC Press.
- King, S. A., Kiremidjian, A., Pachakis, D., and Sarabandi, P. (2004). "Application of Empirical Fragility Functions From Recent Earthquakes." *Proceedings of the 13th World Conference on Earthquake Engineering*, Vancouver, B.C., Canada.
- Kircher, C., Whitman, R., and Holmes, W. (2006). "HAZUS Earthquake Loss Estimation Methods." *Natural Hazards Review*, 7(2), 45–59.
- Lagomarsino, S., and Giovinazzi, S. (2006). "Macroseismic and Mechanical Models for the Vulnerability and Damage Assessment of Current Buildings." *Bulletin of Earthquake Engineering*, 4(4), 415–443.
- Lang, D., Holliday, L., and Beleton, O. G. F. (2007). "Report No. 144: Vivienda De Adobe (Adobe Brick Houses)." *World Housing Encyclopedia*, <<http://www.world-housing.net/wherereport1view.php?id=100162>> (May. 2011).
- Legates, D. R., and McCabe, G. J. (1999). "Evaluating the use of 'goodness-of-fit' measures in hydrologic and hydroclimatic model validation." *Water Resources Research*, 35(1), 233–241.
- Levi, T., Tavron, B., Katz, O., Amit, R., Segal, D., Hamiel, Y., Bar-Lavi, Y., Romach, S., and Salamon, A. (2010). *Earthquake Loss Estimation in Israel Using the New HAZUS-MH Software: Preliminary Implementation*. Geological Survey of Israel, The Ministry of National Infrastructures, Jerusalem.
- Linkimer, L. (2008). "Relationship Between Peak Ground Acceleration and Modified Mercalli Intensity in Costa Rica." *Revista Geológica de América Central*, 38, 81–94.
- Lopez, M. A., Bommer, J. J., and Benavidez, G. (2012). "Report No. 14: Vivienda de Adobe (Adobe house)." *World Housing Encyclopedia*, <<http://www.world-housing.net/wherereport1view.php?id=100047>> (May. 2011).
- Luco, N., and Karaca, E. (2007). "Extending the USGS National Seismic Hazard Maps and ShakeMaps to probabilistic building damage and risk maps." *Proceedings of the 10th International Conference on Applications of Statistics and Probability in Civil Engineering*, Tokyo, Japan.
- Mac Berthouex, P., and Brown, L. (2002). "Chapter 39: The Coefficient of Determination, R^2 ." *Statistics for Environmental Engineers*, CRC Press,

Florida

- Maheri, M. R., Naeim, F., and Mehrain, M. (2005). "Performance of Adobe Residential Buildings in the 2003 Bam, Iran, Earthquake." *Earthquake Spectra*, 21(S1), S337–S344.
- Marshall, J. D., Lang, A. F., Baldrige, S. M., and Popp, D. R. (2011). "Recipe for Disaster: Construction Methods, Materials, and Building Performance in the January 2010 Haiti Earthquake." *Earthquake Spectra*, 27(S1), S323–S343.
- Mathworks. (2012). *Matlab Curve Fitting Toolbox: User's Guide*. The Mathworks Inc.
- Mayorca, P., and Meguro, K. (2004). "Proposal of an Efficient Technique for Retrofitting Unreinforced Masonry Dwellings." *Proceedings of the 13th World Conference on Earthquake Engineering*, Vancouver, B.C., Canada.
- Meli, R., and Alcocer, S. (2004). "Implementation of structural earthquake-disaster mitigation programs in developing countries." *Natural Hazards Review*, 5(1), 29.
- Meli, R., Hernandez, O., and Padilla, M. (1980). "Strengthening of Adobe Houses for Seismic Actions." *Proceedings of the 7th World Conference on Earthquake Engineering*, Istanbul, Turkey, 465–472.
- Moharram, A. M., Elghazouli, A. Y., and Bommer, J. J. (2008a). "A framework for a seismic risk model for Greater Cairo." *Soil Dynamics and Earthquake Engineering*, 28(10-11), 795–811.
- Moharram, A. M., Elghazouli, A. Y., and Bommer, J. J. (2008b). "Scenario-based earthquake loss estimation for the city of Cairo, Egypt." *Georisk: Assessment and Management of Risk for Engineered Systems and Geohazards*, 2(2), 92–112.
- Molina, S., Lang, D. H., and Lindholm, C. D. (2010a). "SELENA – an Open-Source Tool for Seismic Risk and Loss Assessment Using a Logic Tree Computation Procedure." *Computers & Geosciences*, 36(3), 257–269.
- Molina, S., Lang, D. H., Lindholm, C. D., and Lingvall, F. (2010b). *User Manual for the Earthquake Loss Estimation Tool: SELENA (draft)*. International Centre for Geohazards (ICG), NORSAR, University of Alicante (Spain).
- Mouroux, P., and Brun, B. L. (2006). "Presentation of RISK-UE Project." *Bulletin of Earthquake Engineering*, Springer, 4(4), 323–339.
- Mouroux, P., Bertrand, E., Bour, M., Le Brun, B., Depinois, S., Masure, P., RISK-UE Team. (2004). "The European RISK-UE Project: an Advanced Approach to Earthquake Risk Scenarios." *Proceedings of the 13th World Conference on Earthquake Engineering*, Vancouver, B.C., Canada.
- Murao, O., and Yamazaki, F. (2000). "Development of Fragility Curves for

- Buildings Based on Damage Survey Data of a Local Government After the 1995 Hyogoken-Nanbu Earthquake.” *Journal of structural and construction engineering. Transactions of AIJ*, Architectural Institute of Japan, (527), 189–196.
- Nielsen, L. (2011). *Classifications of Countries Based on Their Level of Development: How it is Done and How it Could be Done*. International Monetary Fund, Washington D.C.
- Noy, I. (2009). “The Macroeconomic Consequences of Disasters.” *Journal of Development Economics*, 88, 221–231.
- OCHA. (2006). “Bantul District: House Destroyed/Damaged.” *United Nations Office for the Coordination of Humanitarian Affairs*, Bantul, DI Yogyakarta, Indonesia,
<http://reliefweb.int/sites/reliefweb.int/files/resources/D60347E9963723B0C12571870043AC22-ocha_DMG_idn080606.pdf> (May. 27, 2012).
- Omine, H., Hayashi, T., Yashiro, H., and Fukushima, S. (2008). “Seismic Risk Analysis Method Using Both PGA and PGV.” *Proceedings of the 14th World Conference on Earthquake Engineering*, International Association for Earthquake Engineering, Beijing, China.
- Penelis, G. G., Kappos, A. J., Stylianidis, K. C., and Lagomarsino, S. (2002). “Statistical Assessment of the Vulnerability of Unreinforced Masonry Buildings.” *International Conference Earthquake Loss Estimation and Risk Reduction*, Bucharest, Romania.
- Porter, K. (2003). “Seismic Vulnerability.” *Earthquake Engineering Handbook*, W.-F. Chen and C. Scawthorn, eds. CRC Press.
- Porter, K., Kennedy, R., and Bachman, R. (2007). “Creating Fragility Functions for Performance-Based Earthquake Engineering.” *Earthquake Spectra*, 23(2), 471–489.
- Pramumijoyo, S., and Sudarno, I. (2007). “Surface Cracking due to Yogyakarta Earthquake 2006.” *The Yogyakarta Earthquake of May 27, 2006*, D. Karnawati, S. Pramumijoyo, R. Anderson, and S. Husein, eds. Star Publishing, Belmont, California.
- Rodriguez, M. (2007). “Confined Masonry Construction.” *World Housing Encyclopedia*, <http://www.world-housing.net/wp-content/uploads/2011/05/Confined-Masonry_Rodriguez.pdf> (Feb. 9, 2012).
- Rossetto, T., and Elnashai, A. (2003). “Derivation of Vulnerability Functions for European-Type RC Structures Based on Observational Data.” *Engineering Structures*, 25(10), 1241–1263.
- Rossetto, T., and Elnashai, A. (2005). “A New Analytical Procedure for the Derivation of Displacement-Based Vulnerability Curves for Populations of RC Structures.” *Engineering Structures*, 27(3), 397–409.
- Rota, M., Penna, A., and Magenes, G. (2010). “A Methodology for Deriving Analytical Fragility Curves for Masonry Buildings Based on

- Stochastic Nonlinear Analyses.” *Engineering Structures*, 32(5), 1312–1323.
- Rota, M., Penna, A., and Strobbia, C. L. (2008a). “Processing Italian Damage Data to Derive Typological Fragility Curves.” *Soil Dynamics and Earthquake Engineering*, 28(10-11), 933–947.
- Rota, M., Penna, A., Strobbia, C., and Magenes, G. (2008b). *Derivation of Empirical Fragility Curves from Italian Damage*. Rose School, IUSS Press, Pavia, Italy.
- Ruiz-Garcia, J., and Negrete, M. (2009). “Drift-based fragility assessment of confined masonry walls in seismic zones.” *Engineering Structures*, 31(1), 170–181.
- Sabetta, F., and Pugliese, A. (1987). “Attenuation of Peak Horizontal Acceleration and Velocity From Italian Strong-Motion Records.” *Bulletin of the Seismological Society of America*, 77(5), 1491–1513.
- Sabetta, F., Goretti, A., and Lucantoni, A. (1998). “Empirical fragility curves from damage surveys and estimated strong ground motion.” *Proceedings of the 11th European conference on earthquake engineering, Paris, France*.
- Sarabandi, P., Pachakis, D., and King, S. A. (2004). “Empirical Fragility Functions From Recent Earthquakes.” *Proceedings of the 13th World Conference on Earthquake Engineering*, Vancouver, B.C., Canada.
- Setijadji, L. D., Barianto, D. H., Watanabe, K., Fukuoka, K., Ehara, S., Rahardjo, W., Sudarno, I., Shimoyama, S., Susilo, A., and Itaya, T. (2007). “Searching for the Active Fault of the Yogyakarta Earthquake of 2006 Using Data Integration on Aftershocks, Cenozoic Geo-History, and Tectonic Geomorphology.” *The Yogyakarta Earthquake of May 27, 2006*, D. Karnawati, S. Pramumijoyo, R. Anderson, and S. Husein, eds. Star Publishing, Belmont, California.
- Seyedi, D., Gehl, P., Douglas, J., Davenne, L., Mezher, N., and Ghavamian, S. (2010). “Development of Seismic Fragility Surfaces for Reinforced Concrete Buildings by Means of Nonlinear Time-History Analysis.” *Earthquake Engineering & Structural Dynamics*, 39(1), 91–108.
- Singhal, A., and Kiremidjian, A. S. (1996a). “Method for Probabilistic Evaluation of Seismic Structural Damage.” *Journal of Structural Engineering*, 122, 1459–1467.
- Singhal, A., and Kiremidjian, A. S. (1996b). *A Method for Earthquake Motion-Damage Relationships with Application to Reinforced Concrete Frames*. The John A. Blume Earthquake Engineering Center, Stanford, CA.
- Singhal, A., and Kiremidjian, A. S. (1998). “Bayesian Updating of Fragilities with Application to RC Frames.” *Journal of Structural Engineering*, 124(8), 922–929.

- So, E., and Pomonis, A. (2011). *GEM Technical Report 2011-1 : Events in the GEM Earthquake Consequences Database (GEMECD)*. GEM Foundation, Pavia, Italy.
- Stanganelli, M. (2008). "A new pattern of risk management: The Hyogo Framework for Action and Italian practise." *Socio-Economic Planning Sciences*, 42(2), 92–111.
- Tarque, N., Crowley, H., Pinho, R., and Varum, H. (2010). "Seismic risk assessment of adobe dwellings in Cusco, Peru, based on mechanical procedures." *Proceedings of the 14th European Conference on Earthquake Engineering*, Ohrid, Macedonia.
- Todaro, M. P., and Smith, S. C. (2009). *Economic Development*. Prentice Hall, New Jersey.
- Tselentis, G. A., and Danciu, L. (2008). "Empirical relationships between modified mercalli intensity and engineering ground-motion parameters in Greece." *Bulletin of the Seismological Society of America*, 98(4), 1863–1875.
- UNDP, United Nations Development Programme. (2010). *Human Development Report 2010*. United Nations Development Programme, New York.
- UNDP, United Nations Development Programme. (2011). *Human Development Report 2011*. United Nations Development Programme, New York.
- Ural, A., Doğangün, A., Sezen, H., and Angın, Z. (2012). "Seismic performance of masonry buildings during the 2007 Bala, Turkey earthquakes." *Natural Hazards*, 60(3), 1013–1026.
- USGS. (2010a). "Haiti ShakeMaps." *United States Geological Survey*, <<http://earthquake.usgs.gov/earthquakes/shakemap/global/shake/2010rja6/#Uncertainty>> (Jul. 2012a).
- USGS. (2010b). "Magnitude 6.3 - JAVA, INDONESIA." *U.S. Geological Survey*, <<http://earthquake.usgs.gov/earthquakes/recenteqsww/Quakes/usneb6.php>> (Apr. 13, 2012b).
- Vamvatsikos, D., Kouris, L. A., Panagopoulos, G., Kappos, A. J., Nigro, E., Rossetto, T., Lloyd, T. O., and Stathopoulos, T. (2010). "Structural Vulnerability Assessment Under Natural Hazards: A review." *Proceedings of COST Action C26 Final International Conference on Urban habitat construction under catastrophic events*, Naples, Italy.
- Voight, B., Sukhyar, R., and Wirakusumah, A. D. (2000). "Introduction to the special issue on Merapi Volcano." *Journal of Volcanology and Geothermal Research*, 100.
- Wagner, D., Rabbel, W., Leuhr, B.-G., Wasserman, J., Walter, T. R., Kopp, H., Koulakov, I., Wittwer, A., Bohm, M., and Asch, G. (2007). "Seismic Structure of Central Java." *The Yogyakarta Earthquake of May 27*,

- 2006, D. Karnawati, S. Pramumijoyo, R. Anderson, and S. Husein, eds. Star Publishing, Belmont, California.
- Wald, D. J., Jaiswal, K. S., Marano, K. D., Bausch, D. B., and Hearne, M. G. (2010). *PAGER-Rapid assessment of an earthquake's impact: U.S. Geological Survey Fact Sheet 2010-3036*. United States Geological Survey, Golden, CO.
- Wald, D. J., Quitoriano, V., Heaton, T. H., and Kanamori, H. (1999). "Relationships Between Peak Ground Acceleration, Peak Ground Velocity, and Modified Mercalli Intensity in California." *Earthquake Spectra*, 15(3), 557–564.
- Wald, D. J., Worden, B., Quitoriano, V., and Pankow, K. (2006). *ShakeMap Manual*. United States Geological Survey.
- WB, The World Bank. (2011). *World Development Report 2011*. The World Bank, Washington D.C.
- WB, The World Bank. (2012a). "Rural population growth (annual %)." *The World Bank*, <<http://data.worldbank.org/indicator/SP.RUR.TOTL.ZG>> (Sep. 2012a).
- WB, The World Bank. (2012b). "Urban population growth (annual %)." *The World Bank*, <http://data.worldbank.org/indicator/SP.URB.GROW/countries/1W?order=wbapi_data_value_2010%20wbapi_data_value%20wbapi_data_value-last&sort=desc&display=default> (Sep. 2012b).
- Whitman, R. V., Reed, J. W., and Hong, S.-T. (1973). "Earthquake Damage Probability Matrices." *Proceedings of the 5th World Conference on Earthquake Engineering*, Rome, II, 2531–2540.
- Worden, C. B., Wald, D. J., Allen, T. I., Lin, K., Garcia, D., and Cua, G. (2010). "A Revised Ground-Motion and Intensity Interpolation Scheme for ShakeMap." *Bulletin of the Seismological Society of America*, 100(6), 3083–3096.
- Yamaguchi, N., and Yamazaki, F. (2000). "Fragility curves for buildings in Japan based on damage surveys after the 1995 Kobe earthquake." *Proceedings of the 12th conference on earthquake engineering, Auckland, New Zealand*.
- Yeh, C.-H., Jean, W. Y., and Loh, C. H. (2000). "Building Damage Assessment for Earthquake Loss Estimation in Taiwan." *Proceedings of the 12th World Conference on Earthquake Engineering*, Auckland, New Zealand.
- Yeh, C.-H., Loh, C.-H., and Tsai, K.-C. (2006). "Overview of Taiwan Earthquake Loss Estimation System." *Natural Hazards*, 37(1-2), 23–37.
- Yong, C., Qi-fu, C., and Ling, C. (2001). "Vulnerability Analysis in Earthquake Loss Estimate." *Natural Hazards*, 23(2), 349–364.

Appendix A Fragility Curves (PSA and PGA)

Appendix A contains fragility curves in terms of PGA and PSA fitted with and without the data points for the highest ground motion intervals.

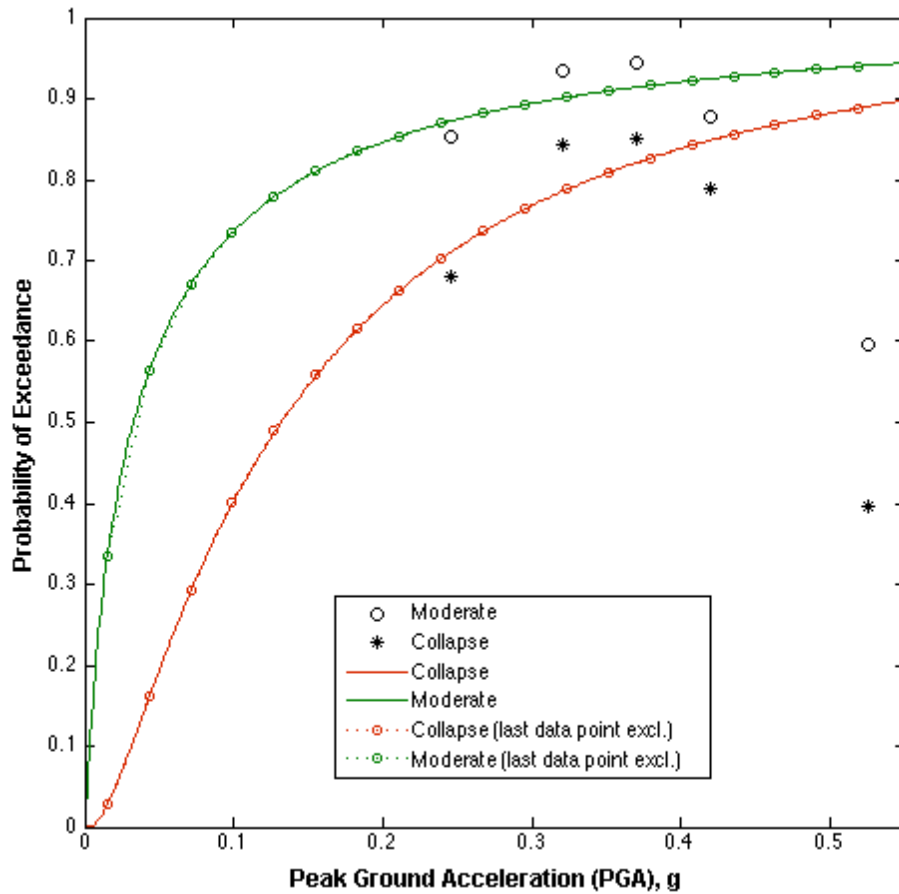


Figure A.1 Cumulative lognormal fragility curve in terms of PGA

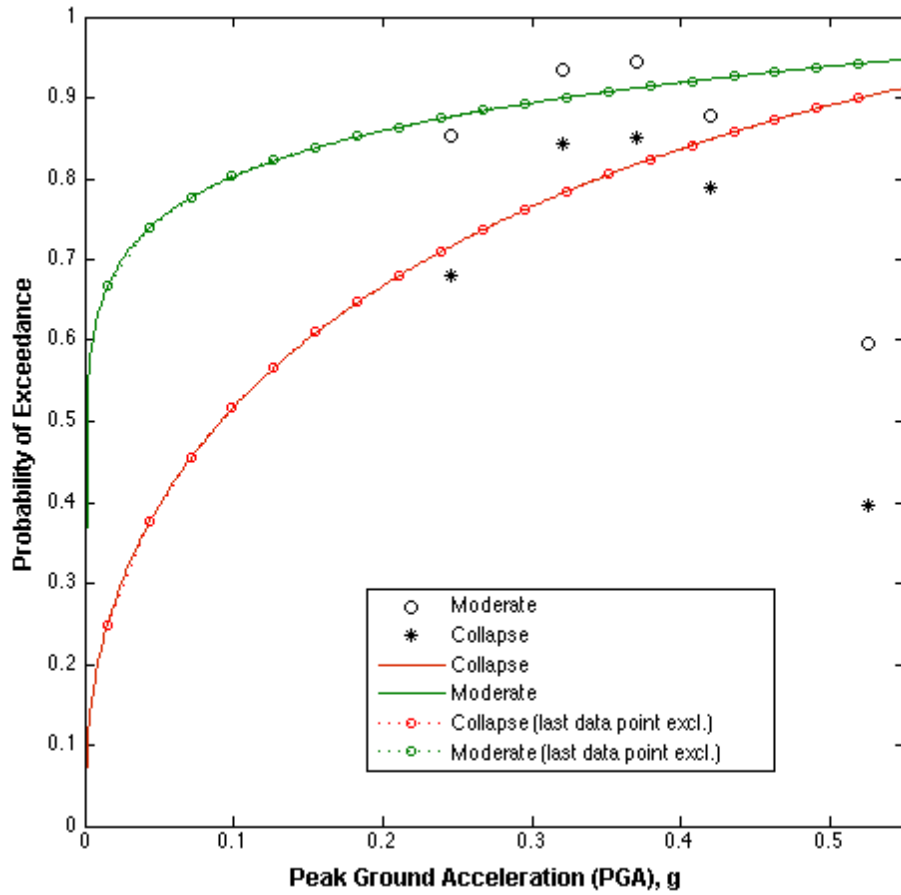


Figure A.2 Cumulative beta fragility curve in terms of PGA

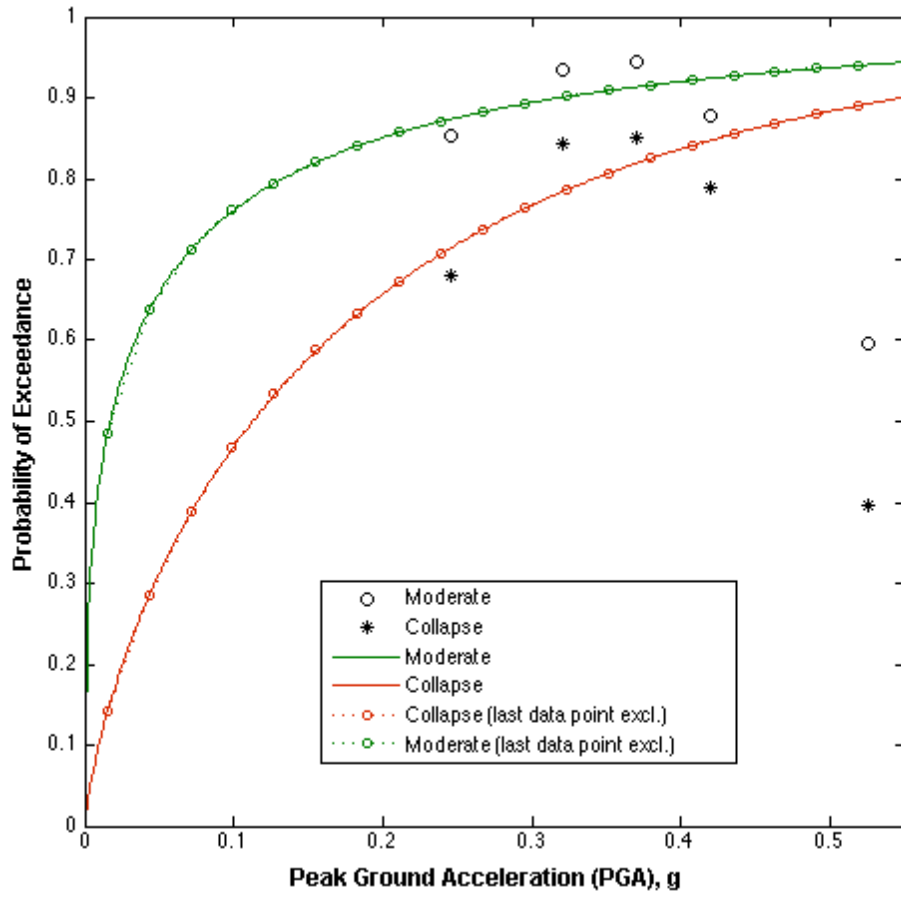


Figure A.3 Exponential fragility curve in terms of PGA

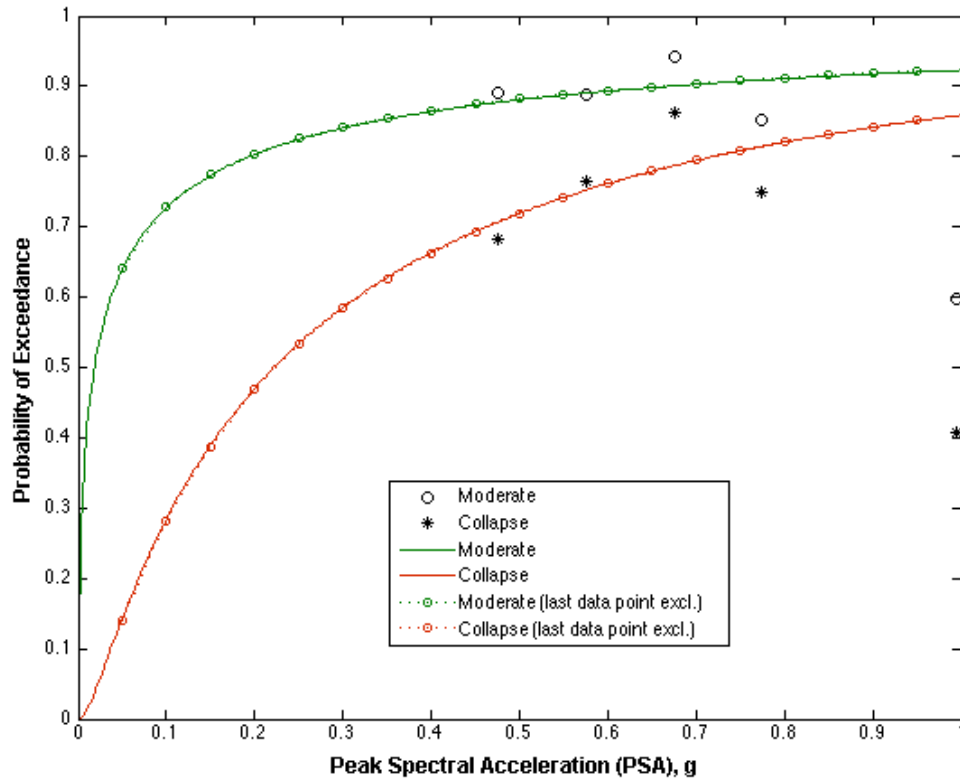


Figure A.4 Cumulative lognormal fragility curve in terms of PSA

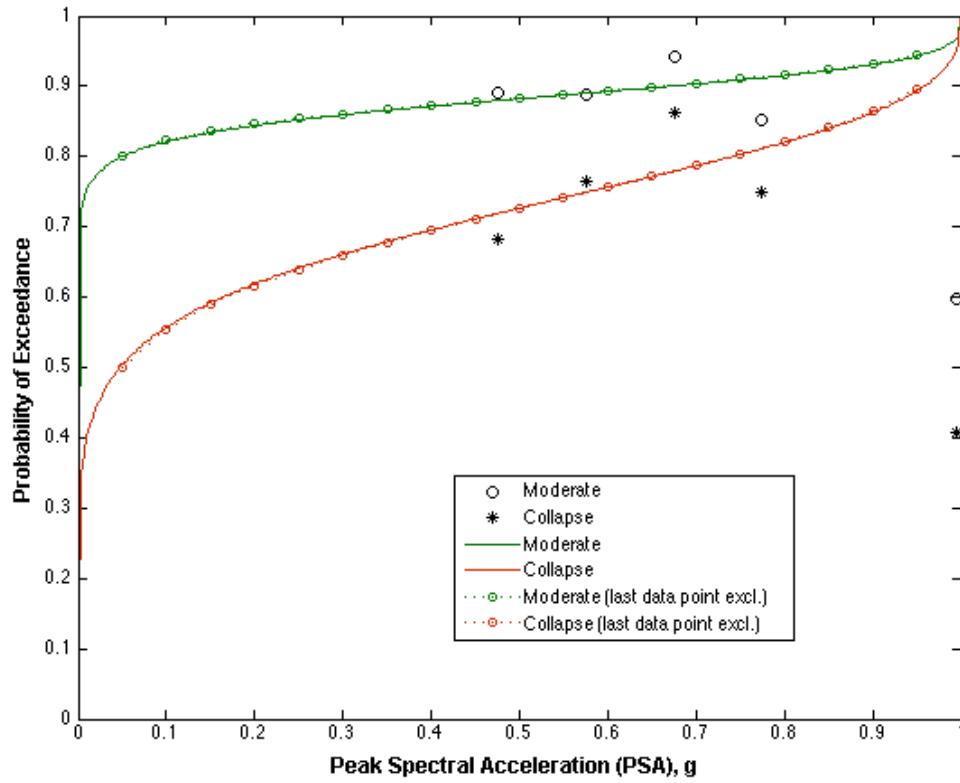


Figure A.5 Cumulative Beta fragility curve in terms of PSA

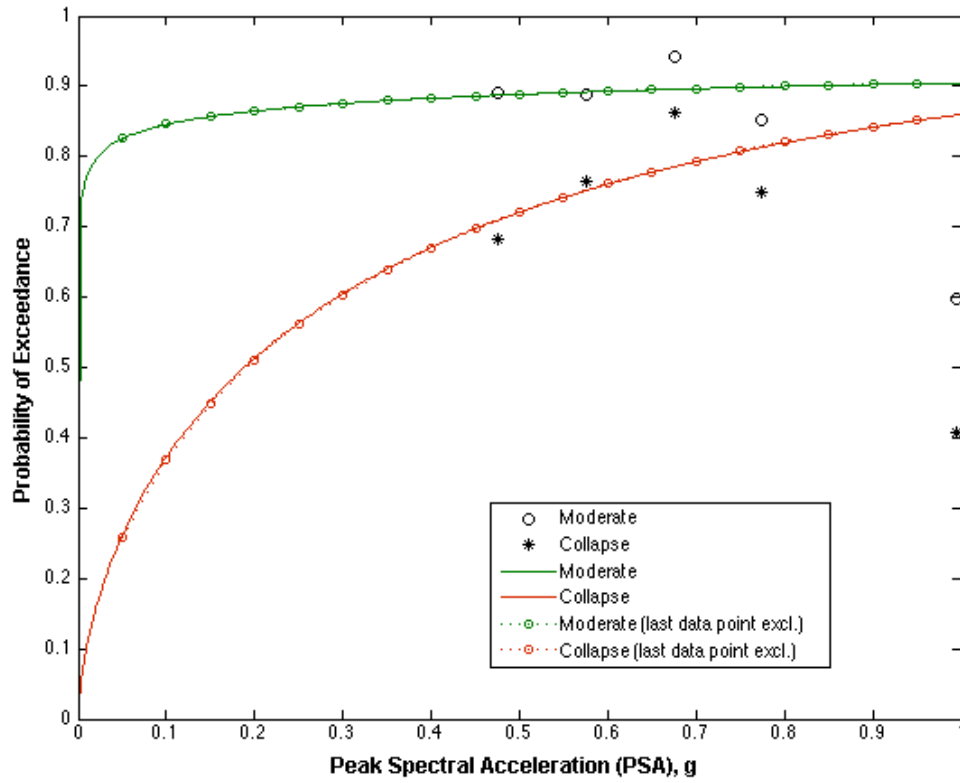


Figure A.6 Exponential fragility curve in terms of PSA